

Dynamics of small particles, passive and active, in complex fluids

by

Charu Datt

B.Tech., National Institute of Technology, Kurukshetra, 2012
M.S., École Polytechnique, 2014

A DISSERTATION SUBMITTED IN PARTIAL FULFILLMENT OF
THE REQUIREMENTS FOR THE DEGREE OF
DOCTOR OF PHILOSOPHY

in

The Faculty of Graduate and Postdoctoral Studies
(Mechanical Engineering)

THE UNIVERSITY OF BRITISH COLUMBIA

(Vancouver)

April 2019

© Charu Datt 2019

The following individuals certify that they have read, and recommend to the Faculty of Graduate and Postdoctoral Studies for acceptance, the dissertation entitled:

Dynamics of small particles, passive and active, in complex fluids
submitted by Charu Datt in partial fulfillment of the requirements for
the degree of Doctor of Philosophy
in Mechanical Engineering

Examining Committee:

Gwynn J. Elfring, Mechanical Engineering
Supervisor

Ian A. Frigaard, Mathematics, and Mechanical Engineering
Supervisory Committee Member

Savvas G. Hatzikiriakos, Chemical and Biological Engineering
Supervisory Committee Member

Anthony Wachs, Mathematics, and Chemical and Biological Engineering
University Examiner

James J. Feng, Mathematics, and Chemical and Biological Engineering
University Examiner

Additional Supervisory Committee Member:

George M. Homsy, Mathematics, and Mechanical Engineering

Abstract

The focus of this thesis is on small non-Brownian particles in fluids that show deviations from *standard* Newtonian fluids. We study the motion of swimmers and sedimenting particles in Newtonian fluids with viscosity gradients, in shear-thinning fluids, and in fluids with viscoelasticity. The work is theoretical; its aim is to study the first effects of non-Newtonian rheology on particle motion and towards this end uses the reciprocal theorem of low Reynolds number hydrodynamics and methods of perturbation expansion. We find that the dynamics of the particles is often qualitatively changed due to the rheological properties of the fluid, and such changes are difficult to predict *a priori*.

Lay Summary

This thesis focusses on understanding the motion of swimmers that are only a few micrometers in size in fluids that are complex. Water is an example of a simple (Newtonian) fluid. But many fluids where microswimmers swim show both fluid-like and solid-like properties. Sperm cells in human cervical mucus and *H. pylori* in gastric mucus are examples of microswimmers in complex fluids.

We study such swimmers theoretically, and demonstrate how their dynamics in complex fluids is different from that in Newtonian fluids. In fact, we find that often the swimming behaviour in complex fluids is totally unexpected beforehand. Noting that designing artificial microswimmers in Newtonian fluids can be challenging, we also show how complexity of the fluid medium may be used to design simpler swimmers. Our work has potential applications in aspects of biomedical engineering focussed at developing microrobots for targeted drug delivery and minimally invasive surgery.

Preface

Parts of this thesis, with minor changes, have been previously published as research articles. These parts are listed below. I have underlined my name among the names of authors to guide the eye.

- Chapter 4 has been previously published as ‘C. Datt & G.J. Elfring, *Dynamics and rheology of particles in shear-thinning fluids*, Journal of non-Newtonian Fluid Mechanics **262** (2018) 107-144’.

C.D. and G.J.E. designed the research. C.D. performed the calculations. C.D. and G.J.E. analyzed the results and wrote the paper. C.D. is the principal contributor to this work. C.D. was supervised by G.J.E.

- Chapter 5 has been previously published as ‘C. Datt, L. Zhu, G.J. Elfring, & O.S. Pak, *Squirring through shear-thinning fluids*, Journal of Fluid Mechanics Rapids, **784** (2015) R1’.

All authors designed the research. C.D. performed the theoretical calculations. L.Z. performed the numerical simulations. All authors analyzed the results. C.D., G.J.E., and O.S.P. wrote the paper with inputs from L.Z. C.D. is the principal contributor to this work. C.D. was supervised by G.J.E.

- Chapter 6 has been previously published as ‘C. Datt, G. Natale, S.G. Hatzikiriakos, & G.J. Elfring, *An active particle in a complex fluid*, Journal of Fluid Mechanics, **823** (2017), 675-688’.

This work is one part of a simultaneously running two-part project. The second part, mentioned later in the preface, is not included in the thesis. All authors contributed to discussion of the project.

C.D. performed the calculations in this work. C.D. and G.J.E. analyzed the results and wrote the paper. C.D. is the principal contributor to this work. C.D. was supervised by G.J.E.

- Chapter 8 has been previously published as ‘C. Datt, B. Nasouri, & G.J. Elfring, *Two-sphere swimmers in viscoelastic fluids*, Physical Review Fluids **3**, 123301 (2018)’.

C.D. designed the research. C.D. performed all calculations in this work except for the section on swimmers with elastic spheres. B.N. performed the calculations for the section on swimmers with elastic spheres. All authors analyzed the results and wrote the paper. C.D. is the principal contributor to this work. C.D. was supervised by G.J.E.

Chapter 7 has been submitted for publication as ‘C. Datt & G.J. Elfring, *A note on higher-order perturbative corrections to squirming speed in weakly viscoelastic fluids*’. C.D. designed the research and performed the calculations. C.D. and G.J.E. analyzed the results and wrote the paper. C.D. is the principal contributor to this work. C.D. was supervised by G.J.E.

Chapter 3 may soon be submitted for publication as ‘C. Datt & G.J. Elfring, *Swimming in viscosity gradients*’. C.D. and G.J.E. have designed the research. C.D. has performed the calculations. C.D. and G.J.E. have analyzed the results and written the article. C.D. is the principal contributor to this work. C.D. was supervised by G.J.E.

Related or directly stemming from the thesis, but not included in it, are two articles that are listed below.

- ‘G. Natale, C. Datt, S. Hatzikiriakos, & G.J. Elfring, *Autophoretic locomotion in weakly viscoelastic fluids at finite Péclet number*, Physics of Fluids **29**, 123102 (2017)’.

This is the second part of the two-part project mentioned above.

G.N. wrote the numerical code for this work. C.D. provided help with the code, contributed to the analyses of results and writing of the paper. C.D. was supervised by G.J.E.

- ‘K. Pietrzyk, H. Nganguia, C. Datt, L. Zhu, G.J. Elfring, & O.S. Pak, *Flow around a squirmer in a shear-thinning fluid*, submitted.’

C.D. contributed to the design of the research, in calculations and in analyses. C.D. was supervised by G.J.E.

Table of Contents

Abstract	iii
Lay Summary	iv
Preface	v
Table of Contents	vii
List of Figures	x
1 Introduction	1
2 The swimmer, the fluids, and the reciprocal theorem . . .	4
2.1 The swimmer	4
2.2 The fluids	6
2.3 The reciprocal theorem	8
3 Swimming in viscosity gradients	12
3.1 Introduction	12
3.2 Theoretical formulation	13
3.2.1 Reciprocal theorem	14
3.2.2 Asymptotic analysis	15
3.2.3 Remarks on the asymptotic analysis	16
3.3 Results and discussion	16
3.3.1 Passive sphere	16
3.3.2 Squirmer	17
3.4 Conclusion	21
4 Dynamics and rheology of particles in shear-thinning fluids	23
4.1 Introduction	23
4.2 Reciprocal Theorem	25
4.3 Shear-thinning fluid	26
4.4 Sedimenting spheres	28

Table of Contents

4.4.1	Single sphere	28
4.4.2	Two spheres	29
4.5	Sedimentation of a rotating sphere	33
4.6	Sphere under an external force in a linear flow of shear-thinning fluid	35
4.7	Suspension of spheres in a shear-thinning fluid	36
4.8	Conclusion	39
5	Squirming through shear-thinning fluids	41
5.1	Introduction	41
5.2	Theoretical framework	43
5.2.1	Shear-thinning rheology: the Carreau-Yasuda model	43
5.2.2	Asymptotic analysis	45
5.2.3	The reciprocal theorem	46
5.2.4	Numerical solution	47
5.3	Results and discussion	47
5.3.1	Drag and thrust	49
5.3.2	Addition of other squirring modes	51
5.4	Conclusion	53
6	An active particle in a complex fluid	54
6.1	Introduction	54
6.2	Modelling active particles	56
6.3	Swimming in a background flow of a weakly non-Newtonian fluid	58
6.4	Janus particle in non-Newtonian fluids	61
6.4.1	Viscoelasticity: second-order fluid	61
6.4.2	Shear-thinning rheology: Carreau model	66
6.5	Conclusion and future work	68
7	A note on higher-order perturbative corrections to squirring speed in weakly viscoelastic fluids	70
7.1	Introduction	70
7.2	Theoretical framework	72
7.2.1	The squirmer model	72
7.2.2	The second-order fluid model	72
7.2.3	The reciprocal theorem	73
7.3	Results and discussion	74
7.3.1	Giesekus fluid	75
7.3.2	A fluid of grade three	78

Table of Contents

7.4	Conclusion	80
8	Two-sphere swimmers in viscoelastic fluids	81
8.1	Introduction	81
8.2	Swimmer in a viscoelastic fluid	84
8.2.1	Two-sphere swimmers	84
8.2.2	Theory for swimming in complex fluids	85
8.2.3	Constitutive equation	87
8.2.4	Small amplitude expansion	88
8.2.5	Results and discussion	90
8.3	Swimmer with elastic spheres	92
8.4	Conclusion	95
9	Conclusion and outlook	96
9.1	The findings	96
9.2	The limitations	98
9.3	The future	99
	Bibliography	101
	 Appendices	
A	Some expressions for motion of spheres	119
B	Linear viscoelasticity	121

List of Figures

3.1	The initial orientation of the swimmers $e_{initial}$ is along the positive x-axis. The viscosity gradient is along the positive y-axis. After sometime all swimmers swim antiparallel to the viscosity gradient. Note that in this orientation, pushers are the fastest, while pullers are the slowest. The trajectories are plotted for time $t = 0$ to $t = 100$	19
3.2	Planar trajectories of pushers (left), neutral swimmers (centre), and pullers (right). The initial position of the swimmers, $(x = 1, y = 1)$, is marked by the red dot. The swimmers originally point in the positive x-axis. The swimmers are in a radial viscosity gradient: viscosity increases radially outward from the point $(0, 0)$, $\delta\eta = \sqrt{x^2 + y^2}$. Pushers find a stable orbit. The trajectory of neutral swimmers is bounded at long times. Pullers perform ‘unstable’ motion about the ‘origin’ of viscosity gradient. Note the farthest the swimmers have travelled from this origin after equal times ($t = 4000$).	20
4.1	a) Variation of non-Newtonian drag F^1 as a function of the distance of separation between the two spheres. b) Normalized drag as a function of this distance. Note that the variation is non-monotonic and that drag reduction is minimized at $h/d \approx 2.35$	32
5.1	In (a) we show results from numerical simulations for a neutral squirmer ($\alpha = 0$, ●), puller ($\alpha = 5$, ▲) and pusher ($\alpha = -5$, ▼) for $\varepsilon = 0.99$ and $n = 0.25$. (b) The non-monotonic variation in velocity is well captured by asymptotics for a neutral squirmer (solid line), and a pusher/puller (dashed line) at $\varepsilon = 0.1$ and $n = 0.25$	48

List of Figures

5.2	In (a), the symbol Δ denotes the difference between drag, or thrust, in a shear-thinning fluid and a Newtonian fluid: the dash-dot curve represents the drag reduction in a shear-thinning fluid compared with a Newtonian fluid, while the solid and dashed curves represent loss in thrust for squirmers with $\alpha = 0$ and $\alpha = \pm 5$ respectively ($n = 0.25$, $\varepsilon = 0.1$). In (b) we show that the difference between drag and thrust is positive both for a neutral squirmer (solid) and a pusher/puller (dashed) in a shear-thinning fluid. All quantities are dimensionless.	50
5.3	In (a) we show the level set curve below which faster swimming occurs for specific values of α and $\zeta = B_3/B_1$ when $Cu \ll 1$. In (b) we show the swimming speed of a neutral squirmer (solid line) and a pusher/puller (dashed line) at values of ζ chosen below the curve in (a) so that the swimming speed is larger than the Newtonian value at small Cu (the upper solid line: $\alpha = 0$, $\zeta = -15$; the upper dashed line: $\alpha = \pm 5$, $\zeta = -4$); conversely, with values of ζ above the curve in (a) the swimmers always swim slower than in a Newtonian fluid as shown (lower solid line: $\alpha = 0$, $\zeta = 15$; lower dashed lines: $\alpha = \pm 5$, $\zeta = 4$). Here $\varepsilon = 0.1$, $n = 0.25$. . .	52
6.1	Self-phoretic particle with two compartments of different activity, A_f and A_b . We consider particles with a constant uniform mobility over the surface. When $\theta_d = \pi/2$, the particle has compartments of equal cover, which we call a symmetric Janus particle.	58
6.2	Variation of the scaled first-order swimming velocity $U_1^{(M)}/U_N$ with θ_d obtained for the first $M + 1$ modes (dashed lines), and $b = 0.2$. $U_1^{(\infty)}$ corresponds to the convergence value ($M = 99$) and is depicted by the solid line. Inset plot shows the relative error.	65
6.3	Variation of the scaled first-order swimming velocity $U_1^{(M)}/U_N$ (obtained for $M + 1$ modes) with Cu for two values of $\mu \equiv \cos \theta_d$. Solid lines correspond to $M = 30$, and $M = 28$ for $\mu = 0$ (symmetric) and $\mu = \pm 0.9$ respectively (additional modes lead to negligible differences). Dashed-lines correspond to the swimming velocity with just the first two modes.	67

List of Figures

7.1	Swimming speeds in the Giesekus fluid as a function of De . The solid lines include corrections up to $\mathcal{O}(De^3)$. The dashed lines are Padé approximations to the series for the speeds in the text. The dotted lines include only $\mathcal{O}(De)$ corrections. The addition of the higher order modes decreases the speeds of the squirmers. As seen here, all squirmers at large values of De swim slower than in a Newtonian fluid, as found in the numerical work of Zhu <i>et al.</i> [217].	77
7.2	Swimming speeds in fluids of grade three. Solid lines: $\mathcal{P} = 3/2$, $\mathcal{Q} = -7$. Dashed lines: $\mathcal{P} = 3/2$, $\mathcal{Q} = 5$. Solid and dashed lines for $\beta = 0$ overlap. Depending on the values of \mathcal{Q} for a given \mathcal{P} , either of the puller or pusher can swim faster or slower than in a Newtonian fluid at small De	79
8.1	Schematic of the two-sphere swimmer. The spheres, labeled \mathcal{B}_1 and \mathcal{B}_2 , have radii $a\alpha$ and a , respectively ($\alpha > 1$). The spheres are (on average) a distance d_0 apart and e_{\parallel} is the unit vector pointing from \mathcal{B}_1 to \mathcal{B}_2	84
8.2	Schematic showing one complete cycle for the two swimmers: (a) The <i>in-phase</i> swimmer maintains the distance between the spheres as it moves forward. (b) In the <i>anti-phase</i> swimmer, the spheres converge and diverge. The steps in grey show the transition from one half cycle to the next. The red dot marks the position of the swimmer.	85
8.3	The swimming speed coefficient \mathcal{U} is plotted with variation in the clearance Δ_c between the two spheres for different size ratios α . The square symbols (connected by dashed lines) represent the anti-phase swimmer and the circles (connected by solid lines) represent the in-phase swimmer. All quantities are dimensionless.	90

Chapter 1

Introduction

This thesis is about the dynamics of small particles in non-Newtonian fluids. A non-Newtonian fluid does not obey Newton’s law of viscosity, i.e., shear stresses in the fluid are not linearly proportional to the rates of strain, and often demonstrates properties like viscoelasticity and shear-thinning viscosity [5, 16]. With viscoelasticity, the fluid retains memory of its flow history and exhibits stress anisotropy, whereas a shear-thinning rheology means that the fluid viscosity decreases with increasing shear rates. We focus on the two properties in incompressible fluids here. We study only small particles, so their motion is dominated by viscous forces, and inertia may be neglected—the motion obeys equations of low Reynolds number hydrodynamics [93]. These particles can be passive or active. Active particles can convert stored or ambient free energy into systematic motion [139, 180]; passive particles are the ones that are not active.

The following is a brief overview of the literature, and an outline of the thesis. The chapters in the thesis that describe our research are written in the format of research articles and have their own literary introduction.

Plastic microbeads in toothpastes, microvesicles in biofluids, and during tertiary oil recovery, oil drops in polymer solution are examples of particles in complex fluids. Such systems range from natural to industrial settings [33], and therefore, it becomes interesting, from both fundamental and engineering point of view, to understand them. The interest in motion of small particles in complex fluids is not new; in fact, one finds review articles by Leal [132, 133] and Brunn [29] in the late 70’s. Even so, sedimentation of a spherical particle in viscoelastic shear flow [64], effects of viscoelasticity on sedimenting anisotropic particles [40], Einstein viscosity for a dilute suspension in viscoelastic fluids [65]—some seemingly canonical problems—were worked out (by others) during the period of this doctorate study. Lest this suggest that progress has not been made in complex fluids, we refer the reader to the recent review articles by Zenit & Feng [216] and D’Avino & Maffettone [49], which also suggest directions for the future of the field. Importantly, it must be pointed out that dealing with complex fluids (in particular, viscoelastic fluids) also meant, and means, tackling some fun-

damental issues [55], like slip or no slip? or the high Weissenberg number problem, which are not present in Newtonian fluids. A sustained, and in fact growing interest in understanding complex fluids, in context of this thesis, is also due to the fast emerging field of microfluidics, where ‘microchannels designed to focus, concentrate, or separate particles suspended in viscoelastic liquids are becoming common’ [47].

The relevant works in the foregoing discussion were centred on passive particles. The focus in this thesis is on “active particles”, a term often interchangeably used with self-propelled particles and microswimmers. Bacteria, which represent the bulk of world’s biomass, are often found in environments, such as gastric mucus (*H. pylori*) and biofilms, which display non-Newtonian rheological properties [127]. Bacteria are examples of active particles. Mammalian sperm cells swimming through cervical mucus [72] are also examples of active particles in complex fluids. Our understanding of active particles has developed enough that we can describe self-sustained turbulent structures in living fluids [60], and also use bacteria in fluids as work horses for turning microscopic gears [185]. This is hardly surprising considering such giants of yesteryears as G. I. Taylor, M. J. Lighthill and E. M. Purcell contributed to the field of microswimming [137, 170, 200]. However, much of this understanding is in Newtonian fluids [129], and understanding in complex fluids is still nascent [164].

Research in swimming in complex fluids has burgeoned after the theoretical work of Lauga [121] where he considered a simple swimmer and compared its swimming speed and its power consumption to those in an equivalent Newtonian fluid: questions regarding the swimming speed and the power consumption of microswimmers in non-Newtonian fluids are now being asked and answered for various model and real swimmers [70, 195]. An important motivation for these studies, other than the fundamental curiosity, remains of creating autonomous devices for targeted drug delivery [79] and other biomedical applications [208] which will swim in non-Newtonian fluids—what most biological fluids are [120, 142]. The work in this thesis was driven by such questions as: how does a small change in rheological property of the fluid affect the swimming motion? can intuitions developed in Newtonian fluids lead to a wrong footing in complex fluids? can the complexity of the fluid be used to our advantage in modelling artificial swimmers?

The work in the thesis is done in the spirit of Leal’s work on passive particles [133] where ‘the particle-motion problem *can* be treated theoretically if the deviations from the “standard conditions” are *small*.’ Chapter 3 talks about a swimmer in a Newtonian fluid with *small* gradients in viscosity.

Chapter 4 is about the dynamics and rheology of passive particles in *weakly* shear-thinning fluids. In Chapter 5, we look at a swimmer in a *weakly* shear-thinning fluid, and in Chapter 6 and 7, in *weakly* viscoelastic fluids. Chapter 8 is about creating an artificial swimmer using the rheological property of the fluid. We end with talking about what we learnt, and the things that interest us for the future in Chapter 9.

Although chapters in this thesis are written in the format of articles, and therefore aimed to be self-contained, we present, in Chapter 2, additional details of the overarching theoretical models and methods that we use for studying swimmers and fluids; the reader not familiar with the field may find these details useful.

Chapter 2

The swimmer, the fluids, and the reciprocal theorem

2.1 The swimmer

Our theoretical microswimmer is a squirmer. As a spherical squirmer, a microswimmer is represented as a sphere with prescribed velocities on its surface [17, 137]. It is only the surface velocities that propel the squirmer. The squirmer was proposed by Lighthill [137] as a finite-body model swimmer that could swim in Newtonian fluids at zero Reynolds number. Recently, the works of Chisholm *et al.* [36], Khair & Chisholm [110], Wang & Ardekani [209] have explored the effect of inertia on the squirmer's motion.

The description below is of an axisymmetric spherical squirmer of radius a , as described in the works of Lighthill [137] and Blake [17] (Blake [17] corrected Lighthill's solution [137]). The surface velocities on such squirmers are represented as

$$(u)_{r=a} = \sum_{n=0}^{\infty} A_n(t) P_n(\cos \theta), \quad (v)_{r=a} = \sum_{n=1}^{\infty} B_n(t) V_n(\cos \theta), \quad (2.1)$$

where u and v are the radial and azimuthal components of the velocity field, respectively. θ is the polar angle (in the spherical coordinate system) measured from the axis of symmetry, and P_n represents the ordinary Legendre polynomial, whereas $V_n = -2/(n(n+1)) P_n^1(\cos \theta)$, P_n^1 being the associated Legendre function of the first kind. In incompressible Newtonian fluids, the surface velocities lead to a propulsion speed (along \mathbf{e}_z , the axis of symmetry) of [17, 137]

$$U = \frac{1}{3} (2B_1 - A_1), \quad (2.2)$$

with the flow field around the squirmer in the lab frame (fluid at infinity is

2.1. The swimmer

at rest) given by [17]

$$u = A_0 \frac{a^2}{r^2} P_0 + \frac{2}{3} (A_1 + B_1) \frac{a^3}{r^3} P_1 + \sum_{n=2}^{\infty} \left[\left(\frac{n}{2} \frac{a^n}{r^n} - \left(\frac{n}{2} - 1 \right) \frac{a^{n+2}}{r^{n+2}} \right) A_n P_n + \left(\frac{a^{n+2}}{r^{n+2}} - \frac{a^n}{r^n} \right) B_n P_n \right], \quad (2.3)$$

$$v = \frac{1}{3} (A_1 + B_1) \frac{a^3}{r^3} V_1 + \sum_{n=2}^{\infty} \left[\left(\frac{n}{2} \frac{a^{n+2}}{r^{n+2}} - \left(\frac{n}{2} - 1 \right) \frac{a^n}{r^n} \right) B_n V_n + \frac{n}{2} \left(\frac{n}{2} - 1 \right) \left(\frac{a^n}{r^n} - \frac{a^{n+2}}{r^{n+2}} \right) A_n V_n \right], \quad (2.4)$$

where r is measured from the centre of the squirmer. When the squirmer does not deform, and its surface impermeable, the radial surface velocities are zero i.e., for all n , $A_n = 0$. With only tangential surface velocities, B_n may be unambiguously referred to as the n^{th} squirring mode. In this work, we restrict our attention to steady squirmers with just tangential surface velocities, and, in the remaining section, will consider only such squirmers.

From equation (2.2), it is clear that, of all the squirring modes, only the first mode B_1 contributes to the swimming speed. From equations (2.3), and (2.4), one also observes that the strongest contribution to the flow field far from the squirmer is due to the second mode B_2 , the flow field due to which decays the slowest, as $1/r^2$. As a consequence, often in Newtonian fluids, the surface velocities are truncated after only the first two modes [165], i.e., $B_n = 0 \forall n > 2$. The ratio $\alpha = B_2/B_1$ decides the type of squirmer [165]. When $\alpha < 0$, the squirmer's centre of thrust is behind its centre of drag, and the squirmer is a pusher-type swimmer. When $\alpha > 0$, the squirmer's centre of thrust is in front of its centre of drag, and the squirmer is a puller-type swimmer. When $\alpha = 0$, the thrust and drag centres coincide, and the squirmer is a neutral-type swimmer. In the absence of any external force, such as weight due to gravity, or torque, the total hydrodynamic force and torque on a squirmer is zero.

Note that both Lighthill [137] and Blake [17] did not consider axisymmetric surface velocities in the azimuthal direction e_ϕ in the squirmer model. These were considered only recently by Pak & Lauga [159], who also provide results for non-axisymmetric squirring motion.

2.2 The fluids

The motion of squirmers, and in general microswimmers, in Newtonian fluids is understood reasonably well [129, 165]. The motivation of this thesis is to understand their dynamics in fluids that are not Newtonian in a ‘standard’ sense; the definition includes not just non-Newtonian fluids, but also Newtonian fluids where the viscosity depends on spatial coordinates due to, for e.g., temperature or concentration gradients. In non-Newtonian fluids, we focus on two common properties, shear-thinning viscosity, and viscoelasticity. Shear-thinning fluids are fluids in which the shear viscosity decreases as applied shear-rates increase. These fluids come under the wider class of generalized Newtonian fluids, for which the deviatoric stress $\boldsymbol{\tau}$

$$\boldsymbol{\tau} = \eta(\dot{\gamma}) \dot{\boldsymbol{\gamma}}, \quad (2.5)$$

where $\eta(\dot{\gamma})$ is the viscosity, and $\dot{\boldsymbol{\gamma}}$ is the strain-rate tensor, and $\dot{\gamma} = \sqrt{\frac{1}{2} \sum_i \sum_j \dot{\gamma}_{ij} \dot{\gamma}_{ji}}$ is the magnitude of the strain-rate tensor [16]. We model shear-thinning viscosity using the Carreau model [16], where

$$\eta(\dot{\gamma}) = \eta_\infty + (\eta_0 - \eta_\infty) \left[1 + \lambda_t^2 |\dot{\gamma}|^2 \right]^{(n-1)/2}. \quad (2.6)$$

Here η_0 is the zero shear-rate viscosity, and η_∞ is the infinite shear-rate viscosity. The parameter λ_t has units of time and gives the strain rate $1/\lambda_t$ at which non-Newtonian effects start becoming important. n is the power law index and is less than 1 for shear-thinning fluids. Note that we do not use the power-law model $\eta = m\dot{\gamma}^{n-1}$, primarily because of the model’s inability to describe viscosities at small strain-rates [16]. The inability can give rise to large errors, even altogether incorrect results, in problems relevant to this thesis (for example, see the discussion of creeping flow around a sphere in shear-thinning fluids by Chhabra [33]).

Viscoelastic fluids show both viscous and elastic properties. Loosely speaking, the response to stress of such fluids is like solids at short times, but as liquids at long times; ‘short’ and ‘long’ are relative to some characteristic timescale of the fluid [150]. Viscoelasticity may be studied under the theory of simple fluids, a lucid description of which can be found in the book by Astarita & Marrucci [5]. The principles that govern simple fluids are determinism of stress, local action, non-existence of a natural state, and fading memory [5]. Determinism of stress means that ‘the stress at a given time is independent of *future deformations*, and only depends on *past deformations*’ [5]. Local action means ‘the stress at a given point is uniquely

2.2. The fluids

determined by the history of deformation of an *arbitrarily small neighborhood* of that material point' [5]. Non-existence of a natural state implies that '*every simple fluid is isotropic*' [5]. Fading memory means 'the influence of past deformations on the present stress is weaker for the distant past than for the recent past' [5]. The principle of fading memory gives rise to the idea of a 'natural time' of the fluid; natural time quantifies the memory span of the material [5]. Natural time is often referred to as the relaxation time.

In this thesis, we study incompressible fluids under two different types of motion, slow flows, and small deformations. In these two types of motions, the general constitutive equation for constant density simple fluids can be expressed as N^{th} order approximations [5]. For slow flows, a general constant density simple fluid at zeroth order is represented by

$$\boldsymbol{\sigma} = -p\mathbf{I}, \quad (2.7)$$

where $\boldsymbol{\sigma}$ is the stress and p is the pressure [5]. Equation (2.7) is the constitutive equation for an incompressible ideal fluid [5]. The first-order approximation gives the constitutive equation for incompressible Newtonian fluids

$$\boldsymbol{\sigma} = -p\mathbf{I} + \eta\dot{\boldsymbol{\gamma}}. \quad (2.8)$$

The popular second-order fluid is the second-order approximation with

$$\boldsymbol{\sigma} = -p\mathbf{I} + \eta_0\dot{\boldsymbol{\gamma}} + \alpha_1\mathbf{A}_2 + \alpha_2\mathbf{A}_1^2, \quad (2.9)$$

where η_0 , α_1 and α_2 are constants, and

$$\begin{aligned} \mathbf{A}_1 &\equiv \mathbf{L} + \mathbf{L}^\top, \\ \mathbf{A}_n &\equiv \frac{D\mathbf{A}_{n-1}}{Dt} + \mathbf{L}^\top\mathbf{A}_{n-1} + \mathbf{A}_{n-1}\mathbf{L}, \end{aligned} \quad (2.10)$$

with $\mathbf{L}^\top = \nabla\mathbf{u}$, and D/Dt representing the material derivative [5, 198]. The term $\alpha_1\mathbf{A}_2$ includes the first effects of memory to an otherwise purely viscous approximation [5]. One can proceed in a similar manner to obtain higher-order approximations (and fluids). In this thesis, we restrict our attention to slow flows of only second-order and third-order fluids.

Under small deformations, say, realized with oscillations of small amplitude of some fluid boundary, simple fluids of constant density at the first-order approximation are represented as

$$\boldsymbol{\sigma} = -p\mathbf{I} + \int_0^\infty f(s)\mathbf{G}^t ds, \quad (2.11)$$

2.3. The reciprocal theorem

where \mathbf{G}^t is the Cauchy strain tensor, and s is the time lag; distant past corresponds to large values of s , recent past to small values of s [5]. Equation (2.11) is the constitutive equation for a linearly viscoelastic fluid. The second-order approximation gives

$$\begin{aligned} \boldsymbol{\sigma} = & -p\mathbf{I} + \int_0^\infty f(s) \mathbf{G}^t ds + \\ & \int_0^\infty \int_0^\infty \left\{ \alpha(s_1, s_2) \mathbf{G}^t(s_1) \cdot \mathbf{G}^t(s_2) + \beta(s_1, s_2) \text{tr} \left[\mathbf{G}^t(s_1) \right] \mathbf{G}^t(s_2) \right\} ds_1 ds_2, \end{aligned} \quad (2.12)$$

where functions $f()$, $\alpha()$ and $\beta()$ depend on the fluid [5]. Details of using equation (2.12) for problems involving oscillating boundaries can be found in the pedagogical description by Böhme [18].

It is to be noted that many viscoelastic models that adequately represent experimental results, and are obtained using kinetic theory of polymers do not come under the umbrella of simple fluids ('equations ...[that] do not allow strain impulses are not included in the general theory of simple fluids with fading memory' [5]). One example is an Oldroyd-B fluid [150]

$$\boldsymbol{\tau} + \lambda \overset{\nabla}{\boldsymbol{\tau}} = \eta \left(\dot{\boldsymbol{\gamma}} + \lambda_r \overset{\nabla}{\dot{\boldsymbol{\gamma}}} \right) \quad (2.13)$$

where the total viscosity $\eta = \eta_s + \eta_p$ is the sum of viscosity of the Newtonian solvent and that due to the polymer contribution. λ is the Maxwell relaxation time, and the retardation time $\lambda_r = \lambda(\eta_s/\eta)$. Other common useful models like FENE-P and Giesekus are not simple fluids either. However, we note that, for flows that are slow or due to small deformations, such models give *qualitatively* the same constitutive relations as one would obtain using equations (2.9) and (2.12), respectively, up to at least the first effects of non-linear rheology.

2.3 The reciprocal theorem

In this thesis, we extensively use the Lorentz reciprocal theorem [93] to obtain results for motion of particles in complex fluids. The form of the theorem for complex fluids has been discussed by Leal [133] for passive particles, and by Lauga [125] for active particles. The formulation below is that of Elfring & Lauga [70], and Elfring [68].

We consider the motion of a particle \mathcal{B} , with surface $\partial\mathcal{B}$,

$$\mathbf{u}(\mathbf{x} \in \partial\mathcal{B}) = \mathbf{U} + \boldsymbol{\Omega} \times \mathbf{x} + \mathbf{u}^S, \quad (2.14)$$

2.3. The reciprocal theorem

in a complex fluid, which is expressed in the form

$$\boldsymbol{\tau} = \eta \dot{\boldsymbol{\gamma}} + \boldsymbol{\tau}_{NN}, \quad (2.15)$$

where the deviatoric stress $\boldsymbol{\tau}$ is written as a sum of ‘Newtonian’ and ‘non-Newtonian’ terms. Non-linearities of the constitutive equation are embedded in $\boldsymbol{\tau}_{NN}$. η represents ‘some’ viscosity of the fluid, $\dot{\boldsymbol{\gamma}}$ is the strain-rate. \mathbf{U} and $\boldsymbol{\Omega}$ are the unknown translational and angular velocities of the particle, respectively, and \mathbf{u}^S represents the prescribed (known) surface velocities on the particle. If the particle is passive, $\mathbf{u}^S = 0$. For the purpose of the derivation here, we consider the particle to be in an otherwise quiescent fluid. The calculation of velocities \mathbf{U} and $\boldsymbol{\Omega}$, if not for the reciprocal theorem, requires solving the Stokes equation (for velocity and pressure fields, \mathbf{u} and p , respectively) with the constitution equation (2.15), and the relevant boundary conditions. Solving for the flow fields in complex fluids analytically is, in general, difficult. The reciprocal theorem provides a shortcut to obtaining \mathbf{U} and $\boldsymbol{\Omega}$, if the solution for the same geometry is known in a Newtonian fluid (or precisely, the resistance or mobility matrices for the geometry are known in a Newtonian fluid [70]). Consider a passive particle, of the same shape as the particle in complex fluid, in an otherwise quiescent Newtonian fluid with viscosity $\hat{\eta}$, i.e.,

$$\hat{\mathbf{u}}(\mathbf{x} \in \partial\mathcal{B}) = \hat{\mathbf{U}} + \hat{\boldsymbol{\Omega}} \times \mathbf{x}. \quad (2.16)$$

The hat quantities represent quantities in Newtonian fluids, and are known. We know that at zero Reynolds number

$$\nabla \cdot \boldsymbol{\sigma} = \nabla \cdot \hat{\boldsymbol{\sigma}} = 0, \quad (2.17)$$

where $\boldsymbol{\sigma}$ and $\hat{\boldsymbol{\sigma}}$ represent the stress in the two fluids. Equation (2.17) is used, rather straightforwardly, to write the reciprocal relation

$$\hat{\mathbf{u}} \cdot (\nabla \cdot \boldsymbol{\sigma}) = \mathbf{u} \cdot (\nabla \cdot \hat{\boldsymbol{\sigma}}) = 0. \quad (2.18)$$

Equation (2.18) can be rewritten, making use of the fact that the stress tensor is symmetric, as

$$\nabla \cdot (\boldsymbol{\sigma} \cdot \hat{\mathbf{u}}) - \boldsymbol{\sigma} : \nabla \hat{\mathbf{u}} = \nabla \cdot (\hat{\boldsymbol{\sigma}} \cdot \mathbf{u}) - \hat{\boldsymbol{\sigma}} : \nabla \mathbf{u} = 0. \quad (2.19)$$

Incompressibility of the fluids demands

$$-p\mathbf{I} : \nabla \hat{\mathbf{u}} = -p\nabla \cdot \hat{\mathbf{u}} = 0, \quad (2.20)$$

$$-\hat{p}\mathbf{I} : \nabla \mathbf{u} = -\hat{p}\nabla \cdot \mathbf{u} = 0, \quad (2.21)$$

2.3. The reciprocal theorem

so that equation (2.19) simplifies to

$$\nabla \cdot (\boldsymbol{\sigma} \cdot \hat{\mathbf{u}}) - \eta \hat{\boldsymbol{\gamma}} : \nabla \hat{\mathbf{u}} - \boldsymbol{\tau}_{NN} : \nabla \hat{\mathbf{u}} = \nabla \cdot (\hat{\boldsymbol{\sigma}} \cdot \mathbf{u}) - \hat{\eta} \hat{\boldsymbol{\gamma}} : \nabla \mathbf{u} = 0, \quad (2.22)$$

on replacing $\boldsymbol{\sigma} = -p\mathbf{I} + \boldsymbol{\tau}$ and $\boldsymbol{\tau} = \eta \hat{\boldsymbol{\gamma}} + \boldsymbol{\tau}_{NN}$ (2.15). From the property of a symmetric tensor in a doubly contracted product, we have

$$\hat{\boldsymbol{\gamma}} : \nabla \mathbf{u} = \hat{\boldsymbol{\gamma}} : \nabla \hat{\mathbf{u}}. \quad (2.23)$$

Using equation (2.23) in the right half of (2.22), and then substituting for the doubly contracted product in the left half gives

$$\nabla \cdot (\boldsymbol{\sigma} \cdot \hat{\mathbf{u}}) - \frac{\eta}{\hat{\eta}} \nabla \cdot (\hat{\boldsymbol{\sigma}} \cdot \mathbf{u}) - \boldsymbol{\tau}_{NN} : \nabla \hat{\mathbf{u}} = 0. \quad (2.24)$$

Taking integral of equation (2.24) over the entire fluid volume, and using the divergence theorem, we get

$$\int_S \mathbf{n} \cdot \boldsymbol{\sigma} \cdot \hat{\mathbf{u}} \, dS - \frac{\eta}{\hat{\eta}} \int_S \mathbf{n} \cdot \hat{\boldsymbol{\sigma}} \cdot \mathbf{u} \, dS + \int_{\mathcal{V}} \boldsymbol{\tau}_{NN} : \nabla \hat{\mathbf{u}} \, dV = 0, \quad (2.25)$$

where n points inside the fluid volume, the surface \mathcal{S} includes the surface of the particle and the bounding surface at infinity, and \mathcal{V} is the fluid volume. For sufficiently fast spatial decay of the integrands above, the surface integrals at infinity do not contribute—this is indeed the case for problems that we consider in the thesis. Neglecting the surface integral at infinity and substituting for surface velocities from equations (2.14) and (2.16), we get

$$\mathbf{F} \cdot \hat{\mathbf{U}} + \mathbf{L} \cdot \hat{\boldsymbol{\Omega}} - \frac{\eta}{\hat{\eta}} \left(\hat{\mathbf{F}} \cdot \mathbf{U} + \hat{\mathbf{L}} \cdot \boldsymbol{\Omega} + \int_{\partial B} \mathbf{n} \cdot \hat{\boldsymbol{\sigma}} \cdot \mathbf{u}^S \, dS \right) + \int_{\mathcal{V}} \boldsymbol{\tau}_{NN} : \nabla \hat{\mathbf{u}} \, dV = 0, \quad (2.26)$$

where \mathbf{F} and $\hat{\mathbf{F}}$, and \mathbf{L} and $\hat{\mathbf{L}}$ represent the total hydrodynamic forces and torques, respectively, on the particles. Using the linearity of the Stokes equations in Newtonian fluids, we write, for compactness, $\hat{\mathbf{u}} = \hat{\mathbf{G}}_U \cdot \hat{\mathbf{U}}$, $\hat{\boldsymbol{\sigma}} = \hat{\mathbf{T}}_U \cdot \hat{\mathbf{U}}$, and $\hat{\mathbf{F}} = -\hat{\mathbf{R}}_{FU} \cdot \hat{\mathbf{U}}$, where $\hat{\mathbf{U}} = [\hat{\mathbf{U}} \ \hat{\boldsymbol{\Omega}}]^\top$, and $\hat{\mathbf{F}} = [\hat{\mathbf{F}} \ \hat{\boldsymbol{\Omega}}]^\top$, and consequently, $\hat{\mathbf{G}}_U$, and $\hat{\mathbf{T}}_U$ are linear operators that map the particle velocity $\hat{\mathbf{U}}$ to the velocity and the stress fields, respectively, whereas the resistance tensor

$$\hat{\mathbf{R}}_{FU} = \begin{bmatrix} \hat{\mathbf{R}}_{FU} & \hat{\mathbf{R}}_{F\Omega} \\ \hat{\mathbf{R}}_{LU} & \hat{\mathbf{R}}_{L\Omega} \end{bmatrix} \quad (2.27)$$

2.3. The reciprocal theorem

links $\hat{\mathbf{U}}$ to the hydrodynamic force and torque on the particle. Rewriting equation (2.26), we get

$$\mathbf{F} \cdot \hat{\mathbf{U}} - \frac{\eta}{\hat{\eta}} \left(\hat{\mathbf{F}} \cdot \mathbf{U} + \int_{\partial\mathcal{B}} \mathbf{n} \cdot \mathbf{u}^S \cdot (\hat{\mathbf{T}}_U \cdot \hat{\mathbf{U}}) \, dS \right) + \int_{\mathcal{V}} \boldsymbol{\tau}_{NN} : \boldsymbol{\nabla} (\hat{\mathbf{G}}_U \cdot \hat{\mathbf{U}}) \, dV = 0, \quad (2.28)$$

which on rearranging terms, cancellation of the arbitrary $\hat{\mathbf{U}}$ on both sides, and using the symmetry of the resistance tensor [93], gives

$$\mathbf{U} = \frac{\hat{\eta}}{\eta} \hat{\mathbf{R}}_{FU}^{-1} \cdot [-\mathbf{F} + \mathbf{F}_T + \mathbf{F}_{NN}], \quad (2.29)$$

where

$$\mathbf{F}_T = \frac{\eta}{\hat{\eta}} \int_{\partial\mathcal{B}} \mathbf{u}^S \cdot (\mathbf{n} \cdot \hat{\mathbf{T}}_U) \, dS, \quad (2.30)$$

is a Newtonian ‘thrust’ due to the surface velocity \mathbf{u}^S , and \mathbf{F}_{NN} is the non-Newtonian contribution (or contribution due to any deviation from Newtonian fluids of uniform viscosity) given by

$$\begin{aligned} \mathbf{F}_{NN} &= - \int_{\mathcal{V}} \boldsymbol{\tau}_{NN} : \boldsymbol{\nabla} \hat{\mathbf{G}}_U \, dV, \\ &= - \int_{\mathcal{V}} \boldsymbol{\tau}_{NN} : \hat{\mathbf{E}}_U \, dV, \end{aligned} \quad (2.31)$$

where $\hat{\mathbf{E}}_U$ is defined as $\hat{\boldsymbol{\gamma}}/2 = \hat{\mathbf{E}}_U \cdot \hat{\mathbf{U}}$. The equivalence in (2.31) comes from using the property of the doubly contracted product when one of tensors is symmetric (here, $\boldsymbol{\tau}_{NN}$) and noting that $\hat{\mathbf{E}}_U$ is the symmetric part (for inner indices) of $\boldsymbol{\nabla} \hat{\mathbf{G}}_U$.

One may easily extend the above derivation to include cases with particles in a background flow [44, 68, 133]. Equation (2.29) is then formulated in terms of disturbance quantities [68], and will be seen in Chapter 4. Note that in the formulation of equation (2.29) as a mobility problem, \mathbf{F}_{NN} as of yet is unknown, since $\boldsymbol{\tau}_{NN}$ has not been calculated in the fluid. Avoiding its calculation was the very reason to use the reciprocal theorem. However, as will become clear in the following chapters, asymptotic analysis in some small parameter, allows one to evaluate $\boldsymbol{\tau}_{NN}$ from the solution in a ‘standard’ Newtonian fluid.

Chapter 3

Swimming in viscosity gradients

Microswimmers swimming in mucus layers and biofilms experience spatial gradients of viscosity. We model the swimmers using the squirmer model, and show how the effects of viscosity gradients on the swimmer motion, leading to the phenomenon of viscotaxis, depend on the swimming gait of the swimmers. We also show how such gradients in viscosity may be used to sort swimmers based on their swimming style.

3.1 Introduction

Cells often swim in environments, such as biofilms and mucus layers, that have spatial gradients of viscosity [194, 211]. Much like the effect of other gradients, such as light (leading to phototaxis [14]), chemical stimuli (chemotaxis [15]), magnetic fields (magnetotaxis [206]), temperature (thermotaxis [7]), or gravitational potential (gravitaxis [176]), gradients of viscosity can lead to viscotaxis in microswimmers. Bacteria like *Leptospira* and *Spiroplasma* are known to move up the viscosity gradients (positive viscotaxis) [41, 196], where as *Escherichia coli* demonstrates negative viscotaxis [182]. It is suggested that viscotaxis plays an adaptive role in microorganisms; it prevents them from being stuck in regions where they are poor swimmers [41, 182, 196]. This migration across regions of different viscosity affects organisms' population distribution, and possibly their virulence [167]. The aggregation of microswimmers in specific regions of viscosity may also be used for sorting of cells [214].

In a recent work, Liebchen *et al.* [136] studied the physical mechanism of viscotaxis. Using assemblies of one, two and three spheres as model swimmers, they showed how viscotaxis can emerge from a mismatch of viscous forces on different parts of the swimmer, thereby demonstrating the possibility of both positive and negative viscotaxis. In this work, we study viscotaxis using a general model to study microswimmers—the squirmer model

[17, 137, 165]. Squirmers can be used to model different types of swimmers within the same theoretical framework, and have been used in understanding swimming at small scales in both Newtonian (e.g., see [165] and references within) and non-Newtonian fluids (e.g., [44, 45, 51, 122, 135, 217]). The squirmer model allows us to study the response of different classes of microswimmers, namely, pushers, pullers and neutral swimmers, to spatial gradients in viscosity. We find that the three types of swimmers behave differently in viscosity gradients, and their different swimming dynamics can be used to sort them based on their swimming style.

We present the theoretical formulation of the problem in the next section, followed by a section on results and discussion, where we briefly discuss how viscotaxis may be used as an effective mechanism for sorting cells.

3.2 Theoretical formulation

We model the microswimmers as spherical squirmers [137]. As a squirmer, a microswimmer is represented as a sphere with some prescribed surface velocity; the surface velocity approximates the detailed propulsion mechanism of the swimmer [137]. We consider axisymmetric squirmers with steady tangential surface velocities ($\mathbf{u}^S = u^s \mathbf{e}_\theta$),

$$u^S = \sum_{l=1}^{\infty} B_l V_l(\theta), \quad (3.1)$$

where $V_l(\theta) = -2P_l^1(\cos\theta)/(l(l+1))$ with P_l^1 being the associated Legendre function of the first kind and θ the polar angle measured with the axis of symmetry [17, 137]. The coefficients B_l are called the squirming modes. In Newtonian fluids, the propulsion velocity of the squirmer is due to just the first mode B_1 , whereas B_2 gives the strongest contribution to the flow far from the swimmer [17, 101]. For swimmers that generate thrust from the front, the puller type (like *Chlamydomonas*), the ratio $\alpha = B_2/B_1$ is greater than zero, and for those that generate thrust from the rear (like *Escherichia coli*), $\alpha < 0$. Swimmers in which the thrust and drag centres coincide are modelled with $\alpha = 0$ and are called neutral squirmers. Pak & Lauga [159] provide a detailed description of general, non-axisymmetric, squirming modes.

We consider fluids which have spatial gradients of viscosity. These gradients may arise due to temperature or due to gradients in the concentration of solute in real systems. In order to study swimming in such fluids theoretically, we consider only small variations in viscosity, representing the viscosity field as $\eta(\mathbf{x}) = \eta_0 + \varepsilon\delta\eta(\mathbf{x})$. Here ε is a small dimensionless parameter.

3.2. Theoretical formulation

In physical terms, with this form of viscosity field, we have assumed that the deviations in viscosity on the scale of the particle are small i.e., $\mathcal{O}(\varepsilon)$, where $\varepsilon = a/L$, a being the length scale of the particle, and L is some length over which the viscosity changes are considerable ($\mathcal{O}(1)$). Our considerations of only small variations in viscosity are in the spirit of the recent work by Oppenheimer *et al.* [157], who also consider small viscosity variations due to the temperature difference between the swimmer and its surroundings. The novelty of the present work lies in the fact that the viscosity variations are externally imposed and are independent of the swimmer or its position. The small viscosity variations, of $\mathcal{O}(\varepsilon)$, allow us to obtain the first effects of viscosity gradients on the swimmer motion with the relative ease of using the reciprocal theorem of low Reynolds number flows [93]. We primarily consider two types of gradients, $\nabla(\delta\eta(\mathbf{x})/\eta_0) \sim \mathbf{e}_x$ (or a similar form), and $\nabla(\delta\eta(\mathbf{x})/\eta_0) \sim \mathbf{e}_r$. We term the former as a linear gradient, and the latter as radial.

Note that we neglect any fluid and solid body inertia, and study the microswimmers at zero Reynolds number. Next, we give details of the reciprocal theorem formulation.

3.2.1 Reciprocal theorem

The velocity of a particle in complex fluids (or in fluids that show any deviation from Newtonian fluids with uniform viscosity) is given by

$$\mathbf{U} = \frac{\hat{\eta}}{\eta} \hat{\mathbf{R}}_{FU}^{-1} \cdot [-\mathbf{F} + \mathbf{F}_T + \mathbf{F}_{NN}], \quad (3.2)$$

where $\mathbf{U} = [\mathbf{U} \ \boldsymbol{\Omega}]^\top$ is a six-dimensional vector comprising of rigid-body translational and rotational velocities. The expression (3.2) is obtained using the reciprocal theorem of low Reynolds number flows [93] and its formulation as described in [43, 68].

$$\mathbf{F}_T = \frac{\eta}{\hat{\eta}} \int_{\partial\mathcal{B}} \mathbf{u}^S \cdot (\mathbf{n} \cdot \hat{\mathbf{T}}_U) dS \quad (3.3)$$

represents the Newtonian ‘thrust’ due to any surface deformation or activity \mathbf{u}^S of the particle. Here $\partial\mathcal{B}$ represents the surface of the particle. The non-Newtonian contribution or, pertinent to present work, the contribution due to any deviation from uniform viscosity in Newtonian fluids,

$$\mathbf{F}_{NN} = - \int_{\mathcal{V}} \boldsymbol{\tau}_{NN} : \hat{\mathbf{E}}_U dV, \quad (3.4)$$

3.2. Theoretical formulation

represents the extra force/torque on the particle due to the non-Newtonian deviatoric stress $\boldsymbol{\tau}_{NN}$ in the fluid volume \mathcal{V} in which the particle is immersed; the total deviatoric stress in the fluid is $\boldsymbol{\tau} = \eta_0 \dot{\boldsymbol{\gamma}} + \boldsymbol{\tau}_{NN}$. $\mathbf{F} = [\mathbf{F} \ \mathbf{L}]^\top$ represents the total hydrodynamic force and torque on the particle; in the absence of any external force, $\mathbf{F} = \mathbf{0}$ for a squirmer. The hat quantities are operators from the resistance/mobility problem in a Newtonian fluid (with viscosity $\hat{\eta}$)

$$\hat{\boldsymbol{\gamma}}/2 = \hat{\mathbf{E}}_U \cdot \hat{\mathbf{U}}, \quad (3.5)$$

$$\hat{\boldsymbol{\sigma}} = \hat{\mathbf{T}}_U \cdot \hat{\mathbf{U}}, \quad (3.6)$$

$$\hat{\mathbf{F}} = -\hat{\mathbf{R}}_{FU} \cdot \hat{\mathbf{U}}, \quad (3.7)$$

obtained for the present case of spherical squirmers from the motion of a single sphere in an unbounded and otherwise quiescent Newtonian fluid.

3.2.2 Asymptotic analysis

The viscosity field in the present work is represented as $\eta(\mathbf{x}) = \eta_0 + \varepsilon \delta\eta(\mathbf{x})$. To study the effect of small viscosity variations, quantified by ε , we expand flow quantities in a regular perturbation expansion of ε , e.g.,

$$\{\mathbf{u}, p, \boldsymbol{\tau}\} = \{\mathbf{u}_0, p_0, \boldsymbol{\tau}_0\} + \varepsilon \{\mathbf{u}_1, p_1, \boldsymbol{\tau}_1\} + \varepsilon^2 \{\mathbf{u}_2, p_2, \boldsymbol{\tau}_2\} + \dots, \quad (3.8)$$

where $\{\mathbf{u}_0, p_0, \boldsymbol{\tau}_0\}$ are velocity, pressures and deviatoric stress solutions to the Stokes equations with uniform viscosity η_0 . At the leading order,

$$\boldsymbol{\tau}_0 = \eta_0 \dot{\boldsymbol{\gamma}}_0, \quad (3.9)$$

and at $\mathcal{O}(\varepsilon)$,

$$\boldsymbol{\tau}_1 = \eta_0 \dot{\boldsymbol{\gamma}}_1 + \delta\eta(\mathbf{x}) \dot{\boldsymbol{\gamma}}_0, \quad (3.10)$$

and therefore, $\boldsymbol{\tau}_{NN,1} = \delta\eta(\mathbf{x}) \dot{\boldsymbol{\gamma}}_0$. We consider corrections up to $\mathcal{O}(\varepsilon)$ in this work. Note that the expansion is regular only for $\delta\eta(\mathbf{x}) \sim \mathcal{O}(1)$; for linear gradients of the form $\delta\eta(\mathbf{x}) \sim x$, the expansion is regular only for $x \sim o(1/\varepsilon)$. The evaluation of the volume integral in equation (3.4), for effects of non-*standard* Newtonian rheology on the particle, then, in principle, requires singular perturbation methods. In the next section, we see how the far field contribution from the viscosity gradients that we choose does not affect the answers obtained from the regular expansion of the form in equation (3.8).

3.2.3 Remarks on the asymptotic analysis

The extra force and torque on a particle due viscosity gradients, up to $\mathcal{O}(\varepsilon)$, are given by

$$\begin{aligned}\mathbf{F}_{NN,1} &= \int_{\mathcal{V}} \delta\eta(\mathbf{x}) \dot{\gamma}_0 : \hat{\mathbf{E}}_U dV, \\ \mathbf{L}_{NN,1} &= \int_{\mathcal{V}} \delta\eta(\mathbf{x}) \dot{\gamma}_0 : \hat{\mathbf{E}}_\Omega dV.\end{aligned}\tag{3.11}$$

For a squirmer in linear or radial viscosity variations, $\delta\eta(\mathbf{x}) \sim r$, the far field contribution, from distances $r \sim \mathcal{O}(1/\varepsilon)$, to the extra force in (3.11) is $\mathcal{O}(r \cdot r^{-3} \cdot r^{-2} \cdot r^3) = \mathcal{O}(\varepsilon)$, to torque is $\mathcal{O}(r \cdot r^{-3} \cdot r^{-3} \cdot r^3) = \mathcal{O}(\varepsilon^2)$, and therefore, can be neglected as we consider corrections to Newtonian (uniform viscosity) motion up to only $\mathcal{O}(\varepsilon)$.

As the velocity field due to motion of a passive sphere decays slower compared to that of a squirmer, in principle, one needs to use a singular perturbation approach to evaluate integrals in (3.11). However, for a passive sphere in linear viscosity profiles, the far-field contribution to the integrals at $\mathcal{O}(1)$ is identically zero (due to symmetry), and therefore, such systems may be studied using the regular perturbation scheme. However, for radial profiles, the $\mathcal{O}(1)$ contribution is non-zero and one then needs a singular perturbation approach.

3.3 Results and discussion

Below, we show results for the motion of squirmers in such small viscosity gradients as discussed; our focus is on gradients that are externally imposed and do not depend on the squirmers' positions. We begin by looking at a passive sphere.

3.3.1 Passive sphere

The hydrodynamic force \mathbf{F} and torque \mathbf{L} on a rigid sphere of radius a moving with a velocity \mathbf{U} and rotating with an angular velocity $\boldsymbol{\Omega}$ in a linear viscosity field, e.g., $\delta\eta(\mathbf{x}) \sim x$, is given by, up to $\mathcal{O}(\varepsilon)$,

$$\mathbf{F} = -6\pi a\eta_0\mathbf{U} - 2\pi\varepsilon a^3\boldsymbol{\Omega} \times \nabla\delta\eta,\tag{3.12}$$

$$\mathbf{L} = -8\pi\eta_0 a^3\boldsymbol{\Omega} + 2\pi\varepsilon a^3\mathbf{U} \times \nabla\delta\eta.\tag{3.13}$$

Note that the gradient in viscosity couples the force with the sphere's angular velocity, and the torque with the translational velocity; this is not the

case for a sphere in a Newtonian fluid with uniform viscosity. As discussed previously, we cannot study a passive sphere in radial gradients using a regular perturbation of the form in (3.8).

When the gradients in viscosity are due to the particle itself, as in the study of Oppenheimer *et al.* [157] where the particle is hot compared to its surroundings and the viscosity depends on temperature such that $\delta\eta(\mathbf{x}) = -a\eta_0/r$, the origin being the centre of the particle, we can reproduce their results using equations (3.11) to get

$$\mathbf{F} = -6\pi\eta_0a \left(1 - \frac{5\varepsilon}{12}\right) \mathbf{U}, \quad (3.14)$$

$$\mathbf{L} = -8\pi\eta_0a^3 \left(1 - \frac{3\varepsilon}{4}\right) \boldsymbol{\Omega}. \quad (3.15)$$

It should be noted that in this case the translational and rotational motion are not coupled—because of the symmetry of the gradient—and both the drag and the torque are lower than those for the case of constant viscosity η_0 .

These results for a passive sphere will be useful to contrast the results obtained for spherical squirmers.

3.3.2 Squirmer

The exact expressions for translational and angular velocities of squirmers can be obtained in linear viscosity profiles such as $\delta\eta(\mathbf{x}) \sim x$. These are, up to $\mathcal{O}(\varepsilon)$,

$$\mathbf{U} = \frac{2B_1}{3}\mathbf{e} + \varepsilon\frac{3aB_2}{5\eta_0} \left(\mathbf{e}\mathbf{e} - \frac{\mathbf{I}}{3}\right) \cdot \nabla\delta\eta, \quad (3.16)$$

$$\boldsymbol{\Omega} = \varepsilon B_1 \frac{\nabla\delta\eta}{\eta_0} \times \mathbf{e}, \quad (3.17)$$

where \mathbf{e} is the orientation of the squirmer. Note that the gradient in viscosity affects both the angular and translational velocities of the squirmer; even an axisymmetric squirmer can now rotate due to its own motion. In a Newtonian fluid with uniform viscosity, $\mathbf{U}_N = (2B_1/3)\mathbf{e}$ and $\boldsymbol{\Omega}_N = \mathbf{0}$. The rotation of the squirmer is in the opposite sense to that of a passive sphere dragged along the same direction in the same gradient. This can be understood by decomposing the swimming problem into a thrust problem and a drag problem [45]. In the thrust problem, the squirmer is held fixed and the thrust due to its surface velocity is calculated. In the drag problem,

3.3. Results and discussion

the drag on a passive sphere translating with the velocity of the swimmer is calculated. Here, one finds that for a squirmer, the thrust contribution is opposite and dominating to the drag contribution. Therefore, the squirmer rotates in a direction opposite to that of a passive sphere. Also note that of all squirring modes B_l , only the first two contribute to velocities in the linear gradients considered here.

In the case where the viscosity field due to the squirmer is radially increasing, (in the spirit of [157] where the viscosity field varies radially due to the temperature of the particle), choosing $\delta\eta(\mathbf{x}) = -a\eta_0/r$ where r is measured from the origin at the centre of the squirmer, the translational velocity of the squirmer is given by

$$\mathbf{U} = \frac{2B_1}{3} \left(1 - \frac{\varepsilon}{12}\right) \mathbf{e}, \quad (3.18)$$

i.e., a squirmer swimming in thin shells of radially increasing viscosities around it swims slower than in a Newtonian fluid with uniform viscosity. The thrust and drag decomposition of the swimming problem shows that the viscosity gradient leads to decrease in both the thrust and the drag, but the decrease in the thrust is more pronounced than the drag leading to a slower swimming [45]. The angular velocity of the squirmer is zero in this case because of the symmetry of the problem.

The expressions in (3.16) and (3.17) allow studying the trajectories of squirmers in viscosity gradients. To do so, we first non-dimensionalise the equations; we scale lengths with the swimmer radius a , velocities with the first squirring mode B_1 , and stresses with $\eta_0 B_1/a$. Equations (3.16) and (3.17) then become

$$\mathbf{U} = \frac{2}{3} \mathbf{e} + \varepsilon \frac{3\alpha}{5} \left(\mathbf{e}\mathbf{e} - \frac{\mathbf{I}}{3} \right) \cdot \nabla \delta\eta, \quad (3.19)$$

$$\mathbf{\Omega} = \varepsilon \nabla \delta\eta \times \mathbf{e}, \quad (3.20)$$

and henceforth, all quantities are dimensionless unless stated otherwise. From equations (3.19) and (3.20), we note that as the swimmer moves along the gradient i.e. $\mathbf{e} = \nabla \delta\eta / |\nabla \delta\eta|$, it does not rotate ($\mathbf{\Omega} = 0$), and therefore maintains its original orientation. Depending on its type of propulsion, and consequently, on the sign of α , it can swim faster, slower or at the same speed as in a Newtonian fluid with uniform viscosity. Pusher swimmers ($\alpha < 0$) swim slower, as their thrust generation is from the rear which, when moving along the gradient, is in a fluid less viscous than that in the front. Pullers ($\alpha > 0$), on the contrary, swim faster. Neutral swimmers ($\alpha = 0$), which

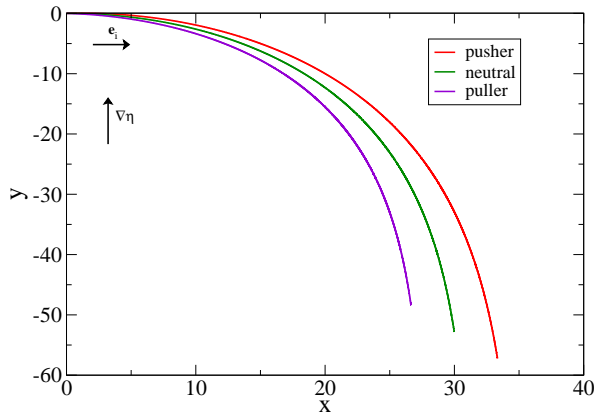


Figure 3.1: The initial orientation of the swimmers $e_{initial}$ is along the positive x-axis. The viscosity gradient is along the positive y-axis. After some time all swimmers swim antiparallel to the viscosity gradient. Note that in this orientation, pushers are the fastest, while pullers are the slowest. The trajectories are plotted for time $t = 0$ to $t = 100$.

have the drag and thrust centres coinciding, swim with the Newtonian speed. The dynamics for pullers and pushers reverses when $e = -\nabla\delta\eta/|\nabla\delta\eta|$.

When the gradient in viscosity is not aligned with the swimmer direction, irrespective of the type of propulsion, squirmers show viscopobicity (negative viscotaxis). They rotate in the direction of lower viscosity. We demonstrate this in figure 3.1, where we consider motion of squirmers only in the plane of viscosity gradients. We consider $\alpha = 0$ for neutral squirmers, $\alpha = 2$ and $\alpha = -2$ for pullers and pushers, respectively, and $\varepsilon = 0.1$. For $\nabla\delta\eta(\mathbf{x})$ parallel to e_y and the initial orientation of swimmers in the positive x-direction, as shown in figure 3.1, the final equilibrium orientation for all the swimmers is antiparallel to the viscosity gradient; however, the trajectories chosen to attain the equilibrium orientation do depend on the type of swimmer. In this equilibrium orientation, as discussed previously, pushers swim the fastest and pullers the slowest. Note that the viscopobicity as demonstrated here can be understood using the thrust and drag decomposition [45]; on the decomposition one finds that the effect of the gradient on the thrust is dominant to that on the drag.

For the same values of α and ε , we also plot trajectories of squirmers mov-

3.3. Results and discussion

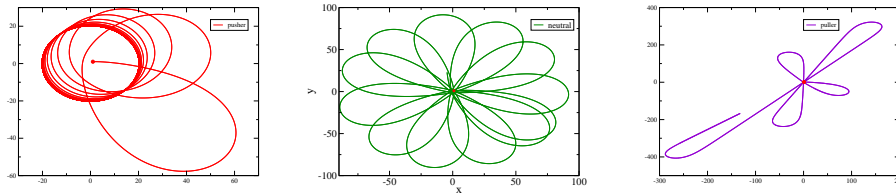


Figure 3.2: Planar trajectories of pushers (left), neutral swimmers (centre), and pullers (right). The initial position of the swimmers, $(x = 1, y = 1)$, is marked by the red dot. The swimmers originally point in the positive x -axis. The swimmers are in a radial viscosity gradient: viscosity increases radially outward from the point $(0, 0)$, $\delta\eta = \sqrt{x^2 + y^2}$. Pushers find a stable orbit. The trajectory of neutral swimmers is bounded at long times. Pullers perform ‘unstable’ motion about the ‘origin’ of viscosity gradient. Note the farthest the swimmers have travelled from this origin after equal times ($t = 4000$).

ing in the plane of radially varying planar viscosity field, $\delta\eta(\mathbf{x}) = \sqrt{x^2 + y^2}$, where the coordinates x and y are measured from an arbitrary point in space which may be seen as a ‘viscosity sink’. It should be noted that we still use expressions (3.19) and (3.20) to calculate the trajectories; we are in want of exact expressions for radial gradients of such types. Although the expressions have been derived only for linear gradients, they are expected to hold for radial gradients as well, for at the scale of the particle, little difference should exist between the two. The trajectories are plotted in figure 3.2. Note the qualitatively different behaviour of the three types of swimmers. The dynamics is discussed in more detail below.

On trajectories of squirmers in radial gradients

The two-dimensional motion of squirmers in the radial gradient discussed above is easier to study with the orientation vector \mathbf{e} represented as $\{\cos \phi, \sin \phi\}$, and the gradient viscosity vector for $\delta\eta(\mathbf{x}) = \sqrt{x^2 + y^2}$, as $\nabla\delta\eta = \{\cos \theta, \sin \theta\}$, where ϕ and θ are measured with the x -axis. Equations (3.19) and (3.20) then become

$$\frac{d\psi}{dt} = \frac{1}{3}\varepsilon \sin \psi - \frac{1}{r} \left(\frac{2}{3} \sin \psi + \frac{3}{10}\varepsilon\alpha \sin 2\psi \right), \quad (3.21)$$

$$\frac{dr}{dt} = \frac{2}{3} \cos \psi + \frac{3}{5}\varepsilon\alpha \left(\frac{2}{3} - \sin^2 \psi \right), \quad (3.22)$$

3.4. Conclusion

where $\psi = \phi - \theta$ and $r = \sqrt{x^2 + y^2}$. For steady state, $\dot{\psi} = 0$, $\dot{r} = 0$, and therefore, when $\alpha \neq 0$, we have

$$r_{eq} = \frac{1}{\varepsilon} \left(2 + \frac{9}{5} \varepsilon \alpha \cos \psi_{eq} \right), \quad (3.23)$$

$$\psi_{eq} = \cos^{-1} \left(-\frac{5}{9\varepsilon\alpha} \left[1 \pm \sqrt{1 + \frac{27\varepsilon^2\alpha^2}{25}} \right] \right). \quad (3.24)$$

When $\alpha = 0$, at equilibrium, we have $\psi_{eq} = \frac{\pi}{2}$ and $r_{eq} = \frac{2}{\varepsilon}$. With $\varepsilon = 0.1$, for $\alpha = \pm 2$ (values for pusher and pullers), we obtain $r_{eq} = 20.21$ and $\psi_{eq} = 1.5114$. For neutral swimmers, $\alpha = 0$, $r_{eq} = 20$ and $\psi_{eq} = \pi/2$.

We study linear stability of the equilibrium values by Taylor expanding equations (3.21) and (3.22) and obtaining

$$\frac{dr'}{dt} = \left(-\frac{2}{3} \sin \psi_{eq} - \frac{3}{5} \varepsilon \alpha \sin 2\psi_{eq} \right) \psi' \quad (3.25)$$

$$\begin{aligned} \frac{d\psi'}{dt} = & \frac{1}{3} \varepsilon (\psi' \cos \psi_{eq}) + \frac{r'}{r_{eq}^2} \left(\frac{2}{3} \sin \psi_{eq} + \frac{3}{10} \varepsilon \alpha \sin 2\psi_{eq} \right) \\ & - \frac{1}{r_{eq}} \left(\frac{2}{3} \psi' \cos \psi_{eq} + \frac{3}{10} \varepsilon \alpha \psi' 2 \cos 2\psi_{eq} \right), \end{aligned} \quad (3.26)$$

where dashed quantities represent small fluctuations from the equilibrium values. We find that for pushers, the equilibrium is a stable spiral, while for pullers, it is an unstable spiral. For neutral swimmers, the equilibrium is a centre. These characteristics are also observed in figure 3.2. For such a simple gradient, we observe very different dynamics of the three types of squirmers.

3.4 Conclusion

We observe that squirmers are, in general, viscopobic (unless they move perfectly aligned with the gradient); they turn towards the less viscous region. Using the squirmer model, we find that the dynamics of microswimmers depend on their propulsion type; even a simple viscosity profile leads to different dynamics for different swimmers. The dynamics of the swimmers, owing to linearity of the problem, can be explained by decomposing the swimming problem into a thrust problem and a drag problem; the effects of the gradients on the thrust are seen to dictate the swimming response. We also show that the differences in the dynamics can be used to sort these

3.4. Conclusion

swimmers by smartly choosing the viscosity profile. As long as the swimmers are not perfectly aligned along (parallel) the gradient direction, and any noise in the system will be helpful towards this end, we find that in linear gradients, pushers will be the farthest from the point of release. In radial gradients, neutral and pusher swimmers will remain bounded / trapped near the viscosity 'sink'. The puller swimmers can therefore be sorted out at farther distances.

Chapter 4

Dynamics and rheology of particles in shear-thinning fluids[†]

Particle motion in non-Newtonian fluids can be markedly different than in Newtonian fluids. Here we look at the change in dynamics for a few problems involving rigid spherical particles in shear-thinning fluids in the absence of inertia. We give analytical formulas for sedimenting spheres, obtained by means of the reciprocal theorem, and demonstrate quantitatively differences in comparison to a Newtonian fluid. We also calculate the first correction to the suspension viscosity, the Einstein viscosity, for a dilute suspension of spheres in a weakly shear-thinning fluid.

4.1 Introduction

Particles in fluids are ubiquitous in both natural and industrial processes. Blood, detergents, paints, aerated drinks, fibre-reinforced polymers, sewage sludges, and drilling muds are some examples where particles—rigid or drops or bubbles—are present in a suspending fluid [9, 33]. The flow behaviour and rheological properties of such suspensions depend on parameters like the particles' shape, size and concentration, particle-particle interaction, particle surface properties, fluid rheology and the type of flow. Even the simplest of such suspensions – small, rigid non-Brownian particles in a Newtonian fluid – exhibits rich rheological properties like shear-thinning, shear-thickening, and normal stress differences which are characteristics of complex fluids [56, 191]. In many common examples like paints, foods, fracking fluids and biological suspensions, the suspending fluid itself is non-Newtonian. The

[†]This chapter has been previously published under the same title in *Journal of Non-Newtonian Fluid Mechanics* 262 (2018) 107–144 by Datt and Elfring. © 2018 Elsevier B.V.

properties of these suspensions is therefore expected to be even more *complex* [143, 155, 212].

In order to understand the properties of these suspensions, it becomes imperative to first understand the interaction of a single particle with the surrounding media and the mutual interaction between two such particles. In fact, it is known that the motion and orientational dynamics of particles can be strongly affected by the rheology of the surrounding fluid medium [29, 49, 132, 133, 216]. For example, at zero Reynolds number, while the center-to-center distance between two equal spherical particles which are sedimenting along their line of centers through a quiescent fluid is fixed indefinitely at its initial value in a Newtonian fluid [192], this distance is found to change in the presence of viscoelasticity of the fluid medium [174]. The understanding of particle dynamics in complex fluids is also important for applications in particle manipulation in microfluidic devices (see recent reviews [47, 138]). Phenomena like cross-stream migration, in which rigid spheres in a pressure-driven tube flow of viscoelastic liquid migrate either towards or away from the wall in the absence of inertia, can be used for cell-trapping in biomedical applications [108].

Towards a fundamental understanding of particle dynamics in non-Newtonian fluids, in this work, we theoretically study the dynamics of rigid non-Brownian spherical particles in shear-thinning fluids in the absence of any fluid or particle inertia. Unlike for viscoelastic fluids, where theoretical studies have been used to develop insights for many experimental observations [49, 132], similar studies have been relatively few in shear-thinning fluids and most of these studies have focussed on using the power-law model [16] to model the shear-thinning rheology [33]. However, as argued by Chhabra *et al.* [34], Chhabra & Uhlherr [35] and Chhabra [33], a fluid model with a zero-shear viscosity should be preferred to the power-law model for slow flows around spheres. Here we use the Carreau model for shear-thinning fluids [16] (discussed in the subsequent section) to study the following problems motivated by some recent experiments:

i) Two equal spherical particles sedimenting along their line of centres through a quiescent fluid. In Newtonian fluids, Stimson & Jeffery [192] showed that the initial distance of separation is maintained as the particles sediment.

ii) Sedimentation of a spherical particle which is also rotating due to some external field. In Newtonian fluids, the sedimenting velocity does not depend on the rotation rate. The translational and rotational motion for a sphere are decoupled in a Newtonian fluid [93].

iii) Sedimentation of a spherical particle in a linear background flow. In

Newtonian fluids, the sedimenting velocity of a sphere depends only on the (local) velocity of the background flow but is independent of the velocity gradient.

iv) The influence of particles on the viscosity of a shear-thinning fluid. For a dilute suspension of neutrally buoyant particles in a Newtonian fluid, it was shown by Einstein [66] that the bulk shear viscosity of the suspension increases due to the presence of particles.

In the following sections, we analyse these problems in shear-thinning fluids in detail, but before that we briefly discuss our theoretical approach and the rheology of shear-thinning fluids.

4.2 Reciprocal Theorem

We are interested here in the motion of, or equivalently forces on, particles in complex fluids. These integrated quantities can be evaluated without resolution of the associated flow field of the complex fluid by employing the reciprocal theorem. This approach was comprehensively reviewed by Leal [133], and we use here a generalized formalism developed in a number of recent papers for active particles [44, 67, 68, 69]. Following Elfring [68], the motion \mathbf{U} or forces \mathbf{F} of N particles in a complex flow may be given by

$$\mathbf{U} = \frac{\hat{\eta}}{\eta} \hat{\mathbf{R}}_{FU}^{-1} \cdot [-\mathbf{F} + \mathbf{F}_T + \mathbf{F}_{NN}], \quad (4.1)$$

where $\mathbf{U} = [\mathbf{U} \ \boldsymbol{\Omega}]$, $\mathbf{F} = [\mathbf{F} \ \mathbf{L}]$ are $6N$ -dimensional vectors comprising translation/rotation and hydrodynamic force/torque respectively on N particles. If the inertia of the particles is negligible (small Stokes numbers), as we will assume here, then the hydrodynamic force must balance any external or applied force (such as weight due to gravity) $\mathbf{F} = -\mathbf{F}_{ext}$. The force

$$\mathbf{F}_T = \frac{\eta}{\hat{\eta}} \int_{\partial\mathcal{B}} (\mathbf{u}^S - \mathbf{u}^\infty) \cdot (\mathbf{n} \cdot \hat{\mathbf{T}}_U) dS, \quad (4.2)$$

is a Newtonian ‘thrust’ due to any surface deformation or activity of the particles \mathbf{u}^S (although in all cases here we consider rigid passive particles, $\mathbf{u}^S = \mathbf{0}$) and ‘drag’ from any background flow \mathbf{u}^∞ . Here $\partial\mathcal{B}$ represents the surfaces of all the particles. The non-Newtonian contribution

$$\mathbf{F}_{NN} = - \int_{\mathcal{V}} \boldsymbol{\tau}'_{NN} : \hat{\mathbf{E}}_U dV, \quad (4.3)$$

4.3. Shear-thinning fluid

represents the extra force/torque on each particle due to a non-Newtonian deviatoric disturbance stress $\boldsymbol{\tau}'_{NN} = \boldsymbol{\tau}_{NN} - \boldsymbol{\tau}_{NN}^\infty$ in the fluid volume \mathcal{V} in which the particles are immersed.

The formulas rely on operators from an N -body resistance/mobility problem in a Newtonian fluid (with viscosity $\hat{\eta}$)

$$\hat{\gamma}'/2 = \hat{\mathbf{E}}_U \cdot \hat{\mathbf{U}}', \quad (4.4)$$

$$\hat{\boldsymbol{\sigma}}' = \hat{\mathbf{T}}_U \cdot \hat{\mathbf{U}}', \quad (4.5)$$

$$\hat{\mathbf{F}}' = -\hat{\mathbf{R}}_{FU} \cdot \hat{\mathbf{U}}'. \quad (4.6)$$

where primes indicate disturbance quantities. The tensors $\hat{\mathbf{E}}$ and $\hat{\mathbf{T}}$ are functions of position in space that map the (arbitrary) motion of all N particles $\hat{\mathbf{U}}$ to the fluid strain-rate and stress fields respectively, while the N -body rigid-body resistance tensor

$$\hat{\mathbf{R}}_{FU} = \begin{bmatrix} \hat{\mathbf{R}}_{FU} & \hat{\mathbf{R}}_{F\Omega} \\ \hat{\mathbf{R}}_{LU} & \hat{\mathbf{R}}_{L\Omega} \end{bmatrix}. \quad (4.7)$$

We note that no specific $\hat{\mathbf{U}}$ needs to be chosen in the rigid-body dual problem as only the linear operators $\hat{\mathbf{E}}_U$, $\hat{\mathbf{T}}_U$ and $\hat{\mathbf{R}}_{FU}$ enter the picture. In many cases there may be symmetries in the problem which simplify these operators substantially, likewise we may know that the forces/torques are in some way simplified (collinear with gravity for instance) and hence need not even determine all components of the operators.

Components of $\hat{\mathbf{E}}_U$, $\hat{\mathbf{T}}_U$ and $\hat{\mathbf{R}}_{FU}$ for a single sphere that we use in this study are provided in Appendix A.

4.3 Shear-thinning fluid

As we outlined in the previous sections, the presence of a non-Newtonian stress $\boldsymbol{\tau}_{NN}$ can significantly alter the motion of particles in flows. In this work, we consider the effects of shear-thinning fluids, which experience a loss in apparent viscosity η with increasing strain-rates $\dot{\gamma}$; specifically, the deviatoric stress

$$\boldsymbol{\tau} = \eta(\dot{\gamma})\dot{\boldsymbol{\gamma}}, \quad (4.8)$$

where the viscosity is modelled using the Carreau model for generalised Newtonian fluids [16]

$$\eta(\dot{\gamma}) = \eta_\infty + (\eta_0 - \eta_\infty) \left[1 + \lambda_t^2 |\dot{\boldsymbol{\gamma}}|^2 \right]^{(n-1)/2}. \quad (4.9)$$

4.3. Shear-thinning fluid

Here, η_0 is the zero-shear-rate viscosity, η_∞ is the infinite-shear rate viscosity, n is the power law index ($n < 1$ for shear-thinning fluids; smaller the value of n , more shear-thinning the fluid is) and λ_t is a time constant. The magnitude of the strain-rate is given by $|\dot{\gamma}| = (\Pi)^{1/2}$ where $\Pi = \dot{\gamma}_{ij}\dot{\gamma}_{ij}$ is the second invariant of the strain-rate tensor. Note that $\lim_{\dot{\gamma} \rightarrow 0} \eta(\dot{\gamma}) = \eta_0$ and $\lim_{\dot{\gamma} \rightarrow \infty} \eta(\dot{\gamma}) = \eta_\infty$, showing that at low and high strain rates the fluid behaves like a Newtonian fluid with viscosity η_0 and η_∞ , respectively. λ_t sets the cross-over strain-rates at which non-Newtonian effects start to become important.

In this work, we investigate strain-rates such that $\lambda_t \ll 1/\dot{\gamma}_c$, where $\dot{\gamma}_c$ is the characteristic strain-rate of the flow. In this case it is useful to write the constitutive equation in the form

$$\boldsymbol{\tau} = \eta_0 \dot{\boldsymbol{\gamma}} + (\eta(\dot{\boldsymbol{\gamma}}) - \eta_0) \dot{\boldsymbol{\gamma}}. \quad (4.10)$$

Although, we note that this rearrangement is not in any way restricted to low strain rates. Writing the equation as such, it is clear that the non-Newtonian contribution $\boldsymbol{\tau}_{NN} = (\eta(\dot{\boldsymbol{\gamma}}) - \eta_0) \dot{\boldsymbol{\gamma}}$.

In dimensionless form, one may decouple the Newtonian and non-Newtonian contribution for a Carreau fluid as

$$\boldsymbol{\tau}^* = \dot{\boldsymbol{\gamma}}^* + \left\{ \beta - 1 + (1 - \beta) \left[1 + Cu^2 |\dot{\boldsymbol{\gamma}}^*|^2 \right]^{(n-1)/2} \right\} \dot{\boldsymbol{\gamma}}^*, \quad (4.11)$$

where stars (*) represent dimensionless flow quantities. The Carreau number $Cu = \dot{\gamma}_c \lambda_t$ is the ratio of the characteristic strain rate in the flow $\dot{\gamma}_c$ to the crossover strain rate $1/\lambda_t$. The viscosity ratio is given by $\beta = \eta_\infty/\eta_0 \in [0, 1]$. The characteristic length of the particle is chosen as the length scale in the problems and as we consider only spherical particles, the length scale is a , the radius of the particles. $\eta_0 \dot{\gamma}_c$ is the scale for stresses; the appropriate characteristic strain-rate, $\dot{\gamma}_c$, varies depending on the problem and therefore, is defined separately in each of the problems below.

In this work, we consider the fluid behaviour to be weakly shear-thinning, in the sense that $Cu \ll 1$ [45], and therefore the viscosity is assumed to not deviate substantially from the zero-shear viscosity η_0 . We then explore the leading-order weakly shear-thinning effects of the fluid rheology on particle motion. To this end, we assume a regular perturbation expansion of all fields, e.g. $\mathbf{u} = \mathbf{u}_0 + Cu^2 \mathbf{u}_1 + \dots$, and find the non-Newtonian stress to be

$$\boldsymbol{\tau}_{NN}^* = -\frac{1}{2} Cu^2 (1 - n) (1 - \beta) |\dot{\boldsymbol{\gamma}}_0^*|^2 \dot{\boldsymbol{\gamma}}_0^* + \mathcal{O}(Cu^4), \quad (4.12)$$

where for shear-thinning fluids $\beta < 1$ and $n < 1$. We consider only the leading-order effects of shear-thinning viscosity and by using (4.12), we may obtain the non-Newtonian force on particles at the expense of an integration (4.3) which then only requires the Newtonian flow field \mathbf{u}_0 .

4.4 Sedimenting spheres

Due to their symmetry, a number of classic results involving motion of spheres in Newtonian fluids can be predicted directly by employing the kinematic reversibility of the field equations and it is insightful to consider examples where dynamics are altered (or not) by shear-thinning rheology. In this section, we explore one such case of two spheres sedimenting along their line of centres but before that, it is instructive to first examine the simple case of a single sphere moving through a shear-thinning fluid and to see how the force-motion relationship is affected by the medium rheology.

4.4.1 Single sphere

The drag force on a sphere of radius a , moving with a velocity \mathbf{U} is given by $\mathbf{F} = -6\pi a\eta\mathbf{U}$ (dimensional), where η is the viscosity of the fluid. In a shear-thinning fluid with zero-shear rate viscosity $\eta_0 = \eta$, the drag force is expected to be less than the Newtonian value. This is because one expects the apparent viscosity around the sphere to decrease below η due to the strain-rates ensuing from the motion of the sphere. Quantitatively, the drag force in shear-thinning fluid can be evaluated using the reciprocal theorem. For a single sphere, we expect this force to be colinear with the velocity by symmetry. Simplifying (4.3) we may write

$$\mathbf{F} = -6\pi\eta_0 a\mathbf{U} - \int_{\mathcal{V}} \boldsymbol{\tau}_{NN} : \hat{\mathbf{E}}_U dV, \quad (4.13)$$

where $\hat{\mathbf{E}}_U$ (such that $\hat{\gamma}/2 = \hat{\mathbf{E}}_U \cdot \hat{\mathbf{U}}$) is well known for a sphere translating in Stokes flow [89]. The integral above may be easily evaluated to leading order as then the non-Newtonian stress depends only on the solution of a translating sphere in a Newtonian fluid i.e. $\boldsymbol{\tau}_{NN}[\mathbf{u}_0]$ (from(4.12)). In dimensionless form we find the drag in a shear-thinning fluid to be

$$\mathbf{F}^* = -6\pi\mathbf{U}^* \left(1 - \frac{1}{2}(1-\beta)(1-n)Cu^2 \frac{942}{2275} |\mathbf{U}^*|^2 \right). \quad (4.14)$$

If we (sensibly) take as the characteristic strain-rate $\dot{\gamma}_c = |\mathbf{U}|/a$ then $\mathbf{U}^* = \mathbf{e}$ is simply the unit vector in the direction of the motion (a convention we use

4.4. Sedimenting spheres

below). The term in the brackets is then an analytical calculation of the drag correction factor (often given the symbol X in the literature [30, 35]) valid to $\mathcal{O}(Cu^2)$.

We see that, as expected, the drag force on a sphere decreases in a shear-thinning fluid as compared to a Newtonian fluid. It should be noted that the reduction in drag below the Newtonian value is at odds with the conclusions reached using the power-law fluid model which predict an increase in the drag force [33] because (as argued in that work) the power-law fluid model does not incorporate a zero shear-rate viscosity which is important in modelling slow flows involving stagnation points and vanishingly small shear rates. In contrast, (4.14) predicts the reduction in drag observed in experimental results [35], and qualitatively agrees with a variational estimate by Chhabra & Uhlherr [35], and numerical results from Bush & Phan-Thien [30], which both used the Carreau fluid model to characterise the fluid rheology.

It is straightforward to invert the drag force to obtain the velocity given a prescribed external force (for example weight due to gravity in sedimentation)

$$\mathbf{U}^* = \frac{\mathbf{F}_{ext}^*}{6\pi} \left(1 + \frac{1}{2} (1 - \beta) (1 - n) Cu^2 \frac{942}{2275} \frac{|\mathbf{F}_{ext}^*|^2}{(6\pi)^2} \right). \quad (4.15)$$

In this case an appropriate strain-rate scale is $\dot{\gamma}_c = |\mathbf{F}_{ext}^*| / (\eta_0 a^2)$ in which case \mathbf{F}_{ext}^* would be a unit vector.

4.4.2 Two spheres

We now consider sedimentation of two spheres of equal radii along the line joining their centres. In a Newtonian fluid, one can use arguments of kinematic reversibility and symmetry to find that the two spheres will sediment with equal velocities and will maintain their initial distance of separation [89]. Stimson & Jeffery [192] solved the hydrodynamically equivalent problem of two spheres moving with a constant velocity along their line of centres and calculated the flow field and the forces on the spheres. When their radii are equal, it was found that the forces on each of the two spheres are indeed equal but each less than on single sphere moving in a quiescent fluid with the same velocity. Quantitatively, the force on either sphere can be written as $\mathbf{F} = -6\pi\eta a \mathbf{U} \lambda$ (dimensional), where λ is a coefficient which depends on the separation between the two spheres [192]. $\lambda \rightarrow 1$ as the distance between the two spheres approaches infinity, i.e. when the two spheres do not

4.4. Sedimenting spheres

interact hydrodynamically with each other. It was also found that value of λ decreases as the distance between the two spheres decreases. However, the method of Stimson & Jeffery [192] could not be applied to the case of two spheres in contact with each other. This case was later solved by Cooley & O'Neill [38] who found $\lambda = 0.645$ (for the two sphere touching case). These results and values of λ have also been observed experimentally [93].

Non-Newtonian rheology can break kinematic reversibility and indeed viscoelasticity is known to change these results qualitatively. Where in Newtonian fluids two equal sedimenting spheres maintain their initial distance of separation, it was found in the experiments of Riddle *et al.* [174] and analyses of Brunn [28] and Ardekani *et al.* [4] that the two particles showed a tendency to aggregate in viscoelastic fluids. This effect of normal stresses on particle dynamics has been commented upon by Joseph & Feng [104].

In shear-thinning fluids, it was observed in the experiments of Daugan *et al.* [46] that the two spheres would aggregate provided the initial distance of their separation was smaller than some critical distance. Yu *et al.* [215], in their experimental study, argued that in fact this tendency towards aggregation was due to thixotropy (memory of shear-thinning) and the corridors of reduced viscosity in the wake of sedimenting particles lead to aggregation [46, 105]. In the absence of memory, the two spheres would maintain their initial distance of separation [215]. Here, we theoretically study the equivalent problem of two equal spheres moving with a constant velocity along their line of centres, as considered by Stimson & Jeffery [192], but in a shear-thinning fluid.

We use the reciprocal theorem to calculate the forces on the two spheres. By (4.1) the force on the particles can be written generally as

$$\mathbf{F} = -\frac{\eta}{\hat{\eta}} \hat{\mathbf{R}}_{FU} \cdot \mathbf{U} + \mathbf{F}_{NN}. \quad (4.16)$$

For two equal spheres moving along their line of centres, by symmetry, we expect all vectors in the problem to be collinear, which significantly simplifies the more general problem of the motion of two spheres. When the motion of two bodies is collinear (only translational motion is considered), it is useful to decompose the motion into a mean velocity $\bar{\mathbf{U}}$ and relative velocity $\Delta\mathbf{U}$ such that the velocity of each sphere may be written as $\mathbf{U}_1 = \bar{\mathbf{U}} + \Delta\mathbf{U}$ and $\mathbf{U}_2 = \bar{\mathbf{U}} - \Delta\mathbf{U}$. In this basis, the relevant resistance/mobility problems for the reciprocal theorem are i) two (equal) spheres translating with equal velocity along the line joining their centres in a Newtonian fluid (corresponding to $\bar{\mathbf{U}}$ as in this case $\Delta\mathbf{U} = 0$) with solution by Stimson & Jeffery [192] and ii) two (equal) spheres approaching each other with equal speed along the line

4.4. Sedimenting spheres

joining their centres in a Newtonian fluid with solution due to Maude [141] and Brenner [23] (corresponding to $\Delta\mathbf{U}$ as in this case $\overline{\mathbf{U}} = 0$). Note that one requires two resistance/mobility problems for evaluating the force on each of the two spheres. The resistance tensor for this problem is diagonal in the sense that in a Newtonian fluid mean translation leads only to a mean force and likewise for relative force. The reciprocal theorem given above leads to expression for mean and relative force in a non-Newtonian fluid given by

$$\overline{\mathbf{F}} = -\frac{\eta_0}{\hat{\eta}} \hat{\mathbf{R}}_{\overline{\mathbf{U}}} \cdot \overline{\mathbf{U}} - \frac{1}{2} \int_{\mathcal{V}} \boldsymbol{\tau}_{NN} : \hat{\mathbf{E}}_{\overline{\mathbf{U}}} dV, \quad (4.17)$$

$$\Delta\mathbf{F} = -\frac{1}{2} \int_{\mathcal{V}} \boldsymbol{\tau}_{NN} : \hat{\mathbf{E}}_{\Delta\mathbf{U}} dV, \quad (4.18)$$

where $\hat{\mathbf{R}}_{\overline{\mathbf{U}}}$ is the (mean) translational resistance of the two spheres in a Newtonian fluid and $\hat{\mathbf{E}}_{\overline{\mathbf{U}}}$ and $\hat{\mathbf{E}}_{\Delta\mathbf{U}}$ correspond to the strain-rate due to mean and relative motion respectively. Note that $\boldsymbol{\tau}_{NN}$ is evaluated using the solution of the problem in Newtonian fluids by Stimson & Jeffery [192] (from (4.12)).

Upon evaluation of (4.18), for weakly non-linear shear-thinning fluids one finds that there is no relative force

$$\Delta\mathbf{F} = \mathbf{0}, \quad (4.19)$$

meaning the forces on two equal spheres are equal in a shear-thinning fluid as in a Newtonian fluid. Although we obtain this result only for a weakly shear-thinning fluid, we expect this to be the case for all generalized Newtonian fluids, regardless of the parameter regime. The reason is that the stress $\boldsymbol{\tau}_{NN}$ maintains the symmetry of the Newtonian problem while the Maude-Brenner problem (and thus the operator $\hat{\mathbf{E}}_{\Delta\mathbf{U}}$) displays a mirror-image symmetry and therefore the integral over the entire fluid volume must be zero. In fact, Brunn [29] briefly comments on this property of generalized Newtonian fluids where results may come out to be similar to Newtonian fluids.

As the force on the two spheres in a weakly shear-thinning fluid are equal, two sedimenting spheres do not show any tendency to aggregate in a shear-thinning fluid without memory, as was also found in the numerical work of Yu *et al.* [215] discussed previously. We can further calculate the force on each of the spheres, and compare it to the force on a single sphere in a shear-thinning fluid from section 4.4.1. Since there is no difference in

4.4. Sedimenting spheres

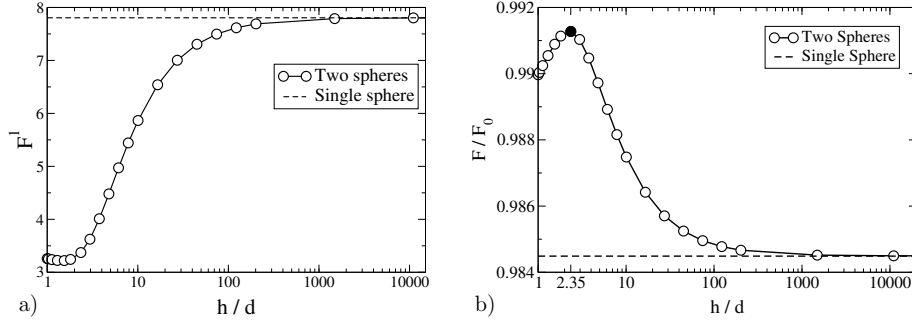


Figure 4.1: a) Variation of non-Newtonian drag F^1 as a function of the distance of separation between the two spheres. b) Normalized drag as a function of this distance. Note that the variation is non-monotonic and that drag reduction is minimized at $h/d \approx 2.35$.

drag force, the mean in (4.17) represents the hydrodynamic drag on each sphere. The form of the force (dimensionless) is

$$\overline{\mathbf{F}}^* = \overline{\mathbf{F}}_0^* + \frac{1}{2}Cu^2(1-\beta)(1-n)F^1\mathbf{e} + \mathcal{O}(Cu^4), \quad (4.20)$$

where $\overline{\mathbf{F}}_0^*$ is the force on each sphere in a Newtonian fluid [192]. Here we have non-dimensionalised lengths with sphere radius a and stresses with $\eta_0 U/a$ where U is the magnitude of velocity of the spheres such that $\mathbf{U}^* = \mathbf{e}$. Both $\overline{\mathbf{F}}_0^*$ and the coefficient F^1 obtained by evaluating the integral in (4.17) numerically, depend on the ratio of the centre distance between the spheres to their diameter, h/d , as shown in Figure 4.1a). Note that F^1 is positive, meaning the correction to drag force is in the direction of the motion \mathbf{e} and so the drag in a shear-thinning fluid is less than in a Newtonian fluid. To contrast the results with the Newtonian fluids case, we also plot the ratio of the magnitude of the force in a weakly shear-thinning fluid (correct to $\mathcal{O}(Cu^2)$) to the drag in an equivalent Newtonian fluid for same configuration in Figure 4.1b). This is plotted in Figure 4.1b) for $Cu^2 = 0.1$, $\beta = 0.001$ and $n = 0.25$.

We note that the ratio F/F_0 is always less than 1 which shows that the drag in a shear-thinning fluid is less than that in Newtonian fluid for the same configuration. This is expected as the viscosity in a shear-thinning fluid decreases with strain-rate leading to less drag on each sphere when compared to in Newtonian fluid. But what is perhaps surprising is the variation of force with distance between the two spheres. We first note that as this distance becomes large, the drag reduction on each sphere asymptotes

to that on a single sphere in shear-thinning fluid. The drag reduction when the two spheres essentially do not interact hydrodynamically with each other is greater than for any other distance of separation. Shear-thinning effects are maximum in this configuration. When the spheres interact hydrodynamically the effective strain rates are reduced (due to screening) and thus the drag reduction on each is always lower than for a single sphere. On the other end of the distances, we have the configuration when the two spheres are in contact with each other. This, interestingly, is not the configuration to observe minimum shear-thinning effects. In fact, the minimum shear-thinning effects or equivalently the maximum of the ratio F/F_0 is observed when the clearance between the two spheres is of the order of their diameter i.e. when $h/d \approx 2.35$. We believe that this nontrivial result may be due to the complex flow field around the spheres, which also includes ring vortices, and its effect on the dissipation rates [50].

4.5 Sedimentation of a rotating sphere

We now consider the case of a sphere which translates as well as rotates in a shear-thinning fluid. The calculations are inspired by the recent experimental work of Godínez *et al.* [82] who study the hydrodynamically equivalent problem of sedimentation of a rotating sphere in a power-law fluid. By imposing a controlled rotation on a sedimenting sphere, Godínez *et al.* [82] measured the increase in the sedimentation velocity, which could then be used to predict the values of power law indices of the fluids. They considered rotation of the sphere only about the sedimenting axis. Here we consider the problem more generally.

Translation and rotation of a sphere in a Newtonian fluid are decoupled and owing to the linearity of the Stokes flow, one may superimpose the solution of translation alone and rotation alone to get the solution of a translating-rotating sphere in a Newtonian fluid. In other words a sphere that rotates in a Newtonian fluid will sediment at the same rate as when it does not rotate. This decoupling of translation and rotation is not expected to hold in a non-linear fluid. We explore this for a weakly shear-thinning fluid, again using the reciprocal theorem.

According to the reciprocal theorem, as before, we have

$$\mathbf{F} = -\frac{\eta}{\hat{\eta}} \hat{\mathbf{R}}_{FU} \cdot \mathbf{U} - \int_{\mathcal{V}} \boldsymbol{\tau}_{NN} : \hat{\mathbf{E}}_U \, dV. \quad (4.21)$$

We non-dimensionalise length with the sphere radius, a , stresses by $\eta_0 U/a$ where U is the magnitude of velocity of the sphere and hence $\mathbf{U}^* = \mathbf{e}$. We

4.5. Sedimentation of a rotating sphere

consider a general angular velocity which in dimensionless form, $\boldsymbol{\Omega}^*$, is not necessarily a unit vector. Then from (4.21) we get

$$\mathbf{F}^* = -6\pi\mathbf{e} \cdot \left\{ \mathbf{I} - \frac{1}{2}Cu^2(1-n)(1-\beta) \left(\frac{942}{2275}\mathbf{I} + \frac{552}{385} [2|\boldsymbol{\Omega}^*|^2\mathbf{I} - \boldsymbol{\Omega}^*\boldsymbol{\Omega}^*] \right) \right\}. \quad (4.22)$$

In the absence of any rotation $\boldsymbol{\Omega}^* = \mathbf{0}$, the force corresponds with (4.14) as expected. With nonzero rotation, the drag force is further reduced due to the additional strain-rate caused by rotation. When the rotation is aligned with the translation, $\boldsymbol{\Omega} \propto \mathbf{U}$, for example when the axis of rotation is aligned with gravity for a sedimenting sphere as in the experiments of Godínez *et al.* [82], the drag force remains collinear with \mathbf{U} . When the rotation is not aligned with translation, a lateral force may arise due to the term in the direction of the axis of rotation $\propto (\mathbf{e} \cdot \boldsymbol{\Omega}^*)\boldsymbol{\Omega}^*$. When the rotation is orthogonal to translation there is no lateral drift and the change in the drag force due to rotation is twice that of when the rotation is aligned with translation and so would maximize sedimentation velocity for a given rotation rate. Conversely, in the mobility problem for a given external force \mathbf{F}_{ext}^* , a rotating sphere will sediment with a translational velocity given by

$$\mathbf{U}^* = \frac{\mathbf{F}_{ext}^*}{6\pi} \cdot \left\{ \mathbf{I} + \frac{1}{2}Cu^2(1-n)(1-\beta) \left(\frac{942}{2275} \frac{|\mathbf{F}_{ext}^*|^2}{(6\pi)^2} \mathbf{I} + \frac{552}{385} [2|\boldsymbol{\Omega}^*|^2\mathbf{I} - \boldsymbol{\Omega}^*\boldsymbol{\Omega}^*] \right) \right\}, \quad (4.23)$$

where \mathbf{F}_{ext}^* is a unit vector if the strain rate scale $\dot{\gamma}_c$ is chosen as $|\mathbf{F}_{ext}^*|/(\eta_0 a^2)$. On comparison with the experimental results, it is noted that Godínez *et al.* [82] find a power law dependence of the sedimenting velocity on the rotation rate, $|\mathbf{U}| \propto |\boldsymbol{\Omega}|^{(1-n)}$, across a range of rotation rates such that strain-rate around the sphere is predominantly due to rotation and not due to translation, our analytical result in equation (4.23), valid for small Carreau numbers, draws a similar picture, namely, increasing the rotation rate and decreasing the power-law index, n , increase the sedimentation velocity of the sphere.

We also calculate the hydrodynamic torque on the particle

$$\mathbf{L}^* = -8\pi\boldsymbol{\Omega}^* \cdot \left\{ \mathbf{I} - \frac{1}{2}Cu^2(1-n)(1-\beta) \left(\frac{24}{5}|\boldsymbol{\Omega}^*|^2\mathbf{I} + \frac{414}{385}[2\mathbf{I} - \mathbf{e}\mathbf{e}] \right) \right\}. \quad (4.24)$$

The first term in the shear-thinning correction is due to the particle rotation alone as there is a reduction in the torque due to the shear-thinning caused by the rotation. The second term in the correction is due to both the

translation and rotation of the sphere and may generate a torque which is not aligned with the direction of rotation. Clearly, in a shear-thinning fluid translational and rotational dynamics are coupled.

4.6 Sphere under an external force in a linear flow of shear-thinning fluid

We now consider the dynamics of a spherical particle driven by an external force in an unbounded linear-flow. In a Newtonian fluid, we know that the sedimenting velocity of a sphere is not altered by the velocity gradient in simple shear flow. However, this may not be the case in non-linear fluids. In fact, in viscoelastic fluids, it is found that the terminal velocity of a sphere decreases when the applied shear-flow is perpendicular to gravity in what is called a cross-shear-flow [27, 49, 96]. Gheissary & van den Brule [80] used sedimentation of a sphere in cross-shear flow to predict the rheological properties of different shear-thinning fluids. The cross-shear flow is a model system used for transport of particles in hydraulically-induced fractures [8]. Einarsson & Mehlig [64] recently extended the analyses in viscoelastic fluids to the case when gravity (or another external force) and the vorticity direction of the applied flow are not aligned. Here, we perform a similar analysis for a shear-thinning fluid.

Using the reciprocal theorem we calculate the velocities (both rotational and angular) of the particle as

$$\mathbf{U} = \frac{\hat{\eta}}{\eta} \hat{\mathbf{R}}_{FU}^{-1} \cdot \left[\mathbf{F}_{ext} - \frac{\eta}{\hat{\eta}} \int_{\partial\mathcal{B}} \mathbf{u}^\infty \cdot (\mathbf{n} \cdot \hat{\mathbf{T}}_U) dS - \int_{\mathcal{V}} \boldsymbol{\tau}'_{NN} : \hat{\mathbf{E}}_U dV \right], \quad (4.25)$$

where $\mathbf{F}_{ext} = [\mathbf{F}_{ext} \ 0]^T$. Here, \mathbf{F}_{ext} is an arbitrary external force acting on the particle. The particle is immersed in a 2D linear flow given by $\mathbf{u}^{\infty*} = \mathbf{A}^{\infty*} \cdot \mathbf{x}^*$ (dimensionless), in a Cartesian basis we may write

$$\mathbf{A}^{\infty*} = \begin{bmatrix} 1 + \lambda & 1 - \lambda & 0 \\ -(1 - \lambda) & -(1 + \lambda) & 0 \\ 0 & 0 & 0 \end{bmatrix} \quad (4.26)$$

where we have scaled length with the radius of the sphere and stresses with $\eta_o \dot{\gamma}_c$, where $\dot{\gamma}_c$ is characteristic of the applied strain-rate such that we have $\mathbf{A}^{\infty*}$ in the form above. It is useful to also decompose $\mathbf{u}^{\infty*} = \frac{1}{2} \dot{\boldsymbol{\gamma}}^{\infty*} \cdot \mathbf{x}^* + \boldsymbol{\Omega}^{\infty*} \times \mathbf{x}^*$ into symmetric and antisymmetric parts associated with strain-rate and rotation-rate respectively. Note that $\lambda = -1$ corresponds to purely rotational flow, $\lambda = 0$ is shear flow and $\lambda = 1$ extensional flow [119].

4.7. Suspension of spheres in a shear-thinning fluid

On evaluating (4.25) we get the translational velocity of the particle

$$\mathbf{U}^* = \left\{ \mathbf{I} + \frac{1}{2}Cu^2(1-\beta)(1-n) \left[\frac{942}{2275} \frac{|\mathbf{F}_{ext}^*|^2}{(6\pi)^2} \mathbf{I} + \frac{695}{539} |\dot{\gamma}^{\infty*}|^2 \mathbf{I} + \frac{10037}{7007} \dot{\gamma}^{\infty*} \cdot \dot{\gamma}^{\infty*} \right] \right\} \cdot \frac{\mathbf{F}_{ext}^*}{6\pi}. \quad (4.27)$$

The first two terms on the right hand side correspond to the velocity due to an external force in an otherwise quiescent shear-thinning fluid as in (4.15). The remaining terms demonstrates the coupling between the background flow field and external force. When the force is perpendicular to the plane of applied flow, we see that the velocity of the particle is further increased above its quiescent fluid value due to the thinning of the fluid by the external flow field. However, interestingly, for any general direction of the external force, the velocity of the particle may not be in the direction of the forcing. This is due to the lack of symmetry of the background flow field in one direction. It is also worth noting that for a purely rotational flow, one does not see a shear-thinning effect arising from the background flow.

Using (4.25) we also evaluate the angular velocity of the sphere, which is given by

$$\boldsymbol{\Omega}^* = \boldsymbol{\Omega}^{\infty*} + \frac{1}{2}Cu^2(1-\beta)(1-n) \frac{3189}{4004} \left[\frac{\mathbf{F}_{ext}^*}{6\pi} \times \dot{\gamma}^{\infty*} \cdot \frac{\mathbf{F}_{ext}^*}{6\pi} \right]. \quad (4.28)$$

Note that in the absence of any forcing the sphere rotates with just the background angular velocity just like in a Newtonian fluid where the angular velocity of the sphere in a background flow is independent of viscosity. This was also found in the numerical simulations of D'Avino *et al.* [48]. Also, if the external force is along any of the principal directions of strain, or the background flow is purely rotational, the angular velocity of the sphere will be just due to the rotational component of the background flow. However, for an arbitrary direction of the external force, the angular velocity may be different than that imposed by background flow field.

4.7 Suspension of spheres in a shear-thinning fluid

Suspensions of particles in shear-thinning fluids are encountered in a wide range of chemical, biochemical and material processing industries, and as such there has been considerable interest in studying the flow properties of such suspensions [32, 90, 114, 130, 161, 199]. Most of these studies consider

4.7. Suspension of spheres in a shear-thinning fluid

particles in power-law fluids, in other words, it is assumed that the strain-rates are large enough so that the fluid rheology is captured by a power law model. Here, we complement these studies by quantifying the first effects of the non-Newtonian rheology of the suspending fluid in the realm of small strain-rates.

We calculate the average stress in a dilute suspension of neutrally buoyant rigid spheres in a weakly shear-thinning fluid, subject to a linear background flow

$$\mathbf{u}^{\infty*} = \mathbf{A}^{\infty*} \cdot \mathbf{x}^* \quad (4.29)$$

as discussed in the previous section. The average stress in a suspension of rigid spheres in a weakly shear-thinning fluid, correct to $\mathcal{O}(Cu^2)$, is evaluated as

$$\langle \widehat{\boldsymbol{\sigma}}^* \rangle = \langle \dot{\boldsymbol{\gamma}}^* \rangle - \frac{1}{2} Cu^2 (1 - \beta) (1 - n) \langle |\dot{\boldsymbol{\gamma}}^*|^2 \dot{\boldsymbol{\gamma}}^* \rangle + \langle \widehat{\boldsymbol{\sigma}}_p^* \rangle, \quad (4.30)$$

where $\boldsymbol{\sigma}_p$ is the additional stress within the suspended particles, and the average quantities (denoted with angular brackets) are obtained by taking an ensemble average over all possible configurations of the particles [10, 116, 173]. We use the wide hat symbol $\widehat{}$ to refer to the symmetric and deviatoric component of a second-order tensor and note that the isotropic terms in the average stress do not contribute to suspension rheology [65, 173]. In a homogeneous and dilute suspension of particles, we know

$$\langle \widehat{\boldsymbol{\sigma}}_p^* \rangle = n \widehat{\mathbf{S}}^* \quad (4.31)$$

where n is the particle number density equal to ϕ/V_p , where $\phi \ll 1$ is the particle volume fraction, V_p is the volume of a single particle, and \mathbf{S} is the particle stresslet [10, 116] defined as

$$\mathbf{S} = \int_{\partial\mathcal{B}} \frac{1}{2} [\mathbf{n} \cdot \boldsymbol{\sigma} \mathbf{r} + \mathbf{r} \mathbf{n} \cdot \boldsymbol{\sigma}] dS. \quad (4.32)$$

In order to calculate the average stress in the suspension, we start by evaluating the particle stresslet using the reciprocal theorem [65, 68, 128]. Elfring [68] derives an expression for the stresslet in a weakly non-Newtonian fluid which is (in dimensional form)

$$\mathbf{S} = \mathbf{S}^\infty - \frac{\eta}{\hat{\eta}} \int_{\partial\mathcal{B}} \mathbf{u}^\infty \cdot (\mathbf{n} \cdot \hat{\mathbf{T}}_E) dS - \int_{\mathcal{V}} \boldsymbol{\tau}'_{NN} : \hat{\mathbf{E}}_E dV. \quad (4.33)$$

4.7. Suspension of spheres in a shear-thinning fluid

Clearly, evaluation of the stresslet \mathbf{S} up to $\mathcal{O}(Cu^2)$ using equation (4.32) would require calculating the first correction to the flow field in the shear-thinning fluid; however, equation (4.33), obtained using the reciprocal theorem, bypasses this calculation and the first correction to the stresslet is obtained by using the Newtonian flow field.

We first evaluate the stresslet \mathbf{S}^∞ due to the stress $\boldsymbol{\sigma}^\infty$ from the background flow. In the absence of particles, the background stress $\boldsymbol{\sigma}^\infty$ is simply

$$\boldsymbol{\sigma}^{\infty*} = \boldsymbol{\gamma}^{\infty*} - \frac{1}{2}Cu^2(1-n)(1-\beta)|\dot{\boldsymbol{\gamma}}^{\infty*}|^2\dot{\boldsymbol{\gamma}}^{\infty*} + \mathcal{O}(Cu^4), \quad (4.34)$$

where $\dot{\boldsymbol{\gamma}}^{\infty*} = \mathbf{A}^{\infty*} + \mathbf{A}^{\infty*\top}$ is the applied strain rate. Using the definition of the stresslet (4.32), we therefore have, up to $\mathcal{O}(Cu^2)$,

$$\mathbf{S}^{\infty*} = \frac{4\pi}{3}\dot{\boldsymbol{\gamma}}^{\infty*} - \frac{1}{2}Cu^2(1-\beta)(1-n)\frac{4\pi}{3}|\dot{\boldsymbol{\gamma}}^{\infty*}|^2\dot{\boldsymbol{\gamma}}^{\infty*}. \quad (4.35)$$

Evaluating the integral terms in (4.33), we obtain

$$\mathbf{S}^* - \mathbf{S}^{\infty*} = 2\pi\dot{\boldsymbol{\gamma}}^{\infty*} - \frac{1}{2}Cu^2(1-\beta)(1-n)\frac{68469\pi}{17017}|\dot{\boldsymbol{\gamma}}^{\infty*}|^2\dot{\boldsymbol{\gamma}}^{\infty*}, \quad (4.36)$$

and therefore altogether have

$$\mathbf{S}^* = \frac{10\pi}{3}\dot{\boldsymbol{\gamma}}^{\infty*} - \frac{1}{2}Cu^2(1-\beta)(1-n)\left(\frac{273475\pi}{51051}\right)|\dot{\boldsymbol{\gamma}}^{\infty*}|^2\dot{\boldsymbol{\gamma}}^{\infty*}. \quad (4.37)$$

The first term on the right hand side is the stresslet in a Newtonian fluid. From the equation above, it can be seen that the total stresslet in a shear-thinning fluid is less than that in Newtonian fluid.

We now proceed to calculate the average stress in equation (4.30). We note that the mean Newtonian viscous stress, $\langle\dot{\boldsymbol{\gamma}}^*\rangle$, is equal to the bulk applied strain-rate $\dot{\boldsymbol{\gamma}}^{\infty*}$ [89, 116]. The second term on the right hand side in equation (4.30) can be evaluated by first performing a formal ensemble average based on the ergodic hypothesis [173] on $\langle|\dot{\boldsymbol{\gamma}}^*|^2\dot{\boldsymbol{\gamma}}^*\rangle$. Writing the strain-rate in terms of the mean and fluctuating components $\dot{\gamma}_{ij}^* = \langle\dot{\gamma}_{ij}^*\rangle + \dot{\gamma}'_{ij*}$, we obtain

$$\langle|\dot{\boldsymbol{\gamma}}^*|^2\rangle = \langle\dot{\gamma}_{ij}^*\dot{\gamma}_{ij}^*\rangle = \langle\dot{\gamma}_{ij}^*\rangle\langle\dot{\gamma}_{ij}^*\rangle + \langle\dot{\gamma}'_{ij*}\dot{\gamma}'_{ij*}\rangle, \quad (4.38)$$

where dashed quantities are fluctuating values. Here, we have used the fact $\langle\dot{\gamma}'_{ij*}\langle\dot{\gamma}_{ij}^*\rangle\rangle = 0$ and as such, obtain $\langle|\dot{\boldsymbol{\gamma}}^*|^2\rangle = 2\dot{\gamma}'_{ij*}\langle\dot{\gamma}_{ij}^*\rangle + \dot{\gamma}'_{ij*}\dot{\gamma}'_{ij*} - \langle\dot{\gamma}'_{ij*}\dot{\gamma}'_{ij*}\rangle$. Using

these, the ensemble average:

$$\langle |\dot{\gamma}|^{2*} \dot{\gamma}^* \rangle = \langle |\dot{\gamma}|^{2*} \rangle \langle \dot{\gamma}^* \rangle + \langle |\dot{\gamma}|^{2'*} \dot{\gamma}'^* \rangle \quad (4.39)$$

$$= \left(\langle \dot{\gamma}_{ij}^* \rangle \langle \dot{\gamma}_{ij}^* \rangle + \langle \dot{\gamma}_{ij}'^* \dot{\gamma}_{ij}'^* \rangle \right) \langle \dot{\gamma}^* \rangle + 2 \langle \dot{\gamma}_{ij}'^* \dot{\gamma}_{ij}^* \rangle \dot{\gamma}'^* + \langle \dot{\gamma}_{ij}'^* \dot{\gamma}_{ij}'^* \dot{\gamma}'^* \rangle. \quad (4.40)$$

Performing this ensemble averaging step has been shown [173] to remove terms that in a volume average give rise to divergent integrals for dilute suspensions in second-order fluids [87, 95]. We now replace ensemble average by volume average in (4.40), and evaluate the quantities both inside the solid spheres and in the fluid volume, noting that inside the solid particles $\dot{\gamma}'^* = -\dot{\gamma}^{\infty*}$, since the total strain-rate inside the particle is zero [116].

Following Koch & Subramanian [116], evaluation of (4.40) gives

$$\langle |\dot{\gamma}_0^*|^2 \dot{\gamma}_0^* \rangle = \left(1 + \frac{125\phi}{28} \right) |\dot{\gamma}^{\infty*}|^2 \dot{\gamma}^{\infty*}. \quad (4.41)$$

Summing all the contributions to the average stress in equation (4.30), we have, finally,

$$\langle \widehat{\sigma}^* \rangle = \left[1 + 2.5\phi - \frac{1}{2} Cu^2 (1 - \beta) (1 - n) (1 + b\phi) |\dot{\gamma}^{\infty*}|^2 \right] \dot{\gamma}^{\infty*}. \quad (4.42)$$

where $b = 288675/34034$. The term inside the square bracket gives the effective viscosity of the suspension. The presence of particles thickens the fluid at the leading order (Einstein viscosity) where as at $\mathcal{O}(Cu^2)$ it decreases the effective viscosity due to enhanced thinning of the fluid. We also note that decreasing n linearly reduces the total correction to fluid viscosity from the Einstein correction as discussed by Tanner *et al.* [199] for dilute suspensions in power law fluids. The presence of particles in a shear-thinning fluid could lead to interesting rheological behaviour when the thickening and thinning effects of particles compete at the same order. Also, the form of above expression suggests that a dilute suspension of rigid spheres in a Carreau fluid will behave as a Carreau fluid. In fact, our results agree with recent results by Domurath *et al.* [58] who use a numerical homogenization technique to obtain the effective viscosity of a dilute suspension in a Bird-Carreau model and find that the effective viscosity too can be modelled using a Bird-Carreau model with modified values of the parameters.

4.8 Conclusion

In this work, we considered a few problems involving spheres in shear-thinning fluids at zero Reynolds number. Using the reciprocal theorem, we

4.8. Conclusion

analytically demonstrated how shear-thinning rheology may lead to qualitative changes in the particle dynamics compared to Newtonian fluids. Specifically, we showed that the translational and rotational dynamics of a sphere are coupled in shear-thinning fluids which can lead to interesting dynamics in problems involving sedimentation of rotating spheres (a setup which may be used as a rheometer) and sedimentation in a background flow field. We also showed that for two equal spheres sedimenting along the line joining their centres, the symmetry arguments used in Newtonian fluids will predict the observed result in a generalised Newtonian fluid. Although these two spheres will sediment maintaining their initial distance of separation, the variation of the shear-thinning effects with initial separation distance is non-monotonic. Finally, we considered a dilute suspension of spheres in a weakly shear-thinning fluid and showed that the resulting suspension will also be a weakly shear-thinning fluid with a viscosity that varies due to competing effects arising from the presence of particles: the particles thicken the fluid (the Einstein viscosity correction) but also increase effective strain-rates thereby enhancing shear-thinning. At higher strain-rates, outside the scope of our weakly non-linear assumption, it would be interesting to investigate strain rates at which the thinning effect supersedes the thickening one.

Chapter 5

Squirming through shear-thinning fluids †

Many microorganisms find themselves immersed in fluids displaying non-Newtonian rheological properties such as viscoelasticity and shear-thinning viscosity. The effects of viscoelasticity on swimming at low Reynolds numbers have already received considerable attention, but much less is known about swimming in shear-thinning fluids. A general understanding of the fundamental question of how shear-thinning rheology influences swimming still remains elusive. To probe this question further, we study a spherical squirmer in a shear-thinning fluid using a combination of asymptotic analysis and numerical simulations. Shear-thinning rheology is found to affect a squirming swimmer in nontrivial and surprising ways; we predict and show instances of both faster and slower swimming depending on the surface actuation of the squirmer. We also illustrate that while a drag and thrust decomposition can provide insights into swimming in Newtonian fluids, extending this intuition to problems in complex media can prove problematic.

5.1 Introduction

Self-propulsion at small length scales is widely observed in biology; common examples include spermatozoa reaching the ovum during reproduction, microorganisms escaping predators and microbes foraging for food [21, 72]. While swimming at low Reynolds numbers is well studied for Newtonian fluids [129], an understanding of the effects of complex (non-Newtonian) fluids on locomotion is still developing. Many biological fluids, such as blood or respiratory and cervical mucus, display complex rheological properties including viscoelasticity and shear-thinning viscosity [120, 142]. A viscoelastic fluid retains a memory of its flow history, whereas the viscosity of a

†This chapter has been previously published under the same title in *Journal of Fluid Mechanics Rapids*, 784 (2015) R1 by Datt *et al.* © 2015 Cambridge University Press.

5.1. Introduction

shear-thinning fluid decreases with the shear rate. While it is important to elucidate how non-Newtonian fluid rheology influences propulsion at low Reynolds numbers because microorganisms swim through biological fluids possessing these properties, an improved understanding may also guide the design of artificial microswimmers [172] and novel microsystems [140] exploiting these nonlinear fluid properties.

Recent research has begun to shed light on the effects of viscoelasticity (see the reviews by Sznitman & Arratia [195] and Elfring & Lauga [70]), but much less is known about swimming in shear-thinning fluids at low Reynolds numbers. Dasgupta *et al.* [42] measured a decreased swimming speed of a waving sheet in a shear-thinning viscoelastic fluid relative to a Newtonian fluid. In contrast, an asymptotic study of a sheet driven by small-amplitude waves showed that the swimming speed of a waving sheet remains unchanged in an inelastic shear-thinning fluid compared to that in a Newtonian fluid [205]. A recent experiment by Gagnon *et al.* [77] on the locomotion of the nematode *Caenorhabditis elegans* has also suggested that shear-thinning viscosity does not modify the nematode's beating kinematics or swimming speed. In addition, numerical studies [148, 149] examined a variety of two-dimensional swimmers and showed that faster or slower swimming in shear-thinning fluids can occur depending on the class of swimmer and its swimming gait. The results were understood in terms of the fluid viscosity distribution surrounding the thrust and drag elements of the swimmer. By estimating separately the propulsive thrust and drag force on the swimmer, Qiu *et al.* [172] obtained a scaling relation predicting the swimming velocity of a single-hinge swimmer (a microscallop), which is enabled to move at low Reynolds numbers by shear-thinning rheology.

The question that emerges from recent literature is when (and why) a swimmer goes faster or slower in a shear-thinning fluid [126]. To address this question we study a canonical idealized model swimmer, the squirmer, in a shear-thinning fluid described by the Carreau-Yasuda model using a combination of asymptotic analysis and numerical simulations. We predict and show instances of both faster and slower swimming depending on the surface actuation of the squirmer. We also explore separately the effects of shear-thinning on the propulsive thrust generated by the squirmer and the drag force it experiences, and demonstrate that extension of these findings to swimming in non-Newtonian fluids can prove problematic.

5.2 Theoretical framework

The hydrodynamics of spherical bodies propelling themselves with surface distortions, otherwise known as squirmers, was first studied by Lighthill [137] and Blake [17]. We follow this approach and model a squirmer with prescribed time-independent tangential surface distortions. The resulting slip velocity around the squirmer is decomposed into a series of Legendre polynomials of the form $u_\theta(r = a, \theta) = \sum_{l=1}^{\infty} B_l V_l(\theta)$, where $V_l(\theta) = -(2/l(l+1))P_l^1(\cos\theta)$ with P_l^1 being the associated Legendre function of the first kind and θ the polar angle measured with the axis of symmetry.

The coefficients B_l are related to Stokes flow singularity solutions. In a Newtonian fluid, the B_1 mode (a source dipole) is the only mode contributing to the swimming velocity, and the B_2 mode (the stresslet) is the slowest decaying spatial mode and thus dominates the far field velocity generated by squirmers. Therefore, often only the first two modes, B_1 and B_2 , of the expansion are considered [59, 101, 213]. The ratio of the two modes, $\alpha = B_2/B_1$, characterises the type of swimmer in a Newtonian fluid: $\alpha > 0$ describes a puller, which generates impetus from its front end (*e.g.* the alga *Chlamydomonas*), whereas $\alpha < 0$ represents a pusher, which generates propulsion from its rear part (*e.g.* the bacterium *Escherichia coli*), and the $\alpha = 0$ case corresponds to a neutral squirmer which induces a potential velocity field. In a Newtonian fluid, the swimming speed of a squirmer $U_N = 2B_1/3$ [17, 137], which is independent of the fluid viscosity because drag and thrust change equally with viscosity. Any modes other than B_1 only modify the surrounding flow structure but do not contribute to the swimming speed of a squirmer. This simple picture, however, does not apply to squirming in a shear-thinning fluid, as we discuss later, where all modes can potentially contribute to the swimming velocity, and adding any other modes to B_1 will nontrivially affect the locomotion of the squirmer.

5.2.1 Shear-thinning rheology: the Carreau-Yasuda model

Shear-thinning fluids experience a loss in apparent viscosity with applied strain rates, a property that results from changes in the fluid microstructure. As the rate of strain exceeds the rate of structural relaxation, one observes microstructural ordering in the fluid [26]. Here, we capture the change in apparent viscosity due to this ordering using the Carreau-Yasuda model for generalised Newtonian fluids [16]. The variation of viscosity with applied

5.2. Theoretical framework

strain rate is given by

$$\eta = \eta_\infty + (\eta_0 - \eta_\infty) \left[1 + \lambda_t^2 |\dot{\gamma}|^2 \right]^{\frac{n-1}{2}}, \quad (5.1)$$

where η_0 and η_∞ are the zero- and infinite-shear rate viscosities respectively. The power law index n characterises the degree of shear-thinning ($n < 1$) and the relaxation time λ_t sets the crossover strain rate at which non-Newtonian behaviour starts to become significant. The magnitude of the strain rate tensor is given by $|\dot{\gamma}| = (II/2)^{1/2}$, where $II = \dot{\gamma}_{ij}\dot{\gamma}_{ij}$ is the second-invariant of the tensor. As an example, measured values for human cervical mucus can be fitted by the Carreau-Yasuda model with values $\eta_0 = 145.7$ Pa.s, $\eta_\infty = 0$ Pa.s, $\lambda_t = 631.04$ s and $n = 0.27$ [99, 205].

We non-dimensionalise the flow quantities taking the first mode, B_1 , of the surface actuation as the scale for velocity and the radius, a , of the squirmer as the characteristic length scale. The strain rates are scaled with $\omega = B_1/a$ and the stresses by $\eta_0\omega$, such that the constitutive equation takes the dimensionless form

$$\boldsymbol{\tau}^* = \left\{ \beta + (1 - \beta) \left[1 + Cu^2 |\dot{\gamma}^*|^2 \right]^{\frac{n-1}{2}} \right\} \dot{\gamma}^*, \quad (5.2)$$

where $\boldsymbol{\tau}$ is the deviatoric stress tensor, and dimensionless quantities are denoted by stars (*). The Carreau number $Cu = \omega\lambda_t$ is the ratio of the characteristic strain rate, defined by the surface actuation ω , to the crossover strain rate, defined by the fluid relaxation $1/\lambda_t$. The viscosity ratio is given by $\beta = \eta_\infty/\eta_0 \in [0, 1]$.

It is evident from (5.2) that when the actuation rate ω is much smaller or much larger than the fluid relaxation rate $1/\lambda_t$, *i.e.* when $Cu \rightarrow 0$ or $Cu \rightarrow \infty$, the shear-thinning fluid reduces to a Newtonian fluid of constant viscosity η_0 (dimensionless viscosity 1) or η_∞ (dimensionless viscosity β) respectively. Recalling that for a given surface actuation the swimming speed of a squirmer in the Newtonian regime is independent of the fluid viscosity, we therefore expect the swimming speed of a squirmer in a shear-thinning fluid to converge to its Newtonian value in the limits $Cu \rightarrow 0$ or $Cu \rightarrow \infty$. Non-monotonic variation of the swimming speed with Cu is expected for any swimmer with prescribed kinematics and has been observed by Montenegro-Johnson *et al.* [148] for some two-dimensional model swimmers. In this study we employ both asymptotic analysis and numerical simulations to investigate these effects of shear-thinning rheology on swimming at low Reynolds numbers.

5.2.2 Asymptotic analysis

The deviatoric stress tensor $\boldsymbol{\tau}^*$ in (5.2) is a non-linear function of the strain rate tensor $\dot{\boldsymbol{\gamma}}^*$. Assuming only a weak nonlinearity, we may uncouple the Newtonian and non-Newtonian contributions, writing

$$\boldsymbol{\tau}^* = \dot{\boldsymbol{\gamma}}^* + \varepsilon \mathbf{A}^*, \quad (5.3)$$

with $\varepsilon \ll 1$ as a dimensionless measure of the deviation from the Newtonian case ($\varepsilon = 0$).

We observe that in the limits $Cu = 0$ or $\beta = 1$, (5.2) reduces to a Newtonian constitutive equation. Thus, one may expect weakly nonlinear behaviour when the fluid relaxation rate is much faster than the surface actuation rate ($\varepsilon = Cu^2 \ll 1$), or when the zero-shear-rate viscosity is very close to the infinite-shear-rate viscosity ($\varepsilon = 1 - \beta \ll 1$).

Henceforth we shall work in dimensionless quantities and therefore drop the stars (*) for convenience.

Expansion in Carreau number

Expanding all fields in regular perturbation series in $\varepsilon = Cu^2$, we obtain, order by order, the constitutive equations

$$\begin{aligned} \boldsymbol{\tau}_0 &= \dot{\boldsymbol{\gamma}}_0, \\ \boldsymbol{\tau}_1 &= \dot{\boldsymbol{\gamma}}_1 + \frac{(n-1)}{2} (1-\beta) |\dot{\boldsymbol{\gamma}}_0|^2 \dot{\boldsymbol{\gamma}}_0, \end{aligned} \quad (5.4)$$

hence $\mathbf{A} = \frac{(n-1)}{2} (1-\beta) |\dot{\boldsymbol{\gamma}}_0|^2 \dot{\boldsymbol{\gamma}}_0$ to leading order in (5.3). It should be noted that the first correction to the Newtonian behaviour is linear in n , which points to a linear dependence of the swimming speed on n upon using (5.8), elucidating the trend suggested by the two-dimensional numerical findings in Montenegro-Johnson *et al.* [149]. We also remark that this expansion is valid only when $Cu^2 |\dot{\boldsymbol{\gamma}}|^2$ is $o(1)$ and is therefore not uniformly valid across all values of strain rates.

Expansion in viscosity ratio

Expanding in perturbation series with $\varepsilon = 1 - \beta$ gives us, order by order, the constitutive equations

$$\boldsymbol{\tau}_0 = \dot{\boldsymbol{\gamma}}_0, \quad (5.5)$$

$$\boldsymbol{\tau}_1 = \dot{\boldsymbol{\gamma}}_1 + \left\{ -1 + \left(1 + Cu^2 |\dot{\boldsymbol{\gamma}}_0|^2 \right)^{\frac{n-1}{2}} \right\} \dot{\boldsymbol{\gamma}}_0, \quad (5.6)$$

where in this limit $\mathbf{A} = \left\{ -1 + (1 + Cu^2|\dot{\gamma}_0|^2)^{\frac{n-1}{2}} \right\} \dot{\gamma}_0$ to leading order in (5.3). It should be noted that this asymptotic expansion is uniformly valid for all strain rates or Carreau numbers, which permits a full-range study of the non-monotonic swimming behaviour.

5.2.3 The reciprocal theorem

Stone & Samuel [193] demonstrated the use of the Lorentz reciprocal theorem in low-Reynolds-number hydrodynamics [93] to obtain the swimming velocity of a squirmer for a given prescribed surface actuation \mathbf{u}^S without calculation of the unknown flow field, provided one can solve the resistance/mobility problem for the swimmer shape (with surface S). Lauga [122, 125] then developed integral theorems extending this method for use with complex fluids. We use these methods in the subsequent calculations to obtain the swimming velocity of a squirmer in a shear-thinning fluid; the methodology adopted below closely follows the formulation in Elfring & Lauga [70].

We represent the velocity field and the associated total stress tensor for a force- and torque-free swimmer with \mathbf{u} and $\boldsymbol{\sigma}$ respectively. We consider the corresponding resistance problem in a Newtonian fluid to simplify the calculation of the swimming velocity. The resistance problem (denoted with a hat) involves the rigid-body motion with translational velocity $\hat{\mathbf{U}}$ and rotational velocity $\hat{\boldsymbol{\Omega}}$, and the corresponding velocity field and associated stress tensor are represented by $\hat{\mathbf{u}}$ and $\hat{\boldsymbol{\sigma}}$ respectively. Due to the linearity of the Stokes equation, we may write $\hat{\mathbf{u}} = \hat{\mathbf{L}} \cdot \hat{\mathbf{U}}$, $\hat{\boldsymbol{\sigma}} = \hat{\mathbf{T}} \cdot \hat{\mathbf{U}}$ and $\hat{\mathbf{F}} = -\hat{\mathbf{R}} \cdot \hat{\mathbf{U}}$. Here, for compactness, both the translational and the rotational components of velocity are contained in $\hat{\mathbf{U}}$ and, similarly, the corresponding matrices contain both the translational and rotational terms. In weakly nonlinear complex fluids, the swimming velocities $\mathbf{U} = [\mathbf{U} \ \boldsymbol{\Omega}]^\top$ are given by

$$\mathbf{U} = \hat{\mathbf{R}}^{-1} \cdot \left[\int_S \mathbf{u}^S \cdot (\mathbf{n} \cdot \hat{\mathbf{T}}) \, dS - \varepsilon \int_V \mathbf{A} : \nabla \hat{\mathbf{L}} \, dV \right]. \quad (5.7)$$

The integral over the volume of fluid V external to S in the equation measures the change in swimming dynamics due to the non-Newtonian behaviour of the fluid. For a spherical squirmer with axisymmetrical tangential surface distortions, there is no rotational motion and the translational velocity is given simply by

$$\mathbf{U} = -\frac{1}{4\pi} \int_S \mathbf{u}^S \, dS - \frac{\varepsilon}{8\pi} \int_V \mathbf{A} : \left(1 + \frac{1}{6} \nabla^2 \right) \nabla \mathbf{G} \, dV, \quad (5.8)$$

where $\mathbf{G} = \frac{1}{r} \left(\mathbf{I} + \frac{\mathbf{r}\mathbf{r}}{r^2} \right)$ is the Oseen tensor (or Stokeslet). The first term on the right-hand side is the result of swimming in a Newtonian fluid [193], and the last term in the equation contains the weakly nonlinear effect, which can be evaluated analytically in some special cases and can be computed in general by numerical quadrature readily.

5.2.4 Numerical solution

The numerical simulations of the momentum equations at zero Reynolds number with the Carreau-Yasuda constitutive relation (5.1) are implemented in the finite element method software COMSOL. We use a square computational domain of size $500a \times 500a$, discretized by approximately 30000–50000 Taylor-Hood ($P2 - P1$) triangular elements. The mesh is refined near the squirmer in order to properly capture the spatial variation of the viscosity. Since slowly decaying flow fields are expected at low Reynolds numbers, a large domain size is important to guarantee accuracy. The simulations are performed in a reference frame moving with the swimmer and the far-field (inlet) velocity is varied to obtain a computed zero force on the squirmer. In addition to comparing with the asymptotic analysis in this work, we have validated our implementation against the analytical results for a three-dimensional squirmer in a Newtonian fluid [17, 137] and a two-dimensional counterpart in a shear-thinning fluid [149].

5.3 Results and discussion

As a first step we investigate the effect of shear-thinning rheology upon swimming speed by considering the small- Cu regime and use (5.8) to derive an analytical formula for the leading-order swimming speed U of a two-mode squirmer (with B_1 and B_2 modes)

$$\frac{U}{U_N} = 1 + Cu^2 (1 - \beta) \frac{(n - 1)}{2} C_1 \left[1 + C_2 \alpha^2 \right], \quad (5.9)$$

where $C_1 = 0.49$ and $C_2 = 2.25$ are numerical constants, and U_N is the Newtonian swimming speed. In a shear-thinning fluid we have $n < 1$ and $\beta < 1$, and hence we find that this two-mode squirmer can only swim slower than in a Newtonian fluid ($U/U_N < 1$) in the small- Cu regime. The two-dimensional numerical simulations in Montenegro-Johnson *et al.* [149] reported that a neutral squirmer ($\alpha = 0$) swims slower in a shear-thinning fluid, which is consistent with our analytical results for a three-dimensional

5.3. Results and discussion

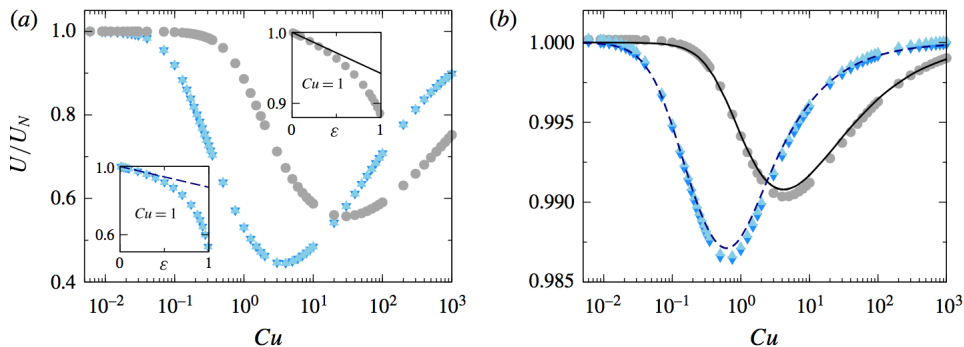


Figure 5.1: In (a) we show results from numerical simulations for a neutral squirmer ($\alpha = 0$, \bullet), puller ($\alpha = 5$, \blacktriangle) and pusher ($\alpha = -5$, \blacktriangledown) for $\epsilon = 0.99$ and $n = 0.25$. (b) The non-monotonic variation in velocity is well captured by asymptotics for a neutral squirmer (solid line), and a pusher/puller (dashed line) at $\epsilon = 0.1$ and $n = 0.25$.

squirmer (5.9) in the small- Cu regime, but we also find that the same conclusion of a decreased swimming speed holds for pushers ($\alpha < 0$) and pullers ($\alpha > 0$) as well. In contrast to the case of swimming in a viscoelastic fluid, where the pusher and puller attain different velocities given the same magnitude of α [217], (5.9) reveals that in a shear-thinning fluid a pusher and puller have the same swimming velocity because the function for swimming speed is even in α ; this asymptotic result is verified by numerical simulations to hold for different ranges of Cu and β (as shown by the overlapping of the upper and lower triangles in figure 5.1).

To further characterise the variation of swimming speed, over the full range of Cu , we consider the asymptotic limit $\epsilon = 1 - \beta \ll 1$, aided by numerical simulations for larger values of ϵ . Biological fluids often have a small viscosity ratio β and hence $\epsilon = 1 - \beta$ is typically close to 1. In figure 1a, we present the numerical results for a neutral squirmer, pusher, and puller in the biological limit using the values $\epsilon = 0.99$ and $n = 0.25$ to emulate human cervical mucus [99, 205]. We demonstrate in the upper inset (neutral squirmer) and lower inset (pusher and puller) in figure 1a that the numerical solutions for the swimming speed ratio converge to the asymptotic solutions (solid line in the upper inset; dashed line in the lower inset) when $\epsilon \rightarrow 0$. In figure 1b, the results are presented at $\epsilon = 0.1$ and we note that all qualitative features of the impact of a shear-thinning fluid in the biological limit ($\epsilon \approx 1$, figure 1a) on the swimming speed are well captured by the asymptotic analysis (when $\epsilon \ll 1$, figure 1b) and as expected, the numerical

simulations (symbols) agree very well with the asymptotic theory (lines) when ε is small (figure 1b).

The non-monotonic variation of the swimming speed with Cu may be expected based on the asymptotic behaviour of the constitutive relation discussed at the end of section 5.2.1. To understand the variation more quantitatively, recall the form of \mathbf{A} in (5.6) and observe from the integral expression for swimming velocity (5.8) that at low strain rates, the non-Newtonian contribution $\mathbf{A} \sim \frac{1}{2}Cu^2(n-1)|\dot{\gamma}_0|^2\dot{\gamma}_0$ vanishes as $Cu \rightarrow 0$. At high strain rates, $\mathbf{A} \sim -\dot{\gamma}_0 + (Cu|\dot{\gamma}_0|)^{n-1}\dot{\gamma}_0$; the first term, $-\dot{\gamma}_0$, vanishes under the integration in (5.8) [70], and the remaining term gives a non-Newtonian contribution that vanishes as $Cu \rightarrow \infty$ because for a shear-thinning fluid $n < 1$. The swimming speed therefore displays a non-monotonic variation with Cu , and since the speed decreases when Cu is small as shown by (5.9), a minimum swimming speed may be expected to occur at intermediate values of Cu (the ‘power-law’ regime of the model), where the non-Newtonian effect is most significant. However, for a given swimming gait, if the actuation rate of the swimmer is small enough or large enough, the shear thinning fluid may appear to have no effect at all on the swimming speed.

To understand the reduction in swimming speed, inspired by the qualitative descriptions given in Montenegro-Johnson *et al.* [149], we look into the thrust and the drag of the swimming problem separately.

5.3.1 Drag and thrust

We separate the swimming problem into a drag problem (a sphere undergoing rigid body translation \mathbf{U} inducing hydrodynamic drag) and a thrust problem (a sphere held fixed undergoing only tangential surface distortions thereby generating thrust). The superposition of these two sub-problems gives the entire swimming problem in a Newtonian fluid in the Stokes regime; this is obviously not the case in a shear-thinning fluid due to its nonlinear constitutive equation. However, by looking at the thrust and the drag problems, one may gain insight into the more complex non-Newtonian swimming problem [149, 172].

We derive the expressions for drag and thrust in a shear-thinning fluid again via the reciprocal theorem approach (section 5.2.3) by utilizing the solution to the resistance problem in a Newtonian fluid. The drag force on a sphere moving with a velocity \mathbf{U} in weakly shear-thinning fluid is given by $\mathbf{F}_D = -6\pi\mathbf{U} - \frac{3}{4}\varepsilon \int_V \mathbf{A}_D : \left(1 + \frac{1}{6}\nabla^2\right) \nabla\mathbf{G} dV$, where \mathbf{A}_D is formed by the solution to the Newtonian drag problem. Similarly, the thrust force generated by a sphere held stationary with surface actuation \mathbf{u}^S in a weakly shear-

5.3. Results and discussion

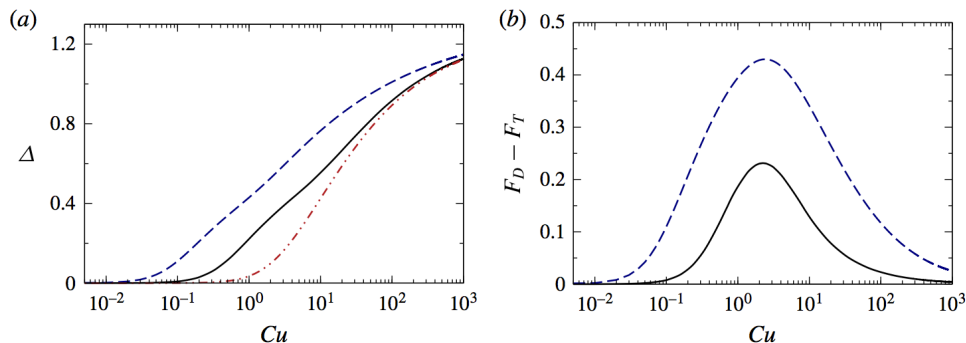


Figure 5.2: In (a), the symbol Δ denotes the difference between drag, or thrust, in a shear-thinning fluid and a Newtonian fluid: the dash-dot curve represents the drag reduction in a shear-thinning fluid compared with a Newtonian fluid, while the solid and dashed curves represent loss in thrust for squirmers with $\alpha = 0$ and $\alpha = \pm 5$ respectively ($n = 0.25$, $\varepsilon = 0.1$). In (b) we show that the difference between drag and thrust is positive both for a neutral squirmer (solid) and a pusher/puller (dashed) in a shear-thinning fluid. All quantities are dimensionless.

thinning fluid is given by $\mathbf{F}_T = -\frac{3}{2} \int_S \mathbf{u}^S dS - \frac{3}{4} \varepsilon \int_V \mathbf{A}_T : \left(1 + \frac{1}{6} \nabla^2\right) \nabla \mathbf{G} dV$, where \mathbf{A}_T is formed by the solution to the Newtonian thrust problem.

One could expect a drag reduction when a rigid sphere is pulled with a constant velocity through a shear-thinning fluid since the fluid viscosity is reduced by the fluid straining motion. However, it is interesting to see in figure 5.2a that the thrust reduction caused by the shear-thinning rheology is larger than the drag reduction for a large range of Cu . This more severe reduction in thrust than drag then suggests slower swimming speeds compared with the Newtonian case, which correctly predicts the trend found by detailed calculations (figure 5.1). In addition, for very small or large values of Cu , the difference between the magnitudes of drag and thrust ($F_D - F_T$) vanishes as shown in figure 5.2b, respecting the limits where the swimming speed should recover the Newtonian value (figure 5.1).

Although conceptually intuitive, the drag and thrust decomposition is not complete as it neglects the contribution of non-linear products in the non-Newtonian stress to the full swimming problem, namely $\mathbf{A} \neq \mathbf{A}_T + \mathbf{A}_D$, due to the non-linearity in the constitutive equation. We will give a counter-example in section 5.3.2 below to illustrate a scenario when these intuitive arguments fail.

5.3.2 Addition of other squirmer modes

The results from the detailed asymptotic and numerical analysis as well as the intuitive model for a two-mode squirmer seem to suggest that the shear-thinning rheology acts to hinder the locomotion. This raises the simple question of whether this conclusion still holds if other modes of surface actuation are present. The picture is clear for a Newtonian fluid: only the B_1 mode contributes to swimming and the addition of other modes does not alter the swimming speed. However, can the shear-thinning rheology render other modes, typically not considered in the Newtonian analysis, effective for propulsion? We address these questions using the asymptotic and numerical tools developed in the previous sections.

We first note that the B_3 mode alone leads to locomotion in a shear-thinning fluid in stark contrast to a Newtonian fluid as only the B_1 mode has a non-zero surface average (see (5.8)). Indeed any odd mode alone may lead to locomotion in a shear-thinning fluid (even modes alone do not swim by symmetry). We also find quite distinctive behaviour when the B_3 mode is combined with other modes. In the $Cu \ll 1$ regime, we can derive an analytical expression allowing us to predict the values of α and $\zeta = B_3/B_1$ for faster or slower swimming. To quadratic order in Cu , we find

$$\frac{U}{U_N} = 1 + Cu^2 (1 - \beta) \frac{(n-1)}{2} C_1 [1 + C_2 (1 + C_3 \zeta) \alpha^2 + C_4 (C_5 \zeta^2 + C_6 \zeta - 1) \zeta], \quad (5.10)$$

where the additional numerical constants are given by $C_3 = 0.51$, $C_4 = 0.70$, $C_5 = 0.18$, and $C_6 = 1.66$. Again the swimming speed is even in α and we recover (5.9) when $\zeta = 0$ as expected. From (5.10) we can predict that faster swimming ($U/U_N > 1$) will occur if

$$\left. \frac{\partial^2 U}{\partial Cu^2}(\alpha, \zeta) \right|_{Cu=0} > 0, \quad (5.11)$$

in other words when the term in the square brackets in (5.10) is negative. In figure 5.3a we plot the level set curve below which faster swimming occurs in the small Cu regime; we find that this can only occur when ζ is negative for any α . For example, when $\alpha = 0$ we must have $\zeta < -10.11$, while $\alpha = \pm 5$, $\zeta < -2.22$ leads to faster swimming.

In figure 5.3b we show the variation of swimming speed for two swimmers with α and ζ chosen below the level set curve (the upper solid and dashed lines) and two swimmers with α and ζ chosen above the level set curve (the lower solid and dashed lines). We note that the swimming speeds of

5.3. Results and discussion

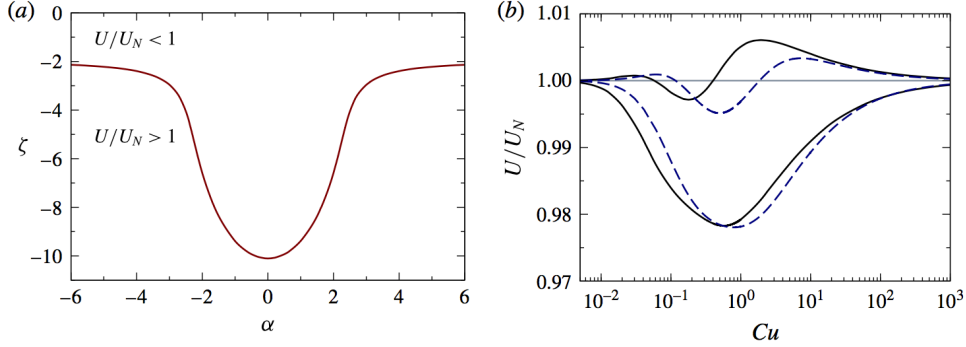


Figure 5.3: In (a) we show the level set curve below which faster swimming occurs for specific values of α and $\zeta = B_3/B_1$ when $Cu \ll 1$. In (b) we show the swimming speed of a neutral squirmer (solid line) and a pusher/puller (dashed line) at values of ζ chosen below the curve in (a) so that the swimming speed is larger than the Newtonian value at small Cu (the upper solid line: $\alpha = 0$, $\zeta = -15$; the upper dashed line: $\alpha = \pm 5$, $\zeta = -4$); conversely, with values of ζ above the curve in (a) the swimmers always swim slower than in a Newtonian fluid as shown (lower solid line: $\alpha = 0$, $\zeta = 15$; lower dashed lines: $\alpha = \pm 5$, $\zeta = 4$). Here $\varepsilon = 0.1$, $n = 0.25$.

the faster swimmers in the small- Cu regime experience a subsequent fall below the Newtonian value and then a rise above it as Cu increases, before asymptoting to the Newtonian swimming speed at high Cu . This indicates that microorganisms (with a given swimming gait) can swim both faster and slower than in a Newtonian fluid depending on the actuation rate of that gait. In contrast, the two swimmers that swim slower in a Newtonian fluid in the small- Cu regime remain slower for larger Cu with a non-monotonic variation similar to that observed previously (see figure 5.1). These results also hold qualitatively for large values of ε .

We emphasize that the thrust and drag reduction model is unable to explain the faster swimming speed with the addition of a B_3 mode because in these cases the thrust still decreases more than the drag over a wide range of Carreau numbers, if they are considered separately. This serves as a counter-example demonstrating how analyzing drag and thrust separately may not adequately describe swimming in complex media. This fact points specifically to the interaction between thrust and drag fields, due to the non-linearity in the constitutive equation, as the cause of faster than Newtonian swimming.

5.4 Conclusion

We show in this work that shear-thinning rheology affects a squirmer with a prescribed swimming gait in nontrivial and surprising ways; we predict, analytically, instances of both faster and slower swimming than in a Newtonian fluid depending on the details of the prescribed boundary conditions. Indeed we demonstrate that even with the same squirming modes a squirmer can swim faster or slower depending on its rate of actuation. In general, these results point to the importance of both the spatial and the temporal details of the swimming gait of a microorganism and ultimately the difficulty in predicting the resulting effect of the non-Newtonian fluid *a priori*. In light of this, an important next step would be to incorporate models of internal force generation for biological swimmers and determine how the fluid rheology affects the resultant gait itself in concert with propulsion. Finally, we remark that the drag and thrust decomposition of the swimming problem is indeed effective in Newtonian fluids and may also be insightful in complex fluids in some instances, but one should use caution when extending the results to non-Newtonian swimming as the inherent non-linearity of the problem can be significant enough for a Newtonian-like decomposition to yield qualitatively flawed predictions as illustrated by the example we provide.

Chapter 6

An active particle in a complex fluid §

In this work, we study active particles with prescribed surface velocities in non-Newtonian fluids. We employ the reciprocal theorem to obtain the velocity of an active spherical particle with an arbitrary axisymmetric slip velocity in an otherwise quiescent second-order fluid. We then determine how the motion of a diffusiophoretic Janus particle is affected by complex fluid rheology, namely viscoelasticity and shear-thinning viscosity, compared to a Newtonian fluid, assuming a fixed slip velocity. We find that a Janus particle may go faster or slower in a viscoelastic fluid, but is always slower in a shear-thinning fluid as compared to a Newtonian fluid.

6.1 Introduction

Active particles are self-driven units which can convert stored or ambient free energy into systematic motion [139, 180]. These particles are found on length scales from subcellular to oceanic, and range from aquatic, terrestrial and aerial flocks to colloidal particles propelled through fluid by catalytic activity at their surfaces. The interactions of active particles with the medium they are found in, and amongst themselves, give rise to fascinating collective behaviour and beautiful pattern formation [139]. Active particles in fluid media can be either living, like swimming microorganisms [129], or synthetic, like crystals of light-activated colloidal surfers [162], swimming droplets [202] and chemically self-propelled nano-motors [107]. For sufficiently small sizes of active particles, inertial forces are negligible compared to viscous forces, and one may assume the fluid to be under an instantaneous equilibrium of forces [170].

Several microorganisms propel themselves using small surface distortions as in the coordinated beating of cilia on *Opalina* and *Paramecium* [184]. As

§This chapter has been previously published under the same title in *Journal of Fluid Mechanics*, 823, (2017) 675–688 by Datt *et al.* © 2017 Cambridge University Press.

such, these swimmers are often modelled as spheres with a prescribed surface slip velocity [165]; the slip velocity serves as a coarse-grained description of any deformation or dynamics on the particle body that leads to its motion [17, 137]. Likewise, a chemically active colloidal particle with asymmetric catalytic properties generates a non-uniform distribution of reaction products and hence, also a flow within a thin ‘inner’ region near the particle’s surface [2]. The surface flow and the resultant diffusiophoretic motion may also be modelled by prescribing an apparent slip velocity on the particle surface [106]. The motion of these particles, arising due to a surface slip velocity is, by now, well-understood for particles that move in Newtonian fluids at low Reynolds numbers [22, 71]. In general, the propulsive force generated by the surface slip velocity balances the hydrodynamic drag force due to the rigid body motion of the particle. For simple bodies, the swimming velocity is given directly by the surface average of the prescribed slip velocity [67] and because of this simplification, detailed models of the surface slip velocity for living and synthetic active particles are often unnecessary.

In contrast, an understanding of dynamics of active particles in non-Newtonian fluids is still developing [164]. Unlike in Newtonian fluids, the constitutive equation for stress is nonlinear in non-Newtonian fluids and as a result a straightforward linear decomposition of the flow field into drag and thrust components fails [45]. Consequently, a surface average of the slip velocity does not yield the velocity of the particle, and so a detailed description of the surface slip velocity may be significant in complex fluids. Despite this, many recent studies consider, as a point of comparison with Newtonian fluids, the *two-mode* swimmer model [52, 135, 149, 217], although recently it was shown that neglected details of the surface slip velocity can have a qualitative effect on the motion of the particle in a shear-thinning fluid [45].

In this work, we analyse the motion of an active particle in a weakly nonlinear complex fluid with a *general* axisymmetric slip velocity by means of the reciprocal theorem [125, 193]. This allows us to consider a complete range of prescribed motions on the particle surface and to determine what details matter and why. We note that the swimming gait (apparent surface slip velocity) of the swimmer may itself be affected in complex fluids as compared to Newtonian fluids, due to, for example, constraints on power for biological swimmers or changes in solute diffusivity for diffusiophoretic particles. Here, however, we consider swimmers with the same swimming gait as in Newtonian fluids. As an example, we consider the slip velocity of self-diffusiophoretic *Janus* particles and discuss the effects of viscoelasticity and shear-thinning rheology on the particles’ propulsion velocity. These

active colloidal particles, at times, may swim through polymer suspensions [31], and an understanding of their dynamics in complex fluids may lead to interesting applications in biological and chemical engineering [169]. Recent studies on the effects of rheology on the motion of Janus particles [86, 157] have shown that the particle translational and rotational dynamics are coupled in media with viscoelasticity or local viscosity variations. Further, motivated by recent works on the dynamics of active particles in background flow of non-Newtonian fluids [3, 51, 140], we generalise the reciprocal theorem formulation [70, 125, 128] to include a background flow in the spirit of previous classical work on passive particles in weakly nonlinear flows [133].

6.2 Modelling active particles

Biological microswimmers possess variety of different geometries and swimming modes; many, like ciliates (*Opalina*) and multicellular colonies of flagellates (*Volvox*), are approximately spherical in shape and propel due to the beating of closely packed cilia on their surface [184]. These swimmers, in an idealised model, are mathematically represented as spheres with small amplitude radial and tangential motions of elements of the surface. The original model (now known as the squirmer model), by Lighthill [137] and Blake [17], considered only axisymmetric surface distortions so the swimmers could swim only along their axis of symmetry. Recently, Pak & Lauga [159] extended the model to arbitrary surface deformations allowing three-dimensional translational and rotational swimming kinematics of the swimmer.

Synthetic active particles too can be conceived in many shapes with a variety of propulsion mechanisms [207]. Self-phoretic particles, in particular, are colloids which are able to generate local gradients through the catalytic physiochemical properties on their surface [84, 85, 145]. The short-range interaction between the surface of the swimmer and the self-generated outer field gradient (solute concentration, temperature or electric field) locally creates fluid motion in the vicinity of particle boundary that leads to particle propulsion due to phoresis [2]. When the interaction layer is thin compared to the particle size, phoretic effects can be represented by the generation of slip velocities on the particle surface [106, 145].

In this work, we focus on spherical phoretic particles [85, 145], with an

axisymmetric slip velocity expressed here as

$$\mathbf{u}^S(\theta, t) = \sum_{p=1}^{\infty} \alpha_p(t) K_p(\cos \theta) \hat{\mathbf{e}}_{\theta} \quad (6.1)$$

with

$$K_p(\cos \theta) = \frac{(2p+1)}{p(p+1)} P'_p(\cos \theta) \sin \theta, \quad (6.2)$$

where $\hat{\mathbf{e}}_{\theta}$ is a unit vector in the direction of increasing polar angle θ in spherical coordinates and P_p is the p^{th} Legendre polynomial [144]. The flow field due to the swimmer in Newtonian fluids is completely characterised and determined by the intensities of the ‘squirming’ modes, α_p [17]. Of particular significance are the first two modes: α_1 , which fixes the swimming velocity [137], and α_2 , which defines the strength of the force dipole generated by the swimmer $\Sigma = 10\pi\alpha_2$ [145]. Consequently, for analyses of collective behaviour [54, 218], or transport of nutrients [100, 144], in Newtonian fluids, active particles are very often modelled with a truncated slip velocity expansion which retains only the first two terms. We consider here only steady slip velocities on the particle surface, which is often appropriate for phoretic particles; however, in general, especially for models of biological organisms where the surface motion arises from a cyclical deformation, the slip velocities may depend on time t [166]. This time dependence of the surface actuation is then particularly important for fluids which possess history dependence, like polymer solutions, especially when the time scale of surface actuation is of the same order as the fluid relaxation time [69].

Self-diffusiophoretic particles propel due to asymmetric surface chemical reactions [2, 20, 84] which cause an induced imbalance of osmotic effects in a thin interaction layer on the particle surface. The resulting flow in this thin layer, the apparent slip velocity, is proportional to the local solute concentration gradient and the specifics of solute–surface interactions (phoretic mobility). Under the assumption that diffusion is fast enough so that the chemical reaction at the surface is controlled by the far-field solute concentration (fixed-flux formulation, Damkohler number = 0) and on neglecting the distortion of solute distribution due to flow resulting from phoretic effects (Péclet number = 0), one obtains the squirming modes in (6.1)

$$\alpha_p = \frac{pA_p}{2p+1} \frac{M}{D}, \quad (6.3)$$

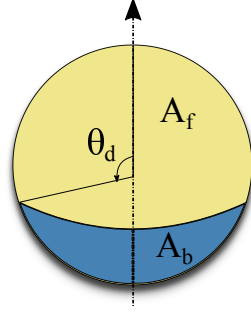


Figure 6.1: Self-phoretic particle with two compartments of different activity, A_f and A_b . We consider particles with a constant uniform mobility over the surface. When $\theta_d = \pi/2$, the particle has compartments of equal cover, which we call a symmetric Janus particle.

where the surface activity $A(\theta) = \sum A_p P_p(\cos \theta)$ (and positive values denote absorption of solute), the phoretic mobility M is assumed to be constant over the surface and D is the solute diffusivity (see Michelin & Lauga [145] for details).

We consider Janus-type particles with a discontinuous change in activity between two distinct compartments of the surface activity, $A(\theta) = A_f$ for $\theta < \theta_d$ while $A(\theta) = A_b$ for $\theta > \theta_d$ as illustrated in figure 6.1. Here, we take the rear compartment to be inert, $A_b = 0$, in which case the coefficients are given by [145]

$$A_0 = \frac{A_f}{2} (1 - \cos \theta_d), \quad A_n = \frac{A_f}{2} [P_{n-1}(\cos \theta_d) - P_{n+1}(\cos \theta_d)] \quad (n \geq 1), \quad (6.4)$$

which then set the squirring modes and the entire flow field for Janus particles in Newtonian fluids.

6.3 Swimming in a background flow of a weakly non-Newtonian fluid

Consider a general active particle (or swimmer) \mathcal{B} with surface $\partial\mathcal{B}$ immersed in a background flow \mathbf{u}^∞ of an incompressible and weakly nonlinear complex fluid. The velocity on the swimmer surface $\partial\mathcal{B}$ is

$$\mathbf{u}(\mathbf{x} \in \partial\mathcal{B}) = \mathbf{U} + \boldsymbol{\Omega} \times \mathbf{x} + \mathbf{u}^S, \quad (6.5)$$

6.3. Swimming in a background flow of a weakly non-Newtonian fluid

where \mathbf{U} is the translational velocity of the particle, $\mathbf{\Omega}$ is the rotational velocity and \mathbf{u}^S is the prescribed deformation velocity on its surface (the swimming gait).

The rheology of the non-Newtonian fluid is assumed to be only weakly nonlinear [70, 125], and thus, a constitutive equation of the form

$$\boldsymbol{\tau} = \eta \dot{\boldsymbol{\gamma}} + \varepsilon \mathbf{A}[\mathbf{u}], \quad (6.6)$$

where $\boldsymbol{\tau}$ is the deviatoric stress, η is the viscosity and $\dot{\boldsymbol{\gamma}}$ the strain-rate tensor such that $\eta \dot{\boldsymbol{\gamma}}$ gives the Newtonian contribution. $\mathbf{A}[\mathbf{u}]$ is a symmetric tensor and a nonlinear functional of \mathbf{u} and ε is a small dimensionless parameter characterising the deviation from Newtonian behaviour, for example, small Deborah number in case of viscoelastic fluids or small Carreau number for shear-thinning fluids.

We consider the flow field to be inertialess and in mechanical equilibrium with $\nabla \cdot \boldsymbol{\sigma} = \mathbf{0}$, where $\boldsymbol{\sigma}$ is the stress tensor corresponding to the velocity field \mathbf{u} . We define disturbance fields $\mathbf{u}' = \mathbf{u} - \mathbf{u}^\infty$ and $\boldsymbol{\sigma}' = \boldsymbol{\sigma} - \boldsymbol{\sigma}^\infty$ where \mathbf{u}^∞ and $\boldsymbol{\sigma}^\infty$ correspond to the velocity and stress fields of the background flow in the absence of the particle. Due to the nonlinearity of constitutive equation (6.6), \mathbf{u}' and $\boldsymbol{\sigma}'$, in general, do not represent velocity and stress fields of the same problem (except when $\varepsilon = 0$).

Stone & Samuel [193] demonstrated a shortcut to obtain the swimming velocity of an arbitrary swimmer in a Newtonian fluid with a given prescribed surface actuation \mathbf{u}^S without calculation of its unknown flow field using the Lorentz reciprocal theorem in low Reynolds number hydrodynamics [93], provided one can solve the rigid-body resistance/mobility problem for a body of the same shape. Using this approach Lauga [122, 125] then developed integral theorems to determine the swimming velocity in complex fluids. We use these methods below, following the formulation in [69, 70], to obtain the swimming velocity of a swimmer in a weakly non-Newtonian fluid but include the possibility of a non-zero background flow for generality.

For the resistance problem (denoted with a hat), we consider rigid-body motion with translational velocity $\hat{\mathbf{U}}$ and rotational velocity $\hat{\mathbf{\Omega}}$, through a Newtonian fluid with corresponding velocity field $\hat{\mathbf{u}}$ and associated stress tensor $\hat{\boldsymbol{\sigma}} = \hat{\eta} \hat{\boldsymbol{\gamma}}$. As both flows (due to the swimmer and due to rigid-body motion) are in mechanical equilibrium, we have

$$\hat{\mathbf{u}} \cdot (\nabla \cdot \boldsymbol{\sigma}') = \mathbf{u}' \cdot (\nabla \cdot \hat{\boldsymbol{\sigma}}) = 0. \quad (6.7)$$

Integrating over the volume of fluid, \mathcal{V} , exterior to \mathcal{B} and applying the divergence theorem while enforcing the incompressibility of the flows, we

6.3. Swimming in a background flow of a weakly non-Newtonian fluid

get

$$\int_{\partial\mathcal{V}} \mathbf{n} \cdot \boldsymbol{\sigma}' \cdot \hat{\mathbf{u}} \, dS + \int_{\mathcal{V}} \boldsymbol{\tau}' : \nabla \hat{\mathbf{u}} \, dV = \int_{\partial\mathcal{V}} \mathbf{n} \cdot \hat{\boldsymbol{\sigma}} \cdot \mathbf{u}' \, dS + \int_{\mathcal{V}} \hat{\boldsymbol{\tau}} : \nabla \mathbf{u}' \, dV = 0, \quad (6.8)$$

where we have defined $\boldsymbol{\tau}' = \eta \dot{\boldsymbol{\gamma}}' + \varepsilon \mathbf{A}'$ and $\mathbf{A}' = \mathbf{A}[\mathbf{u}] - \mathbf{A}[\mathbf{u}^\infty]$. The surface $\partial\mathcal{V}$ that bounds the fluid volume \mathcal{V} is composed of the body surface, $\partial\mathcal{B}$, and an outer surface (fluid or solid, possibly at infinity). Here, \mathbf{n} is the normal to the surface, $\partial\mathcal{V}$, pointing into \mathcal{V} .

Provided the fields, \mathbf{u}' and $\boldsymbol{\sigma}'$, decay appropriately in the far field, we may neglect the outer surface of $\partial\mathcal{V}$ (we shall show this is the case for weakly viscoelastic linear background flows in a subsequent work). For flows bounded by no-slip walls these terms will be identically zero. Upon substitution of the boundary conditions on $\partial\mathcal{B}$ for each field and enforcing that the net hydrodynamic force, $\mathbf{F} = \int_{\partial\mathcal{B}} \mathbf{n} \cdot \boldsymbol{\sigma} \, dS$, and torque, $\mathbf{L} = \int_{\partial\mathcal{B}} \mathbf{x} \times (\mathbf{n} \cdot \boldsymbol{\sigma}) \, dS$, are both zero on a free swimmer in the absence of inertia, the left-hand side of (6.8) simplifies to

$$\eta \int_{\mathcal{V}} \dot{\boldsymbol{\gamma}}' : \nabla \hat{\mathbf{u}} \, dV + \varepsilon \int_{\mathcal{V}} \mathbf{A}' : \nabla \hat{\mathbf{u}} \, dV = 0. \quad (6.9)$$

while the right-hand side of (6.8) simplifies to

$$\hat{\mathbf{F}} \cdot \mathbf{U} + \hat{\mathbf{L}} \cdot \boldsymbol{\Omega} + \int_{\partial\mathcal{B}} \mathbf{n} \cdot \hat{\boldsymbol{\sigma}} \cdot (\mathbf{u}^S - \mathbf{u}^\infty) \, dS - \varepsilon \frac{\hat{\eta}}{\eta} \int_{\mathcal{V}} \mathbf{A}' : \nabla \hat{\mathbf{u}} \, dV = 0, \quad (6.10)$$

where we have utilised the fact that $\hat{\boldsymbol{\gamma}} : \nabla \mathbf{u}' = \dot{\boldsymbol{\gamma}}' : \nabla \hat{\mathbf{u}}$. We will here use six-dimensional vectors for compactness, $\mathbf{U} = [\mathbf{U} \ \boldsymbol{\Omega}]^\top$ and $\hat{\mathbf{F}} = [\hat{\mathbf{F}} \ \hat{\mathbf{L}}]^\top$, and from the linearity of the Stokes equation, write $\hat{\mathbf{u}} = \hat{\mathbf{L}} \cdot \hat{\mathbf{U}}$, $\hat{\boldsymbol{\sigma}} = \hat{\mathbf{T}} \cdot \hat{\mathbf{U}}$ and $\hat{\mathbf{F}} = -\hat{\mathbf{R}} \cdot \hat{\mathbf{U}}$, where $\hat{\mathbf{R}}$ is symmetric. Finally, upon combining (6.9) with (6.10) we obtain

$$\mathbf{U} = \hat{\mathbf{R}}^{-1} \cdot \left[\int_{\partial\mathcal{B}} (\mathbf{u}^S - \mathbf{u}^\infty) \cdot (\mathbf{n} \cdot \hat{\mathbf{T}}) \, dS - \varepsilon \frac{\hat{\eta}}{\eta} \int_{\mathcal{V}} \mathbf{A}' : \nabla \hat{\mathbf{L}} \, dV \right], \quad (6.11)$$

which gives us a relation for the propulsion velocity of a swimmer in the background flow of a weakly non-Newtonian fluid. The correction to the Newtonian swimming speed, due to the tensor \mathbf{A}' , typically depends upon the unknown field \mathbf{u} but, upon expanding perturbatively in ε , the correction depends only on the Newtonian solution to leading order.

For a spherical particle of radius a , the translational velocity is given simply by

$$\mathbf{U} = -\frac{1}{4\pi a^2} \int_S (\mathbf{u}^S - \mathbf{u}^\infty) \, dS - \varepsilon \frac{1}{8\pi\eta} \int_{\mathcal{V}} \mathbf{A}' : \left(1 + \frac{a^2}{6} \nabla^2 \right) \nabla \mathbf{G} \, dV \quad (6.12)$$

where $\mathbf{G} = (\mathbf{I} + \mathbf{r}\mathbf{r}/r^2)/r$ is the Oseen tensor (or Stokeslet). As expected, when $\varepsilon = 0$, one obtains the result for a swimmer in a background flow of Newtonian fluid [67].

6.4 Janus particle in non-Newtonian fluids

As examples of an active particle in a complex fluid, we study a Janus particle in a weakly viscoelastic fluid and in a weakly shear-thinning fluid but assume the same surface slip velocity as in the Newtonian fluid (given by (6.3)). We note that we expect the non-Newtonian rheology will also affect the slip velocity for phoretic particles but focus here only on kinematic differences for a fixed swimming gait. Viscoelasticity and shear-thinning rheology are two important non-Newtonian properties [16] and also the characteristics of many biological fluids [120, 142] wherein these artificial swimmers have potential applications [158]. As discussed in §6.2, we assume the diffusion of the solute to be fast enough so that the effects of Péclet and Damköhler number can be neglected and we shall consider the particle in an unbounded and otherwise quiescent background ($\mathbf{u}^\infty = \mathbf{0}$). We first analyse the Janus particle in a weakly viscoelastic fluid.

6.4.1 Viscoelasticity: second-order fluid

Viscoelastic fluids exhibit both viscous and elastic responses to forces. Such fluids possess a memory, and stresses in them depend on the flow history. For flows which are both slow and slowly varying, viscoelasticity may be modelled without any memory of the past stresses as a second-order fluid [150],

$$\boldsymbol{\tau} = \eta \dot{\boldsymbol{\gamma}} - \frac{\Psi_1}{2} \overset{\nabla}{\dot{\boldsymbol{\gamma}}} + \Psi_2 \dot{\boldsymbol{\gamma}} \cdot \dot{\boldsymbol{\gamma}}. \quad (6.13)$$

Here, η is the total viscosity of the solution and Ψ_1 and Ψ_2 are the first and second normal stress-difference coefficients, respectively. The first normal stress difference is generally positive in viscoelastic flows i.e $\Psi_1 > 0$. The triangle denotes the upper-convected derivative

$$\overset{\nabla}{\dot{\boldsymbol{\gamma}}} = \frac{\partial \dot{\boldsymbol{\gamma}}}{\partial t} + \mathbf{u} \cdot \nabla \dot{\boldsymbol{\gamma}} - (\nabla \mathbf{u})^\top \cdot \dot{\boldsymbol{\gamma}} - \dot{\boldsymbol{\gamma}} \cdot \nabla \mathbf{u}. \quad (6.14)$$

In order to study the effect of fluid rheology on the particle, we first non-dimensionalise the equations by scaling lengths with the particle radius, a ; velocities with the first swimming mode α_1 , which without any loss of

6.4. Janus particle in non-Newtonian fluids

generality is assumed to be positive, and stresses with $\eta\omega$, where $\omega = \alpha_1/a$ is the scale of strain rate. The resulting dimensionless constitutive equation is

$$\boldsymbol{\tau}^* = \dot{\boldsymbol{\gamma}}^* - De \left(\overset{\nabla}{\dot{\boldsymbol{\gamma}}}^* + b\dot{\boldsymbol{\gamma}}^* \cdot \dot{\boldsymbol{\gamma}}^* \right), \quad (6.15)$$

with $De = \omega\Psi_1/2\eta$, the Deborah number, which is the ratio of the relaxation time scale of the fluid to the characteristic timescale of the flow and $b = -2\Psi_2/\Psi_1 \geq 0$. Henceforth, we work in dimensionless quantities and drop the stars (*) for the sake of convenience. For small De (weakly viscoelastic limit), we expand the flow quantities in a regular perturbation expansion in De [52, 70, 121] to get, at the leading order,

$$\boldsymbol{\tau}_0 = \dot{\boldsymbol{\gamma}}_0, \quad (6.16)$$

and at $O(De)$

$$\boldsymbol{\tau}_1 = \dot{\boldsymbol{\gamma}}_1 + \mathbf{A}, \quad (6.17)$$

with $\mathbf{A} = -\left(\overset{\nabla}{\dot{\boldsymbol{\gamma}}}_0 + b\dot{\boldsymbol{\gamma}}_0 \cdot \dot{\boldsymbol{\gamma}}_0\right)$. The angular velocity of a spherical swimmer is zero due to axisymmetry while its translational velocity, correct to $O(De)$, is given by (6.12) where now $\epsilon = De$.

The flow field for a swimmer with prescribed surface velocity (6.1) in a quiescent Newtonian fluid is given by [101, see]

$$\begin{aligned} \mathbf{u}_0 = & -\frac{1}{2r^3}\mathbf{e} + \frac{3}{2r^3}\frac{\mathbf{e} \cdot \mathbf{r}}{r}\frac{\mathbf{r}}{r} + \sum_{p=2}^{\infty} \left(\frac{1}{r^{p+2}} - \frac{1}{r^p} \right) \left(p + \frac{1}{2} \right) \Theta_p P_p \left(\frac{\mathbf{e} \cdot \mathbf{r}}{r} \right) \frac{\mathbf{r}}{r} \\ & + \sum_{p=2}^{\infty} \left(\frac{p}{2r^{p+2}} - \left(\frac{p}{2} - 1 \right) \frac{1}{r^p} \right) \left(p + \frac{1}{2} \right) \Theta_p W_p \left(\frac{\mathbf{e} \cdot \mathbf{r}}{r} \right) \left(\frac{\mathbf{e} \cdot \mathbf{r}}{r} \frac{\mathbf{r}}{r} - \mathbf{e} \right), \end{aligned} \quad (6.18)$$

where \mathbf{e} is the swimming direction and \mathbf{r} is the position vector with $r = |\mathbf{r}|$ from the centre of the sphere. $\Theta_p = \alpha_p/\alpha_1$ and $W_p(x) = 2/(n(n+1))P'_p(x)$. Using the Newtonian velocity field, one can calculate the strain-rate field around the swimmer, $\dot{\boldsymbol{\gamma}}_0$, and thus obtain the expression for \mathbf{A} . Substituting the expression for \mathbf{A} in (6.12) and using the orthogonal properties of Legendre polynomials, one obtains, after some lengthy but straightforward calculations,

$$U/U_N = 1 + De(b-1) \sum_{p=1}^{\infty} C_p \Theta_p \Theta_{p+1}, \quad (6.19)$$

where

$$C_p = \frac{6p}{(p+1)^2(p+2)}. \quad (6.20)$$

Recall that $U_N = \alpha_1$ is the (dimensional) swimming speed in Newtonian fluids. Frequently, the slip velocity description is truncated at two modes i.e. $\Theta_p = 0 \forall p > 2$, and depending on whether $\Theta_2 < 0$, $\Theta_2 = 0$ or $\Theta_2 > 0$ the swimmer is identified as a pusher, neutral or puller swimmer, respectively, in Newtonian fluids [71]. However, swimmers like starfish larvae [81] and Janus particles possess significant values of higher modes. When considering such swimmers in non-Newtonian fluids, one should be careful while truncating the series because unlike in Newtonian fluids, swimming speeds may be qualitatively affected by higher modes [45]. Indeed, as can be noted from (6.19), setting the modes $\alpha_1 = 1$, $\alpha_2 = 1$ and $\alpha_3 = 2$ (with appropriate units) produces qualitatively different swimming behaviour than $\alpha_1 = 1$, $\alpha_2 = 1$ and $\alpha_3 = -2$ when just the first three modes are considered. Therefore, the expression (6.19), while giving the contribution of all spectral modes in the slip velocity expansion to the swimming velocity, helps to predict when it may be reasonable to neglect higher modes and use a simple ‘two-mode’ description to obtain the swimming speed.

We consider the case of a symmetric Janus particle, where precisely one half is chemically active and the other inert, $\theta_d = \pi/2$. The spectral coefficients for activity in this case are zero for even modes (from (6.4)), and consequently $\Theta_{2p} = 0$. Hence, from (6.19), one finds that a symmetric Janus particle (with a constant uniform surface mobility) swims only at its Newtonian speed – a result also true for a two-mode neutral swimmer [52] but here obtained without any restriction on the number of modes being considered. Interestingly, one could obtain this result by observing that the non-Newtonian contribution in (6.12) is a volume integral of the contraction of an even tensor \mathbf{A} (under $\mathbf{x} \rightarrow -\mathbf{x}$) and an odd kernel and therefore vanishes. Similarly, looking at the power consumption of a squirmer, P , correct to the first order [52]

$$2P = \int_{\mathcal{V}} \dot{\gamma}_0 : \dot{\gamma}_0 dV + De \int_{\mathcal{V}} \mathbf{A} : \dot{\gamma}_0 dV, \quad (6.21)$$

one finds once again that for a symmetric Janus particle the non-Newtonian contribution gives a null result. Thus, a symmetric Janus particle in a second-order fluid swims and expends power as if in an equivalent Newtonian fluid ($De = 0$), correct to the first order in De , for the same surface slip velocity as in the Newtonian fluid. We note that the non-Newtonian

rheology will affect the solution of the ‘inner’ region for phoretic particles [145]. Additional non-Newtonian stresses arise on the particle surface, and even the solute diffusivity may change due to viscosity variations. For a thin interaction layer, neglecting effects of Péclet and Damköhler number, the slip velocity will change at $O(De)$ similarly to the case of electrophoresis considered by Khair *et al.* [111]. Here, however, our emphasis is on studying the changes in the propulsion velocity from its Newtonian value for a given (but arbitrary) slip velocity on the particle surface.

A similar result was obtained by Leal [131] for axisymmetric passive particles with fore–aft symmetry in a second-order fluid, where such particles translate, to the first approximation, at the same rate as in an equivalent Newtonian fluid. On comparison with present results, one may expect even non-spherical active particles with fore–aft symmetry in second-order fluids to behave as if in equivalent Newtonian fluids.

When the two halves of the Janus particle are not exactly equal, i.e. $\theta_d \neq \pi/2$, then the even spectral modes of the activity, A_{2p} , are no longer equal to zero and hence $\Theta_{2p} \neq 0$. Consequently, the non-Newtonian contribution to the swimming velocity may now be non-zero, and can be easily calculated for any level of active surface coverage, θ_d . We find that when $\theta_d > \pi/2$, the particle swims faster than in a Newtonian fluid and while for $\theta_d < \pi/2$ it swims slower, provided $b < 1$ (see [37] and [53] for a recent discussion on permissible values of b). Interestingly, one can qualitatively predict this result by considering the two-mode description, by observing that $\Theta_2 = 2 \cos \theta_d$. The former particle behaves as a pusher, $\Theta_2 < 0$, and thus swims faster, where as the latter is a puller, $\Theta_2 > 0$, and therefore swims slower than in a Newtonian fluid (from (6.19)), as also reported for two-mode swimmers by De Corato *et al.* [52]. Quantitatively, the viscoelastic contribution decays for higher modes as $C_p \sim 1/p^2$ and a two-mode description gives the viscoelastic contribution with a relative error of less than 0.1 for $|\cos \theta_d| \leq 0.35$; however, the approximation grows worse upon increasing the fore–aft asymmetry of the particle and a three-mode description is better for $|\cos \theta_d| \geq 1/\sqrt{5}$. This is shown in figure 6.2, where we plot the scaled first-order velocity, $U_1^{(M)}/U_N = (b-1) \sum_{p=1}^M C_p \Theta_p \Theta_{p+1}$ from (6.19) for different coverage areas of activity with varying number of modes. Note that as θ_d approaches 0 or π , the Newtonian velocity $U_N \rightarrow 0$ and $U_1^{(M)}/U_N$ diverges.

The asymptotic results for a small De expansion are seen to be valid for only very small values of De (≈ 0.02 for two-mode swimmers with $O(1)$ modes [52]). This may be understood by noting that squirring modes of

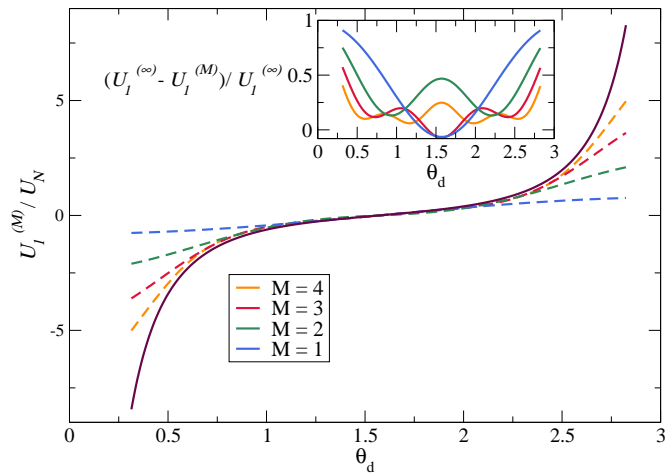


Figure 6.2: Variation of the scaled first-order swimming velocity $U_1^{(M)}/U_N$ with θ_d obtained for the first $M + 1$ modes (dashed lines), and $b = 0.2$. $U_1^{(\infty)}$ corresponds to the convergence value ($M = 99$) and is depicted by the solid line. Inset plot shows the relative error.

magnitude $O(1)$ result in strain rates of magnitude $O(10)$ on the surface of the particle in a Newtonian fluid and, therefore, $O(10^2)$ values of the non-Newtonian contribution \mathbf{A} , which thereby renders the Deborah number expansion accurate for only very small values of De . Numerical results using the Giesekus model, at higher values of De , find all swimmers – pusher, puller and neutral – swimming slower and expending less power than in an equivalent Newtonian fluid [217]; one may also expect results obtained using the second-order fluid model to deviate from those obtained with the Giesekus model, at moderate Deborah numbers, due to the saturation of polymer elongation in the latter and the associated differences in extensional rheology. In the experimental study of Janus particles in viscoelastic fluids by [86], the Deborah (Weissenberg) numbers were quite small, and hence in a regime where one may then expect the second-order model to, at least qualitatively, predict the viscoelastic fluid behaviour [132].

6.4.2 Shear-thinning rheology: Carreau model

Shear-thinning fluids experience a loss of apparent viscosity with applied strain rate. The Carreau model [16] and its perturbation to the form in (6.6) has recently been covered by Datt *et al.* [45]. We consider the perturbation of the flow quantities in the viscosity ratio, $\varepsilon = 1 - \beta$ where $\beta \in [0, 1]$ is the ratio of infinite shear-rate viscosity to zero shear-rate viscosity, as this expansion is uniformly valid for all strain rates and obtain $\mathbf{A} = \left\{ -1 + (1 + Cu^2|\dot{\gamma}_0|^2)^{(n-1)/2} \right\} \dot{\gamma}_0$. Here, Cu , the Carreau number is the ratio of the characteristic strain rate in the flow, to the cross-over strain rate in the fluid and n characterises the degree of shear thinning ($n < 1$). With this form of \mathbf{A} , it is difficult to obtain an analytical expression for the propulsion velocity similar to that obtained for the viscoelastic case (6.19). However, one can numerically calculate the propulsion velocity with higher modes and then compare the results with just the first two modes. This is done in figure 6.3 for $n = 0.25$, where we plot $U_1^{(M)}/U_N$ for two values of $\mu \equiv \cos \theta_d$.

We find that irrespective of the position of θ_d , the Janus particle swims slower in a shear-thinning fluid than in a Newtonian fluid. The non-monotonic variation of the first-order swimming speed with Cu in figure 6.3 is similar to as found by Datt *et al.* [45] for any two-mode squirmer. Though the two-mode description qualitatively predicts the results: all – neutral, pusher and puller – swimmers swim slower, with pusher and pullers swimming at the same velocity [45], it is apparent from figure 6.3 that higher modes may significantly alter the results. Additionally, we note that

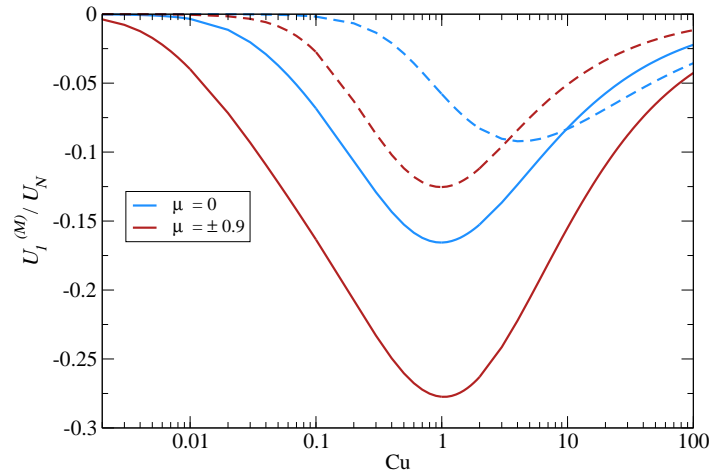


Figure 6.3: Variation of the scaled first-order swimming velocity $U_1^{(M)}/U_N$ (obtained for $M + 1$ modes) with Cu for two values of $\mu \equiv \cos \theta_d$. Solid lines correspond to $M = 30$, and $M = 28$ for $\mu = 0$ (symmetric) and $\mu = \pm 0.9$ respectively (additional modes lead to negligible differences). Dashed-lines correspond to the swimming velocity with just the first two modes.

the values of Θ_2 and Θ_3 for any Janus particle lie in the range where Datt *et al.* [45] predict a smaller swimming velocity than in Newtonian fluids.

6.5 Conclusion and future work

In this work, we studied active particles with prescribed surface velocities in non-Newtonian fluids. Using the reciprocal theorem, we derived a general form of the propulsion velocity of an active particle in a weakly nonlinear background flow. Using this formalism, we calculated the swimming speed for an active particle with a general, axisymmetric slip velocity in an otherwise quiescent second-order fluid extending results previously obtained for a two-mode description. We then considered the motion of diffusiophoretic Janus particles in weakly viscoelastic and shear-thinning fluids. We showed that a Janus particle with two equal halves, in a weakly viscoelastic fluid, will swim at the same speed as in a Newtonian fluid due to its fore-aft symmetry (provided the surface slip velocity remains unchanged). When this symmetry is broken the particle may swim faster or slower than in a Newtonian fluid and this may be predicted by considering the Janus particle as a pusher or puller based on the two-mode squirmer description. Conversely, in a weakly shear-thinning fluid, a Janus particle always swims slower than in a Newtonian fluid.

While analysing Janus particles, we neglected any changes to the slip velocity due to fluid rheology as well any dynamics due to the distortion of the solute concentration field of phoretic particles because of the velocity field. The latter may not be true for large proteins or molecules, when the diffusion constant is small and the Péclet number becomes significant. This coupling of the velocity and concentration field leads to interesting dynamics in Newtonian fluids [145, 146] and is an avenue for further inquiry in non-Newtonian fluids. We also expect the fluid rheology to affect the slip velocity of the particle: the gait of a biological microswimmer may be modified by non-Newtonian stresses, likewise the slip velocity of a diffusiophoretic Janus particle. For a complete understanding of the dynamics of active particles in complex fluids, one should also consider such changes to the gait itself.

Postscript

Consider a squirmer in a 2D linear shear flow, $\mathbf{u}^\infty = \mathbf{\Gamma} \cdot \mathbf{x}$, of a second-order fluid ($\mathbf{A} = \overset{\nabla}{\dot{\boldsymbol{\gamma}}}_0 + b\dot{\boldsymbol{\gamma}}_0 \cdot \dot{\boldsymbol{\gamma}}_0$, where b is the ratio of the two normal stress coefficients). We find that the rotational dynamics of the squirmer at first

order, $O(De)$, is given, in dimensionless form (with the scales used in the current chapter), by

$$\boldsymbol{\omega}_1 = -\frac{5}{6}\Theta_2\mathbf{e} \times (\mathbf{E} \cdot \mathbf{e}) \quad (6.22)$$

where $\mathbf{E} = \boldsymbol{\Gamma} + \boldsymbol{\Gamma}^\top$, $\Theta_2 = \alpha_2/\alpha_1$ and \mathbf{e} is the orientation of the squirmer. Note that at the leading order (in the Newtonian fluid), the squirmer will rotate with just the rotational velocity of the background flow, as the axisymmetric distribution of the slip velocity on its surface does not lead to any self-rotation.

The result in (6.22) shows that of all the modes, only the second mode contributes to the rotational velocity of the swimmer. The expression's resemblance to Jeffery's equations [25, 103] suggests that the slip velocity distribution may render the spherical swimmer appear spheroidal to the fluid flow. We are currently working on the problem, dealing with how to rigorously prove the expression (6.22) (presently, the absence of higher modes in the expression has been tested numerically).

Note that De Corato & D'Avino [51] have already addressed the dynamics of a three mode squirmer in a sheared viscoelastic fluid. The novelty we add is through the form (6.22) with its similarity to Jeffery's equations, and the hypothesis that the result holds for a general n -mode squirmer.

Chapter 7

A note on higher-order perturbative corrections to squirming speed in weakly viscoelastic fluids[¶]

Many microorganisms swim in fluids with complex rheological properties. Although much is now understood about motion of these swimmers in Newtonian fluids, the understanding is still developing in non-Newtonian fluids—this understanding is crucial for various biomimetic and biomedical applications. Here we study a common model for microswimmers, the squirmer model, in two common viscoelastic fluid models, the Giesekus fluid model and fluids of differential type (grade three), at zero Reynolds number. Through this article we address a recent commentary that discussed suitable values of parameters in these models and pointed at higher-order viscoelastic effects on squirming motion.

7.1 Introduction

With ideas of minimally invasive surgery, targeted drug delivery, and other biomimetic applications [79, 154, 208], an understanding of motion of microswimmers in complex fluids has become imperative. Subsequently, many recent articles have focussed on motion of microswimmers in complex fluids (see reviews [70, 195]). While biological fluids demonstrate many non-Newtonian fluid properties [204], one common property is viscoelasticity [120, 201]. We consider this property in this article.

Viscoelastic fluids show both viscous and elastic properties, and retain memory of their flow history [16]. Recent experimental studies on biologi-

[¶]This chapter has been submitted for publication under the same title by Datt and Elfring.

cal swimmers [134, 171, 181] have addressed how an organism may change its swimming stroke as it “senses” the viscoelasticity of the fluid medium. Elastic stresses in the fluid can also directly contribute to changes in the swimming speed given a swimming stroke (see, for e.g., [121]). The present work is a theoretical study of swimmers in viscoelastic fluids. A model of microswimmers conducive to theoretical treatment is the squirmer model [137]. The model, developed by Lighthill [137] and Blake [17], consists of a rigid body that generates thrust due to the presence of (apparent) slip velocities on its surface. It has been used to understand various single and collective behaviours of microswimmers in Newtonian fluids [165]. In viscoelastic fluids, Zhu *et al.* [217] studied the motion of squirmers using numerical simulations and found that all squirmers—pushers, pullers and neutral swimmers—swim slower than in a Newtonian fluid for a wide range of values of the Weissenberg number (measure of viscoelasticity in the fluid). Later, De Corato *et al.* [52] using a theoretical approach (and the squirmer model), showed that in fact for very small values of the Deborah (Weissenberg) number not considered in the work of Zhu *et al.* [217] pusher swimmers swim faster, puller swimmers slower and neutral swimmers at the same speed as in a Newtonian fluid. We note that in these studies, as will be the case in the present study, the swimming speeds in viscoelastic and Newtonian fluids are compared for the same swimming stroke.

The work of De Corato *et al.* [52] used the second-order fluid model to study weakly viscoelastic effects on squirming motion. The use of the second order fluid model with parametric values as chosen by De Corato *et al.* [52] was critiqued by Christov & Jordan [37] who argued that the parametric values be chosen in accordance with thermodynamic constraints and recommended the use of other viscoelastic models which “better elucidate the transient effects of fluid viscoelasticity on a squirmer”. De Corato *et al.* [53] then showed that in fact using the Giesekus model to study weakly viscoelastic effects, to $\mathcal{O}(De)$, gives results identical to those previously obtained by them using the second-order fluid model. The motivation for this work in large part is due to this discussion; here we study the squirming motion to higher orders in Deborah number both in the Giesekus fluid and in fluids of differential type. We find that unlike in a second-order fluid that obeys thermodynamic constraints, weak viscoelastic contributions to the squirming speed are non-zero in a fluid of grade three (third-order fluid) obeying thermodynamic constraints. These contributions are qualitatively different to those obtained due to viscoelasticity as modelled by the Giesekus fluid.

In the following, we briefly discuss the squirmer model and the second-order fluid model with the points of contention, and then present our results.

7.2 Theoretical framework

7.2.1 The squirmer model

The spherical squirmer model consists of a sphere with prescribed axisymmetric surface velocities (surface velocities may be thought of as originating from surface distortions in biological microswimmers like *Opalina*) which generate thrust forces to propel the swimmer [17, 137]. We consider only tangential surface velocities on the swimmer (the swimmer maintains its shape) so that the surface velocity $\mathbf{u}^S = u_\theta^S \mathbf{e}_\theta$, where u_θ^S can be expressed as

$$u_\theta^S = \sum_{l=1}^{\infty} B_l V_l(\theta), \quad (7.1)$$

using $V_l(\theta) = -(2/(l(l+1))) P_l^1(\cos\theta)$; $P_l^1(\cos\theta)$ are associated Legendre polynomials of the first kind, and θ is the polar angle measured from the axis of symmetry [17]. The coefficients B_l are generally referred to as squirmering modes. In Newtonian fluids, the swimming speed of the squirmer is due to just the first mode, $U_N = 2/3B_1$, and the second mode B_2 gives the stresslet due to the squirmer [101]. As velocities due to higher modes decay faster than the first two modes (in fact, B_2 gives the slowest decaying spatial contribution to the flow field), and since higher modes do not contribute to the swimming speed, in Newtonian fluids, often only the first two modes are considered, i.e., $B_n = 0$ for $n > 3$. For the purpose of this study, in accordance with the bulk of literature in the field [165], we too consider only the first two modes. At this point we feel it is important to note that in general considering only the first two modes in complex fluids may be problematic as shown in the recent works of Datt *et al.* [44, 45]. The interested reader may refer to the description of non-axisymmetric squirmering modes in Newtonian fluids by Pak & Lauga [159].

When the ratio $\beta = B_2/B_1$ is negative, the squirmer generates thrust from its rear end, like the bacterium *E. coli.*; when $\beta > 0$ the thrust is generated from the front end, as in the “breaststroking” algae *Chlamydomonas*. When $\beta = 0$, the thrust and drag centres coincide, and flow field around the swimmer is due to a potential dipole. The three types of squirmers are called pushers, pullers, and neutral swimmers, respectively [165].

7.2.2 The second-order fluid model

The deviatoric stress in an incompressible second-order fluid is given by

$$\boldsymbol{\tau} = \eta \mathbf{A}_1 + \alpha_1 \mathbf{A}_2 + \alpha_2 \mathbf{A}_1^2, \quad (7.2)$$

where

$$\begin{aligned}\mathbf{A}_1 &\equiv \mathbf{L} + \mathbf{L}^\top, \\ \mathbf{A}_n &\equiv \frac{D\mathbf{A}_{n-1}}{Dt} + \mathbf{L}^\top \mathbf{A}_{n-1} + \mathbf{A}_{n-1} \mathbf{L},\end{aligned}\tag{7.3}$$

with $\mathbf{L}^\top = \nabla \mathbf{u}$, and D/Dt denoting the material derivative [61, 198]. Here η is the shear viscosity and α_1 and α_2 are material moduli. The second order fluid model has been used to study the first effects of viscoelasticity on the motion of both passive and active particles (see for e.g., [4, 29, 160]). However, there has been much discussion on the permissible values of α_1 and α_2 in the model. Dunn & Fosdick [62] have shown that considering (7.2) as exact, the model is consistent with thermodynamics when

$$\eta \geq 0, \tag{7.4}$$

$$\alpha_1 \geq 0, \tag{7.5}$$

$$\alpha_1 + \alpha_2 = 0. \tag{7.6}$$

However, often these constraints, citing experimental investigations (incorrectly, according to Dunn & Rajagopal [61]), are not strictly adhered to. In particular, α_1 , which corresponds to the first normal stress difference coefficient, is generally taken to be negative [61].

7.2.3 The reciprocal theorem

The reciprocal theorem of low Reynolds number hydrodynamics [93] can be used to calculate the first effects of the fluid rheology on the swimming speed of microswimmers [125]. The details of the reciprocal theorem for the specific case of squirmers in viscoelastic fluids may be found, among others, in the works of Lauga [122], De Corato *et al.* [52] and Datt *et al.* [44].

Consider a weakly non-linear fluid of the form [125]

$$\boldsymbol{\tau} = \eta \dot{\boldsymbol{\gamma}} + \varepsilon \boldsymbol{\Sigma}[\mathbf{u}], \tag{7.7}$$

where $\boldsymbol{\tau}$ is the deviatoric stress, η is the shear viscosity, and $\dot{\boldsymbol{\gamma}}$ is the strain rate tensor so that the first term on the right hand side in (7.7) gives the Newtonian contribution. Here ε is the small parameter that quantifies the deviation from the Newtonian behaviour and $\boldsymbol{\Sigma}$ gives the non-Newtonian contribution. The translational velocity of a squirmer of radius a in such a fluid is, obtained by using the reciprocal theorem,

$$\mathbf{U} = -\frac{1}{4\pi a^2} \int_S \mathbf{u}^S \, dS - \varepsilon \frac{1}{8\pi\eta} \int_S \boldsymbol{\Sigma} : \left(1 + \frac{a^2}{6} \nabla^2\right) \nabla \mathbf{G} \, dV, \quad (7.8)$$

where $\mathbf{G} = (1/r) (\mathbf{I} + \mathbf{r}\mathbf{r}/r^2)$ is the Oseen tensor, and S denotes the surface of the swimmer, and V , the fluid volume [44].

7.3 Results and discussion

De Corato *et al.* [52] studied the motion of a squirmer in a second-order fluid. Considering only small deviations from Newtonian behaviour, they expanded all flow quantities in the small parameter $\varepsilon = De$, where Deborah number $De = -\alpha_1 B_1 / \eta a$ is a measure of the relaxation time scale of the fluid to the characteristic time scale of the flow (note that for steady surface slip velocity squirmers, the Deborah and Weissenberg numbers are equivalent [168]). De Corato *et al.* [52] assumed $\alpha_1 < 0$, in contradiction with the thermodynamic stability criterion as pointed out by Christov & Jordan [37]. The thermodynamic constraint $\alpha_1 + \alpha_2 = 0$ was also relaxed. De Corato *et al.* [52] found that the perturbation calculations predicted that pushers swim faster, pullers slower and neutral swimmers at the same speed as in Newtonian fluids, provided that the swimming gait remains unchanged between the viscoelastic and Newtonian fluids. Their numerical simulations in a Giesekus fluid found the analytical results to hold up to $De \approx 0.02$ [52]. It was commented that the deviation of the results due to theoretical calculations from those due to numerical simulations at larger De was because of higher order viscoelastic effects that were neglected in the analytical results for which only $\mathcal{O}(De)$ corrections were analysed [52].

The critique of the work of De Corato *et al.* [52] by Christov & Jordan [37] was focussed on the former not respecting the thermodynamic constraints of the second-order fluid model. In particular, Christov & Jordan [37] remarked that since $\alpha_1 + \alpha_2$ should be equal to zero, most corrections to flow quantities (but pressure) including the swimming speed of the squirmer will be zero, since all these corrections are proportional to the sum $\alpha_1 + \alpha_2$. Citing [62], Christov & Jordan [37] also pointed out that for $\alpha_1 < 0$ a steady solution to the problem should not be expected. Finally, Christov & Jordan [37] suggested calculating corrections to the swimming motion with the thermodynamic constraints (meaning going to higher powers in De for any non-zero contributions) or using a different viscoelastic model, such as the upper-convected Maxwell model.

De Corato *et al.* [53] showed that even with using a more involved model like the Giesekus fluid model (which reduces to the upper-convected Maxwell model for a choice of a model parameter), one obtains equations identical to the second-order fluid in the limit of small De at $\mathcal{O}(De)$. Further, for its permissible values, the Giesekus fluid gives identical results to those from the second order fluid as used by De Corato *et al.* [52]. In fact, they maintain that the second order fluid model should be seen as an approximation to more complex viscoelastic models in slow and nearly steady flows (and therefore (7.2) not be seen as exact). Perhaps, in order to avoid any confusion, one may restrict the use of the term “second-order fluid model” only when it is treated as an exact model obeying the thermodynamic constraints; where a slow and nearly steady flow approximation is used one can start with a more involved model and reduce it to simpler constitutive equations at each order in the perturbation series in De . Below we use this terminology and study the squirmer in a Giesekus fluid and in fluids of grade n (the second-order fluid is a fluid of grade two) and calculate the corrections to the swimming speed in these fluids up to higher orders in De .

7.3.1 Giesekus fluid

The polymeric stress in an incompressible Giesekus fluid is given as [150]

$$\boldsymbol{\tau}_p + \lambda \overset{\nabla}{\boldsymbol{\tau}}_p + \alpha_m \frac{\lambda}{\eta_p} \boldsymbol{\tau}_p \cdot \boldsymbol{\tau}_p = \eta_p \dot{\boldsymbol{\gamma}}, \quad (7.9)$$

where the mobility factor α_m must take values between 0 and 1/2 [150, 217]. The total deviatoric stress in the fluid is $\boldsymbol{\tau} = \boldsymbol{\tau}_s + \boldsymbol{\tau}_p$ where $\boldsymbol{\tau}_s = \eta_s \dot{\boldsymbol{\gamma}}$ is the contribution from the Newtonian solvent. The total viscosity in the fluid $\eta = \eta_s + \eta_p$. Here we consider the case when $\zeta = \eta_s/\eta = 0$; when $\zeta = 0$ and $\alpha_m = 0$, (7.9) reduces to the upper-convected Maxwell fluid model [150].

We non-dimensionalise equations by scaling lengths by the squirmer radius a , velocities with the first squirring mode B_1 , and stresses with $\eta B_1/a$, and obtain the dimensionless constitutive equation

$$\boldsymbol{\tau}^* + De \overset{\nabla}{\boldsymbol{\tau}}^* + \alpha_m De \boldsymbol{\tau}^* \cdot \boldsymbol{\tau}^* = \dot{\boldsymbol{\gamma}}^*, \quad (7.10)$$

where the Deborah number $De = \lambda B_1/a$. Henceforth, we drop the stars for convenience. We expand all flow quantities in a regular perturbation expansion in De , and using standard methods to calculate the flow fields in

Stokes flow [93] obtain the swimming speed of the squirmer, up to $\mathcal{O}(De^3)$,

$$\begin{aligned}
 U &= \frac{2}{3} + \frac{2}{15}\beta(-1 + \alpha_m)De \\
 &+ \frac{\beta^2(-20568 - 98136\alpha_m + 65266\alpha_m^2) + 84(-193 + 176\alpha_m(-3 + 2\alpha_m))}{45045}De^2 \\
 &+ \frac{\beta}{482431950} \left(170(3005646 + \alpha_m(6190100 + 3\alpha_m(-10014053 + 4815243\alpha_m))) \right. \\
 &\left. + \beta^2(224764987 + \alpha_m(1298121442 + 3\alpha_m(-1659132865 + 875113652\alpha_m))) \right) De^3.
 \end{aligned} \tag{7.11}$$

At this point, examining equation (7.11) for specific values of β and α_m becomes instructive; we choose $\beta = -1$ for pushers, 0 for neutral squirmers, and 1 for puller type squirmers and $\alpha_m = 0.2$. These values correspond to the values used in the work of De Corato *et al.* [52]. From (7.11) we find, for pushers,

$$\frac{U}{U_N} = 1 + 0.16De - 2.05De^2 - 2.62De^3, \tag{7.12}$$

for pullers,

$$\frac{U}{U_N} = 1 - 0.16De - 2.05De^2 + 2.62De^3, \tag{7.13}$$

and for neutral squirmers,

$$\frac{U}{U_N} = 1 - 0.80De^2. \tag{7.14}$$

The swimming speeds in (7.12), (7.13), and (7.14) are plotted in figure 7.1 along with their respective Padé approximant $P_2^1(De)$ [13]. When corrections up to only $\mathcal{O}(De)$ are considered, we note that pushers swim faster, pullers slower and neutral swimmers at the same speed as in a Newtonian fluid; this is shown in the work of De Corato *et al.* [52]. With terms up to $\mathcal{O}(De^3)$, we note that all the squirmers swim slower than in a Newtonian fluid (except for very small values of De) as found in the numerical work of Zhu *et al.* [217]. Clearly, the inclusion of higher order terms changes the theoretical predictions significantly.

One may calculate the higher order terms in the expansion to predict results for larger values of De . This is done by Housiadas & Tanner [97], up to $\mathcal{O}(De^8)$, for steady sedimentation of a passive sphere in a viscoelastic fluid. Housiadas & Tanner [97] also quantify when the results from the series should not be considered (using positive definiteness of the conformation tensor). Sauzade *et al.* [179] and Elfring & Lauga [70] also performed a

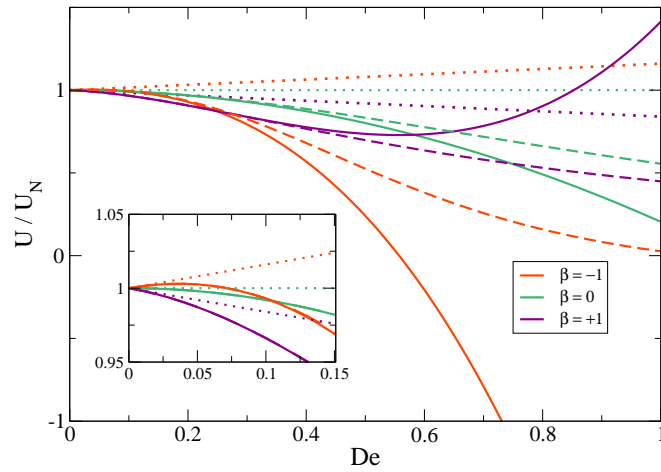


Figure 7.1: Swimming speeds in the Giesekus fluid as a function of De . The solid lines include corrections up to $\mathcal{O}(De^3)$. The dashed lines are Padé approximations to the series for the speeds in the text. The dotted lines include only $\mathcal{O}(De)$ corrections. The addition of the higher order modes decreases the speeds of the squirmers. As seen here, all squirmers at large values of De swim slower than in a Newtonian fluid, as found in the numerical work of Zhu *et al.* [217].

higher-order perturbation analysis, using techniques to improve the convergence properties of the series, for the swimming speed of a two-dimensional swimming sheet where the small parameter was the amplitude of the waves on the sheet. We have not pursued these endeavours here, for the motivation for this study was to see the differences between the different viscoelastic models considering only the first few terms.

The results in the foregoing were obtained using the Giesekus model for viscoelasticity. They would remain qualitatively the same if one were to use the upper-convected Maxwell model. But what happens to a squirmer in a fluid of grade n , when the fluid is “regarded as a fluid in its own right, not necessarily an approximation to any other one” [203] ?

7.3.2 A fluid of grade three

Consider an incompressible fluid of grade three [75]:

$$\boldsymbol{\tau} = \eta \mathbf{A}_1 + \alpha_1 \mathbf{A}_2 + \alpha_2 \mathbf{A}_1^2 + \beta_1 \mathbf{A}_3 + \beta_2 [\mathbf{A}_1 \mathbf{A}_2 + \mathbf{A}_2 \mathbf{A}_1] + \beta_3 (\text{tr} \mathbf{A}_1^2) \mathbf{A}_1, \quad (7.15)$$

where η , α_1 , α_2 , β_1 , β_2 , and β_3 are material moduli. The equation is dimensional. Thermodynamics stipulates [75] that

$$\begin{aligned} \eta \geq 0 \quad \alpha_1 \geq 0, \quad |\alpha_1 + \alpha_2| &\leq \sqrt{24\eta\beta_3}, \\ \beta_1 = 0 \quad \beta_2 = 0 \quad \beta_3 \geq 0. \end{aligned} \quad (7.16)$$

We scale flow quantities as before, and consequently, equation (7.15) with (7.16), in its dimensionless form, becomes

$$\boldsymbol{\tau} = \dot{\boldsymbol{\gamma}} + De \left[\overset{\Delta}{\dot{\boldsymbol{\gamma}}} + \mathcal{Q} \dot{\boldsymbol{\gamma}} \cdot \dot{\boldsymbol{\gamma}} \right] + De^2 [\text{tr} (\dot{\boldsymbol{\gamma}} \cdot \dot{\boldsymbol{\gamma}}) \mathcal{P} \dot{\boldsymbol{\gamma}}], \quad (7.17)$$

where $De = \alpha_1 B_1 / \eta a$, $\mathcal{Q} = \alpha_2 / \alpha_1$ and $\mathcal{P} = \beta_3 \eta / \alpha_1^2$. $\overset{\Delta}{\dot{\boldsymbol{\gamma}}}$ is the lower convected derivative of $\dot{\boldsymbol{\gamma}}$ [150], denoted by \mathbf{A}_2 in equation (7.15). We expand all flow quantities in a regular perturbation expansion of De and calculate the propulsion speed up to $\mathcal{O}(De^2)$, which in dimensionless form comes to be

$$\begin{aligned} U = \frac{2}{3} - \frac{2}{15} \beta (1 + \mathcal{Q}) De \\ - \frac{2\beta^2 (1 + \mathcal{Q}) (161 + 559\mathcal{Q}) - 48 (616 + 1383\beta^2) \mathcal{P}}{45045} De^2. \end{aligned} \quad (7.18)$$

Note that when $\mathcal{P} = 0$, we obtain a fluid of grade two, where $1 + \mathcal{Q} = 0$ (7.6), and consequently, no contribution to the swimming speeds of the squirmers

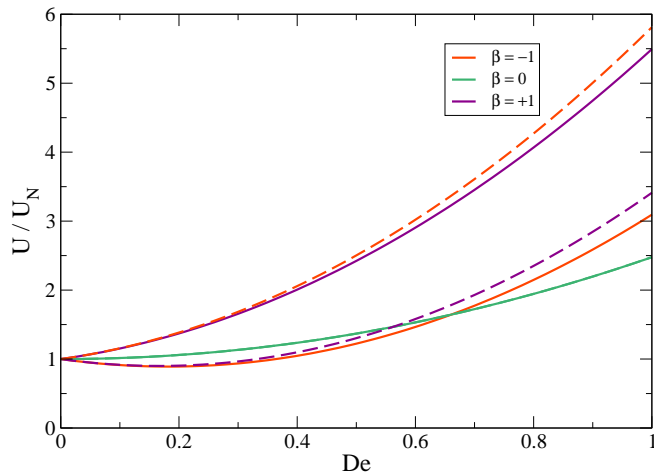


Figure 7.2: Swimming speeds in fluids of grade three. Solid lines: $\mathcal{P} = 3/2$, $\mathcal{Q} = -7$. Dashed lines: $\mathcal{P} = 3/2$, $\mathcal{Q} = 5$. Solid and dashed lines for $\beta = 0$ overlap. Depending on the values of \mathcal{Q} for a given \mathcal{P} , either of the puller or pusher can swim faster or slower than in a Newtonian fluid at small De .

we consider. This is in contradiction to the results obtained through the weak De expansion in a Giesekus fluid to $\mathcal{O}(De)$ where pushers and pullers swim faster and slower, respectively, than in a Newtonian fluid. This was discussed in the exchange between Christov & Jordan [37] and De Corato *et al.* [53] described previously.

To observe the effects of a fluid of grade three, we choose $\mathcal{P} = 3/2$ (an arbitrary choice in as much as the physics of the problem is concerned). From equation (7.16), we know that $-7 \leq \mathcal{Q} \leq 5$. We plot the swimming speeds for two cases: $\mathcal{P} = 3/2$, $\mathcal{Q} = -7$ and $\mathcal{P} = 3/2$, $\mathcal{Q} = 5$ in figure 7.2.

From figure 7.2 and equation (7.18), we see that depending on the value of \mathcal{Q} , either of the puller or the pusher can swim faster than in a Newtonian fluid at $\mathcal{O}(De)$. The higher order correction, $\mathcal{O}(De^2)$, gives a positive contribution to the swimming speed.

In contrast to the results from the Giesekus fluid, the parameters in a fluid of grade three allow for a wider range of possibilities—either of pullers or pushers can swim faster or slower at small values of the Deborah number. Here, we demonstrate this using the parameter \mathcal{Q} for a given \mathcal{P} . About

this range of possibilities, perhaps it is useful to recall the observation from Truesdell [203] that “it is possible that two fluids of grade 3 could behave just alike in every viscometric test yet react altogether differently to some test of a different kind”. At higher De , all squirmers swim faster in fluids of grade three than in a Newtonian fluid, when in Giesekus fluids they would swim slower.

7.4 Conclusion

We calculated the higher order corrections to the swimming speeds in two viscoelastic fluids: the Giesekus fluid and the fluid of grade three. The higher order corrections significantly add to the results at $\mathcal{O}(De)$; even at relatively small values of De , the corrections lead to qualitatively different speeds. This again raises the question about the range of values of De at which the expansion can predict results (also see [44]). Importantly, we observe that the two fluids, the Giesekus fluid and the fluid of grade three, predict qualitatively different swimming speeds for the squirmers. Clearly, the answer to what viscoelastic model to use depends on what all we wish to model—in this, we are guided by experiments.

Chapter 8

Two-sphere swimmers in viscoelastic fluids^{**}

We examine swimmers comprising of two rigid spheres which oscillate periodically along their axis of symmetry, considering when the spheres oscillate both in phase and in anti-phase, and study the effects of fluid viscoelasticity on the swimmers' motion. These swimmers display reciprocal motion in Newtonian fluids and consequently, no net swimming is achieved over one cycle in such fluids. Conversely, in viscoelastic fluids, we find that the effect of viscoelasticity acts to propel the swimmers forward in the direction of the smaller sphere when the two spheres are of different sizes. Finally, we compare the motion of rigid spheres oscillating in viscoelastic fluids with elastic spheres in Newtonian fluids where we find similar results.

8.1 Introduction

Recent review articles on swimming at small length scales [11, 71, 88, 129, 154, 177] point to the immense interest in recent years on understanding the topic that has wide ranging applications from biomedical engineering [208] to autonomous de-pollution of water and soil [78]. Several theoretical models for understanding swimming at low Reynolds number in Newtonian fluids have been developed, such as the swimming sheet [200], and the squirmer [137]. The swimming techniques used in these two seminal models, which were drawn from observing biological swimmers, demonstrate effective ways to circumvent the scallop theorem, which stipulates that a reciprocal swimming gait cannot lead to net motion at low Reynolds numbers in Newtonian fluids [170]. Beyond the swimming sheet and the squirmer, other theoretical models have been proposed; many aiming simplicity. Purcell in his famous 1976 talk “Life at low Reynolds number” proposed the “simplest animal”

^{**}This chapter has been previously published under the same title in *Physical Review Fluids*, 3, 123301 (2018) by Datt, Nasouri, and Elfring. © 2018 American Physical Society.

that could swim: a planar three-linked swimmer, which could move by alternately moving its front and rear segments [12, 170]. The Najafi-Golestanian swimmer [151] propels forward using its collinear assembly of three equal spheres, connected with thin rods which vary in lengths as the spheres oscillate in a non time-reversible way [1, 73, 83]. Avron *et al.* [6] proposed another model, more efficient than the three-sphere model, where the swimmer consists of just a pair of spherical bladders which exchange their volumes while also varying their distance of separation. These models have been instrumental in understanding swimming at low Reynolds number and therefore in designing optimal swimmers in Newtonian fluids [63, 144, 147, 197].

In many instances, microswimmers swim in fluids which are not Newtonian and show complex rheological properties [164]. Among others, one example is of a mammalian sperm in the female reproductive tract [72] where cervical mucus displays viscoelasticity and shear-thinning viscosity [120]. Consequently, several model swimmers studied in Newtonian fluids have also been studied in non-Newtonian fluids for a comparison of their swimming dynamics [39, 44, 45, 76, 94, 121, 149]. The change in the swimmer's dynamics—whether a change in its propulsion velocity for a fixed swimming gait or a change in the gait itself for either a fixed actuation force or fixed energy consumption—is found to be swimmer dependent [70] and in general, we see that it is fraught with peril to generalize results obtained for one swimmer to others [45, 69]. Perhaps more interestingly, and closer to the present work, are strategies that do not lead to swimming in Newtonian fluids but can be useful in complex fluids. Lauga [122] first showed this for a squirmer with a surface velocity distribution that does not lead to any net motion over one cycle in a Newtonian fluid, but does so in a viscoelastic fluid. Keim *et al.* [109] then demonstrated experimentally this elasticity enabled locomotion for a rigid assembly of two connected spheres undergoing rotational oscillations about an axis perpendicular to their mutual axis of symmetry. Böhme & Müller [19] observed the same for axisymmetric swimmers performing reciprocal torsional oscillations. Pak *et al.* [160] modelled a snowman swimmer, which has two unequal spheres that rotate about their common axis, that can swim only in complex fluids. Indeed it is known that the scallop theorem does not hold in complex fluids [124]; fluid inertia, nearby surfaces, elasticity of the swimmer body, or interaction with other swimmers are some other reasons why a reciprocal gait for a swimmer may lead to net motion [124]. In truth, the motivation for this work came from the interesting experimental and computational works of Klotsa *et al.* [115] and Dombrowski *et al.* [57] who show that an assembly of two rigid collinear spheres with a single degree of freedom can swim in the presence of inertia,

and can in fact also reverse its direction at higher Reynolds number. Felderhof [74] then theoretically studied the effect of inertia on the motion of such collinear swimmers.

In this work, we consider two different two-sphere ‘swimmers’. The first is simply an assembly of two spheres connected as a rigid body that is oscillated by some external force aligned along the axis of symmetry of the two spheres. Strictly speaking, this is not a swimmer because the motion of the body arises as a consequence of the external force; however, we will see that by imposing a sinusoidally varying force (with zero mean value) we can achieve a rectified ‘swimming’ motion in a complex fluid. This is similar to the two-sphere system developed by Pak *et al.* [160] that achieved net motion under an imposed torque exerted by an external (magnetic) field, although imposing an oscillatory force is perhaps easier to accomplish experimentally. The second swimmer is a two-sphere assembly where the swimming gait is prescribed as the sinusoidal variation of the distance between the two spheres with no imposed external force. This is similar to the Najafi-Golestani swimmer [151] except that here instead of three spheres we have only two and therefore only a single degree of freedom.

We emphasize that neither of these swimmers can achieve any net motion over a complete cycle in a Newtonian fluid at zero Reynolds number, irrespective of the radii of the spheres. This is due to the reciprocal forcing of the first swimmer and the reciprocal prescribed swimming gait of the second [170]. In contrast, we will show that in a viscoelastic fluid, both swimmers move in the direction of the smaller sphere when the spheres are of unequal radii and nowhere if the spheres are identical. This motion is a nonlinear viscoelastic response elicited from the deformation of the microstructure of the fluid and is therefore absent in Newtonian fluids. In light of this, a two-sphere assembly in a viscoelastic fluid may also be used as a micro-rheometer as previously demonstrated in the works of Khair & Squires [112] and Pak *et al.* [160], but an assembly of two rigidly connected spheres oscillating in a fluid is perhaps the simplest such example of a nonlinear micro-rheometer. Here we use the method of perturbation expansion to study the two-sphere swimmers in an Oldroyd-B fluid which for small extension rates is a reasonable approximation of polymeric fluids [121]. To conclude this work, we compare our results with another two-sphere swimmer wherein the spheres themselves deform elastically in a Newtonian fluid—a comparison of two-sphere swimmers in the presence of elasticity, either of the fluid or the solid.

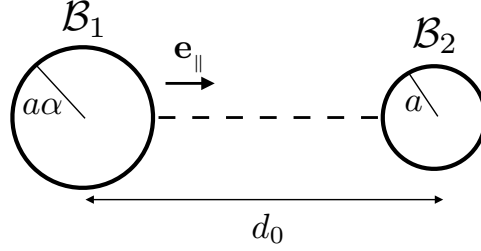


Figure 8.1: Schematic of the two-sphere swimmer. The spheres, labeled \mathcal{B}_1 and \mathcal{B}_2 , have radii $a\alpha$ and a , respectively ($\alpha > 1$). The spheres are (on average) a distance d_0 apart and \mathbf{e}_{\parallel} is the unit vector pointing from \mathcal{B}_1 to \mathcal{B}_2 .

8.2 Swimmer in a viscoelastic fluid

8.2.1 Two-sphere swimmers

In order to describe the motion of a swimming object, we decompose the contributions of the velocity of the body,

$$\mathbf{v}(\mathbf{x} \in \partial\mathcal{B}) = \mathbf{U} + \boldsymbol{\Omega} \times \mathbf{r} + \mathbf{v}^S, \quad (8.1)$$

where \mathbf{U} and $\boldsymbol{\Omega}$ are the rigid-body translation and rotation, and the swimming gait is denoted by \mathbf{v}^S . Here the body \mathcal{B} , with boundary $\partial\mathcal{B}$, is composed of two spheres of radius a and $a\alpha$, labeled \mathcal{B}_2 and \mathcal{B}_1 respectively ($\mathcal{B} = \mathcal{B}_1 \cup \mathcal{B}_2$). Without lack of generality, we assume $\alpha \geq 1$. The distance between the two spheres is d , which is along \mathbf{e}_{\parallel} (from large to small sphere) as shown in figure 8.1.

When the two spheres are connected as a rigid body, the distance between the two sphere centres is a fixed constant $d = d_0$; there is no swimming gait $\mathbf{v}^S = \mathbf{0}$, but an oscillatory external force is applied on the body,

$$\mathbf{F}_{ext} = F \cos(\omega t) \mathbf{e}_{\parallel}. \quad (8.2)$$

This may be imposed by applying an oscillating external magnetic field if the spheres are magnetic, or if the spheres are not density matched with the fluid, simply by oscillating the medium (although in that case there would be a mean force on the spheres as well). We will refer to this as an *in-phase* swimmer because the two spheres move in unison (see figure 8.2a).

In contrast to the first swimmer, the distance d between the spheres of the second swimmer varies sinusoidally according to

$$d = d_0 + 2\delta \sin(\omega t), \quad (8.3)$$

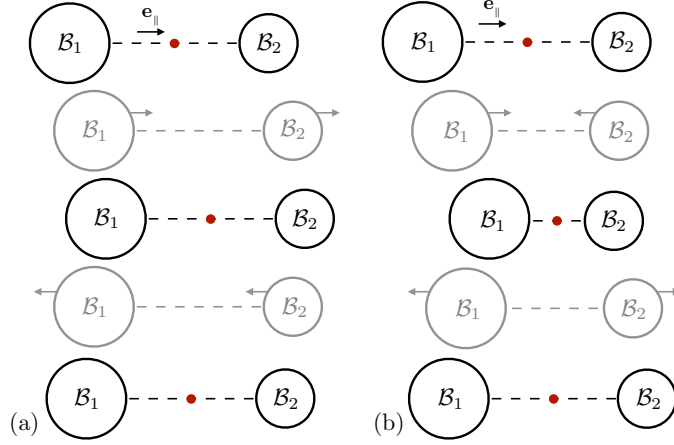


Figure 8.2: Schematic showing one complete cycle for the two swimmers: (a) The *in-phase* swimmer maintains the distance between the spheres as it moves forward. (b) In the *anti-phase* swimmer, the spheres converge and diverge. The steps in grey show the transition from one half cycle to the next. The red dot marks the position of the swimmer.

as equal and opposite velocities are imposed on the two spheres

$$\mathbf{v}^S(\mathbf{x} \in \partial\mathcal{B}_1) = \delta\omega \cos(\omega t) \mathbf{e}_\parallel, \quad (8.4)$$

$$\mathbf{v}^S(\mathbf{x} \in \partial\mathcal{B}_2) = -\delta\omega \cos(\omega t) \mathbf{e}_\parallel. \quad (8.5)$$

Here d_0 is the average distance, δ is the amplitude of oscillation and ω is the frequency. We refer to this swimmer as the *anti-phase* swimmer (see figure 8.2b).

For the sake of comparison between the two swimmers, we set the magnitude of the force F in (8.2) such that to leading order, the magnitude of the velocity of the induced oscillations would also be $\delta\omega$ for the in-phase swimmer (see Appendix B for further details).

8.2.2 Theory for swimming in complex fluids

The motion \mathbf{U} of an arbitrary swimmer (or active particle) in a non-Newtonian fluid, with deviatoric stress

$$\boldsymbol{\tau} = \eta \dot{\boldsymbol{\gamma}} + \boldsymbol{\tau}_{NN}, \quad (8.6)$$

where $\boldsymbol{\tau}_{NN}$ is the additional non-Newtonian stress, at zero Reynolds number is given by

$$\boldsymbol{U} = \frac{\hat{\eta}}{\eta} \hat{\boldsymbol{R}}_{FU}^{-1} \cdot [\boldsymbol{F}_{ext} + \boldsymbol{F}_T + \boldsymbol{F}_{NN}], \quad (8.7)$$

where $\boldsymbol{U} = [\boldsymbol{U} \ \boldsymbol{\Omega}]$ is six-dimensional vector comprising rigid-body translational and rotational velocities, respectively (we use bold sans serif fonts for six-dimensional vectors and tensors and bold serif for three dimensional ones) [43, 68]. The six-dimensional vector $\boldsymbol{F}_{ext} = [\boldsymbol{F}_{ext} \ \boldsymbol{L}_{ext}]$ contains any external force and torque acting on the swimmer. The term

$$\boldsymbol{F}_T = \frac{\eta}{\hat{\eta}} \int_{\partial\mathcal{B}} (\boldsymbol{v}^S - \boldsymbol{v}^\infty) \cdot (\boldsymbol{n} \cdot \hat{\boldsymbol{T}}_U) \, dS, \quad (8.8)$$

is a Newtonian ‘thrust’ due to any surface deformation \boldsymbol{v}^S of the swimmer in a background flow \boldsymbol{v}^∞ . Here, we consider an otherwise quiescent fluid so that $\boldsymbol{v}^\infty = \mathbf{0}$. The non-Newtonian contribution

$$\boldsymbol{F}_{NN} = - \int_{\mathcal{V}} \boldsymbol{\tau}_{NN} : \hat{\boldsymbol{E}}_U \, dV, \quad (8.9)$$

represents the extra force/torque on each particle due to a non-Newtonian deviatoric stress $\boldsymbol{\tau}_{NN}$ in the fluid volume \mathcal{V} in which the particles are immersed.

These formulae rely on operators from a resistance/mobility problem in a Newtonian fluid (with viscosity $\hat{\eta}$)

$$\hat{\boldsymbol{\gamma}} = 2\hat{\boldsymbol{E}}_U \cdot \hat{\boldsymbol{U}}, \quad (8.10)$$

$$\hat{\boldsymbol{\sigma}} = \hat{\boldsymbol{T}}_U \cdot \hat{\boldsymbol{U}}, \quad (8.11)$$

$$\hat{\boldsymbol{F}} = -\hat{\boldsymbol{R}}_{FU} \cdot \hat{\boldsymbol{U}}. \quad (8.12)$$

The tensors $\hat{\boldsymbol{E}}_U$ and $\hat{\boldsymbol{T}}_U$ are functions of position in space that map the rigid-body motion $\hat{\boldsymbol{U}}$ of the swimmer to the fluid strain-rate and stress fields, respectively, while the rigid-body resistance tensor

$$\hat{\boldsymbol{R}}_{FU} = \begin{bmatrix} \hat{\boldsymbol{R}}_{FU} & \hat{\boldsymbol{R}}_{F\Omega} \\ \hat{\boldsymbol{R}}_{LU} & \hat{\boldsymbol{R}}_{L\Omega} \end{bmatrix}. \quad (8.13)$$

Both problems considered here are axisymmetric, with the forcing and the gait aligned with the axis of symmetry of the swimmer. In this case, the resistance matrix $\hat{\boldsymbol{R}}_{FU}$ is diagonal and only translational motion occurs, simplifying matters substantially.

8.2. Swimmer in a viscoelastic fluid

We consider here only the time-averaged or (post-transient) mean velocity of the swimmer,

$$\bar{\mathbf{U}} = \frac{\hat{\eta}}{\eta} \overline{\hat{\mathbf{R}}_{FU}^{-1} \cdot [\mathbf{F}_{ext} + \mathbf{F}_T + \mathbf{F}_{NN}]}, \quad (8.14)$$

where the overline represents a time-averaged quantity. The in-phase swimmer does not change shape therefore the resistance is constant and $\mathbf{F}_T = \mathbf{0}$ because $\mathbf{v}^S = \mathbf{0}$; furthermore, the prescribed force is periodic with zero mean, $\overline{\mathbf{F}_{ext}} = \mathbf{0}$. In contrast, the anti-phase swimmer has no external forcing $\mathbf{F}_{ext} = \mathbf{0}$, but undergoes a reciprocal shape change and so, while the resistance is not constant, we know that $\overline{\hat{\mathbf{R}}_{FU}^{-1} \cdot \mathbf{F}_T} = \mathbf{0}$ by the scallop theorem [102]. We see then that, for both swimmers, the net motion is only due to the non-Newtonian contribution from the rheology of the fluid medium

$$\bar{\mathbf{U}} = \frac{\hat{\eta}}{\eta} \overline{\hat{\mathbf{R}}_{FU}^{-1} \cdot \mathbf{F}_{NN}}. \quad (8.15)$$

By the symmetry of the problem, any net motion must be in the direction of the axis of symmetry \mathbf{e}_{\parallel} i.e. $\bar{\mathbf{U}} = \bar{U} \mathbf{e}_{\parallel}$ with

$$\bar{U} = -\frac{\hat{\eta}}{\eta \hat{R}_{FU_{\parallel}}} \int_{\mathcal{V}} \overline{\boldsymbol{\tau}_{NN} : \hat{\mathbf{E}}_{U_{\parallel}}} dV, \quad (8.16)$$

where $\hat{R}_{FU_{\parallel}} = \mathbf{e}_{\parallel} \cdot \hat{\mathbf{R}}_{FU} \cdot \mathbf{e}_{\parallel}$ is the scalar resistance to translational motion of the two-sphere assembly in the direction of the axis of symmetry, whereas $\hat{\mathbf{E}}_{U_{\parallel}} = \hat{\mathbf{E}}_U \cdot \mathbf{e}_{\parallel}$ is a second order tensor equal to the strain-rate field due to rigid-body translation (with unit speed) in the direction \mathbf{e}_{\parallel} . $\hat{R}_{FU_{\parallel}}$ and $\hat{\mathbf{E}}_{U_{\parallel}}$ are obtained by way of the Stimson-Jeffery solution of two spheres moving with equal velocities along their axis of symmetry in a Newtonian fluid [192]. Finally, we note that although the geometry of the anti-phase swimmer is not constant, we solve the problem asymptotically for small deformations about a mean geometry such that $\hat{R}_{FU_{\parallel}}$, $\hat{\mathbf{E}}_{U_{\parallel}}$, and the boundary of the volume integral in (8.16) are constant, which allows us to pass the time-average operator onto the non-Newtonian stress alone [69, 125].

8.2.3 Constitutive equation

We are interested here in the effects of nonlinear viscoelasticity that enable the net motion of the swimmers. Until this point, we have only assumed that the stress in the fluid may be separated into a Newtonian and non-Newtonian contribution. The deviatoric stress $\boldsymbol{\tau}_{NN}$ in a viscoelastic fluid

typically follows a nonlinear evolution equation. For simplicity, we use the Oldroyd-B constitutive equation [16] but other constitutive relationships can be easily used within this formalism. Oldroyd-B is a single relaxation time viscoelastic (Boger fluid) fluid that is governed by

$$\overset{\nabla}{\boldsymbol{\tau}}_{NN} = \frac{\eta_{NN}}{\lambda} \dot{\boldsymbol{\gamma}} - \frac{1}{\lambda} \boldsymbol{\tau}_{NN}, \quad (8.17)$$

where λ is the relaxation time of the fluid and η_{NN} is an additional viscosity due to the (polymeric) microstructure. The upper convected derivative is defined $\overset{\nabla}{\mathbf{A}} = \partial \mathbf{A} / \partial t + \mathbf{v} \cdot \nabla \mathbf{A} - ((\nabla \mathbf{v})^\top \cdot \mathbf{A} + \mathbf{A} \cdot \nabla \mathbf{v})$ where \mathbf{v} is the fluid velocity field.

The problems we consider here are periodic (with period $\tau = 2\pi/\omega$) and, neglecting any transient evolution from an initial condition, we may simplify matters by assuming that all functions may be written as Fourier series, for example, the velocity field $\mathbf{v} = \sum_p \mathbf{v}^{(p)} e^{pi\omega t}$. Following this for the stress, we have [69]

$$\boldsymbol{\tau}_{NN}^{(p)} = (\eta^*(p) - \eta) \dot{\boldsymbol{\gamma}}^{(p)} + \mathbf{N}^{(p)} \quad (8.18)$$

where the tensor $\mathbf{N}^{(p)}$ represents the contribution of the nonlinear terms to each mode and the complex viscosity

$$\eta^*(p) = \frac{1 + piDe\beta}{1 + piDe} \eta_0. \quad (8.19)$$

The Deborah number, $De = \lambda\omega$, characterizes the relative rate of actuation of the spheres to the relaxation of the fluid. The viscosity ratio $\beta = \eta/\eta_0$ is the relative viscosity of the Newtonian part of the fluid (solvent) where $\eta_0 = \eta + \eta_{NN}$ represents the (total) zero-shear-rate viscosity of the fluid. In particular, by substituting (8.18) into (8.16) one may show that

$$\bar{U} = -\frac{\hat{\eta}}{\eta_0 \hat{R}_{FU\parallel}} \int_{\mathcal{V}} \bar{\mathbf{N}} : \hat{\mathbf{E}}_{U\parallel} dV, \quad (8.20)$$

where $\bar{\mathbf{N}} = \mathbf{N}^{(0)}$, and we see that linear viscoelasticity does not lead to net motion of these swimmers because by definition $\mathbf{N}^{(p)} = \mathbf{0}$ for linearly viscoelastic fluids (see Appendix B for further details).

8.2.4 Small amplitude expansion

We assume that the oscillation amplitudes are much smaller than all other length scales, $\delta \ll a, d_0$, and define dimensionless quantities $\epsilon = \delta/a \ll 1$

8.2. Swimmer in a viscoelastic fluid

and $\Delta = d_0/a$. In addition, we define a dimensionless clearance between the spheres, $\Delta_c = \Delta - (1 + \alpha)$. We solve for the flow by employing a regular perturbation expansion in small deformations ϵ to all flow quantities

$$\{\mathbf{v}, \boldsymbol{\tau}, p, \dots\} = \epsilon \{\mathbf{v}_1, \boldsymbol{\tau}_1, p_1, \dots\} + \epsilon^2 \{\mathbf{v}_2, \boldsymbol{\tau}_2, p_2, \dots\} + \dots \quad (8.21)$$

The swimming speed is then given by

$$\bar{U} = -\epsilon^2 \frac{\hat{\eta}}{\eta_0 \hat{R}_{FU\parallel}} \int_{\mathcal{V}} \bar{\mathbf{N}}_2 : \hat{\mathbf{E}}_{U\parallel} dV + \mathcal{O}(\epsilon^4). \quad (8.22)$$

Because the tensor \mathbf{N} represents the nonlinear terms in the viscoelastic constitutive equation, there are no terms linear in ϵ . The quadratic term depends only on the leading order flow field, $\mathbf{N}_2[\mathbf{v}_1, \boldsymbol{\tau}_1]$, which is a solution to a linearly viscoelastic flow that has exactly the same flow field as a Newtonian flow with equivalent prescribed velocity boundary conditions.

When the spheres move together as a rigid body (the in-phase swimmer), the solution for \mathbf{v}_1 is easily obtained using the solution for two spheres moving with equal velocities along the line joining their centers by Stimson & Jeffery [192]. Similarly when the spheres approach one another (anti-phase swimmer), the solution for \mathbf{v}_1 is available due to the work of Maude [141] for two spheres approaching each other in a Newtonian fluid (see [188] for some corrected errors). Thus knowing the $\mathcal{O}(\epsilon)$ fields, we may evaluate the tensor \mathbf{N}_2 , which for an Oldroyd-B fluid is given by

$$\bar{\mathbf{N}}_2 = -\frac{1}{2} \text{Re} \left\{ \frac{\text{De}(1-\beta)}{(1+i\text{De})} \left[\mathbf{v}_1^{(-1)} \cdot \nabla \dot{\gamma}_1^{(1)} - \left(\nabla \mathbf{v}_1^{(-1)} \right)^\top \cdot \dot{\gamma}_1^{(1)} - \dot{\gamma}_1^{(1)} \cdot \nabla \mathbf{v}_1^{(-1)} \right] \right\}. \quad (8.23)$$

Finally, we obtain the leading order motion for either swimmer by evaluating (8.22) to find

$$\bar{U} = \delta \omega \frac{\delta}{a} \left(\frac{\text{De}(1-\beta)}{1+\text{De}^2} \right) \mathcal{U}, \quad (8.24)$$

where the dimensionless quantity \mathcal{U} is evaluated using numerical integration of an analytical expression.

Note that under this small-amplitude expansion $|\dot{\gamma}| \sim \epsilon \omega$ and consequently Weissenberg numbers, $\text{Wi} = |\dot{\gamma}| \lambda \sim \epsilon \text{De}$, are asymptotically smaller than Deborah numbers. Thus, provided ϵ is made small enough, these results are valid for arbitrary values of Deborah number even for fluids such as Oldroyd-B fluid that are unphysical for order one Weissenberg numbers (see also [121, 125]).

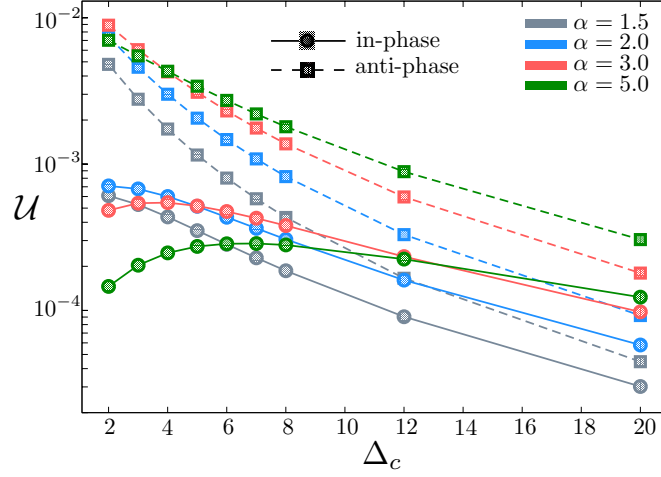


Figure 8.3: The swimming speed coefficient \mathcal{U} is plotted with variation in the clearance Δ_c between the two spheres for different size ratios α . The square symbols (connected by dashed lines) represent the anti-phase swimmer and the circles (connected by solid lines) represent the in-phase swimmer. All quantities are dimensionless.

8.2.5 Results and discussion

We find that the two-sphere assembly can swim in a viscoelastic fluid at finite Deborah numbers, provided the two spheres are of different sizes. The difference in the sphere sizes leads to the fore-aft asymmetry required for swimming. We see from (8.24) that the swimming speed is maximized when $De = 1$. In the limit when the actuation is much slower than the relaxation of the fluid, $De \rightarrow 0$, or much faster, $De \rightarrow \infty$, there is no swimming $\bar{U} = 0$, indeed the term in the brackets of (8.24), which governs this behavior, is simply the dimensionless elastic modulus of the fluid [69]. We report the values of \mathcal{U} for the two swimmers for a few configurations in figure 8.3. Both swimmers swim with the smaller sphere as the head. At small separations, the anti-phase swimmer is an order of magnitude faster; however, at large separations this difference in magnitude fades away.

The direction of the motion of these swimmers can be largely predicted by studying a single sphere oscillating in a viscoelastic fluid. The *viscoelastic steady streaming flow* that results from this motion draws fluid in towards the center of the sphere along the axis of oscillation [18]. Larger spheres generate stronger viscoelastic flows for a given velocity but the relation-

ship is sublinear in radius and so one would expect that when two unequal spheres interact, because of the relative resistances, the net effect of the interacting viscoelastic streaming flows would be to push the assembly in the direction of the smaller sphere. This is essentially a ‘far-field’ superposition argument, where there is no difference between in-phase and anti-phase oscillations, and one should take great care when applying this logic to closely interacting spheres in a nonlinear non-Newtonian fluid; however, this prediction qualitatively agrees with our exact two-body problem solutions. We also note that Keim *et al.* [109] find that a similar two-sphere assembly undergoing rotational oscillations instead moves towards the larger sphere, but in that case the spheres are moving perpendicular to their axis of symmetry and so we expect the viscoelastic steady streaming flow to be reversed along that axis.

Examining more closely first the in-phase swimmer, a rigid body of such shape moving in a weakly viscoelastic fluid (e.g. a second-order fluid under slow flows [16]) will experience a net viscoelastic force pointing towards the smaller sphere and so the total drag on the body when the larger sphere leads increases while it decreases when the smaller sphere is at the front. Leal [131] has also shown that for sedimenting slender bodies, when the trailing end is sharp and the leading edge is blunt the drag increases in a second-order fluid. In light of this, when the two-sphere body oscillates periodically in a viscoelastic fluid, one expects the net viscoelastic contribution to the force on the body over one cycle to point towards the smaller sphere. The speed of the swimming depends on the strength of this viscoelastic contribution and the hydrodynamic resistance to the steady translation of the body. As can be seen from figure 8.3, such a swimmer has an optimum in the swimming velocity at a certain separation for a given ratio of the sphere sizes.

For the anti-phase swimmer, the viscoelastic force seems to depend on the strength of squeeze flow between the two spheres which increases as the separation between the spheres decreases. Combined with the low hydrodynamic resistance of the assembly when the spheres are close, swimming is monotonically faster with smaller separations (for a given size ratio). When the spheres are far apart, the strength of the squeeze flow decreases and the two types of swimmers swim with speeds of the same order.

Clearly, a size ratio of 1 will not lead to swimming. One also expects a very large size ratio to be equally inefficient due to a decrease in the net fore-aft asymmetry over a complete cycle. This non-monotonicity with size ratio is also observed at small distances in figure 8.3, although at very large distances, when the interaction between the spheres has much decreased, higher size ratio leads to better swimming. However, this may not be the

regime one would focus on for optimal swimming.

We also note that the effect of viscoelasticity on the swimmers is found to be opposite to the effect of inertia as described in the analytical work of Felderhof [74]. There, the two-sphere swimmer moves with the larger sphere as the head, as might be expected given that weakly inertial steady-streaming flow can push fluid out from an oscillating sphere along the axis of oscillation [18, 175, 187]. However, recent numerical work by Dombrowski *et al.* [57] reports that the smaller sphere leads at small Reynolds number only to switch to larger sphere leading at higher Reynolds number. We do not observe such switching of swimming direction with the Deborah number in our analysis which is valid for small oscillation amplitudes. We also note that although the results presented here are for an Oldroyd-B fluid, one may perform a small-amplitude analysis with other viscoelastic fluid models like the second-order fluid, Giesekus fluid, and FENE-P [16] and find qualitatively similar results. Any quantitative differences that occur are due to parameter values (concerning for example, the presence or absence of second normal stress differences) particular to the model or slightly different definitions of the Deborah number [121].

In the next section, we study a two-sphere swimmer with elastic spheres in a Newtonian fluid and demonstrate that the direction of propulsion is the same as this two-(rigid)-sphere swimmer in viscoelastic fluid.

8.3 Swimmer with elastic spheres

We now compare the two-sphere swimmers in a viscoelastic fluid with swimmers with elastic spheres in a Newtonian fluid. This calculation closely follows the work of Nasouri *et al.* [153] who studied a two-sphere swimmer with one rigid and other elastic sphere in a Newtonian fluid. Here, similar to the previous section, we consider model swimmers that consist of two spheres of radii a and αa , but this time we relax the rigidity constraint by assuming that the spheres are isotropic, incompressible neo-Hookean solids.

To study the behavior of this system, one must first understand the deformation of a single elastic sphere in Stokes flow. Neglecting inertia, momentum balance for the elastic solid yields

$$\nabla \cdot \boldsymbol{\sigma}_s + \mathbf{f}(t) = \mathbf{0}, \quad (8.25)$$

where $\boldsymbol{\sigma}_s$ is the stress due to elastic deformation and \mathbf{f} is the applied body force density on the sphere. For an isotropic, incompressible neo-Hookean solid, this stress field can be expressed using the displacement vector \mathbf{u} as

[91, 156]

$$\boldsymbol{\sigma}_s = -p_s \mathbf{I} + G (\mathbf{D} \cdot \mathbf{D}^T - \mathbf{I}), \quad (8.26)$$

where G is the shear modulus and $\mathbf{D} = \mathbf{I} + \nabla \mathbf{u}$ is the deformation gradient tensor. The Lagrange multiplier p_s enforces the incompressibility of the solid through

$$\det(\mathbf{D}) = 1, \quad (8.27)$$

where ‘det’ is the determinant. The traction across the solid-fluid interface must be continuous so that

$$\boldsymbol{\sigma}_s \cdot \mathbf{n} = \boldsymbol{\sigma} \cdot \mathbf{n}, \quad (8.28)$$

where \mathbf{n} is the normal vector to the deformed sphere and $\boldsymbol{\sigma}$ is the stress field in the fluid domain which can be determined by solving the Stokes equations over the deformed boundary.

If we scale lengths with a , velocities with $\delta\omega$, forces with G/a , time with $a/\delta\omega$, stress in the solid domain with G and stress in the fluid domain with $\eta\delta\omega/a$, from equation (8.28) a dimensionless parameter $\varepsilon = \eta\delta\omega/aG$ then naturally arises as the ratio of viscous forces to elastic forces. Here we focus on the case wherein the sphere is only weakly elastic; elastic forces are much larger than viscous forces and so $\varepsilon \ll 1$. Since the motion is axisymmetric, one can show that the elastic sphere reaches equilibrium with a relaxation time scale of $\tau_{\text{relax}} \sim \mathcal{O}(a\varepsilon/\delta\omega)$. Thus, under the assumption of $\varepsilon \ll 1$, we can assume that elastic deformations are quasi-static: the sphere deforms instantly and we then have rigid-body motion [98].

Similar to the viscoelastic case, for the in-phase swimmer, for the sake of comparison, we set the magnitude of the applied external force to be $F = \delta\omega R_{FU\parallel}$ so that to leading order the speed of oscillation is $\delta\omega$. For the anti-phase swimmer, we define the gait according to (8.4) and (8.5) but in this case the velocity is prescribed on the deformed boundaries.

We now return to our two-sphere swimmer, with both spheres being weakly elastic. In a Newtonian fluid, the dynamics of the motion of the body is given by

$$\mathbf{U} = \mathbf{R}_{FU}^{-1} \cdot [\mathbf{F}_T + \mathbf{F}_{ext}]. \quad (8.29)$$

The thrust force may be generically decomposed into the thrust generated by each sphere $\mathbf{F}_T = \mathbf{F}_{T_1} + \mathbf{F}_{T_2}$. Because the spheres are deforming, we will

8.3. Swimmer with elastic spheres

assume that the spheres are well separated, and compute the hydrodynamic thrust generated by each sphere with hydrodynamic interactions solved to leading order using a far-field approximation, $\Delta \gg 1$.

For individual spheres, (8.8) reduces to Faxén's first law for each sphere

$$\mathbf{F}_{T_1} = -\mathbf{R}_1 \cdot \left(\mathbf{v}_1^S - \mathcal{F}_1[\mathbf{v}_2^\infty] \right), \quad (8.30)$$

$$\mathbf{F}_{T_2} = -\mathbf{R}_2 \cdot \left(\mathbf{v}_2^S - \mathcal{F}_2[\mathbf{v}_1^\infty] \right), \quad (8.31)$$

where \mathbf{R}_1 and \mathbf{R}_2 are the resistance tensors for each sphere and, \mathcal{F}_1 and \mathcal{F}_2 are the respective Faxén operators. Here, \mathbf{v}_1^∞ is the background flow field induced by sphere \mathcal{B}_1 , and vice versa for \mathbf{v}_2^∞ . Recalling that spheres are only weakly elastic (since $\varepsilon \ll 1$), the spheres only slightly deviate from their spherical shape so that the hydrodynamic resistance and Faxén's laws are unchanged from an undeformed sphere to leading order [24, 113]. The net thrust generated by the swimmer at the leading order is thereby

$$\mathbf{F}_T = 6\pi\eta a \left(-\alpha \mathbf{v}_1^S + \alpha \mathbf{v}_{2,1}^\infty - \mathbf{v}_2^S + \mathbf{v}_{1,2}^\infty \right), \quad (8.32)$$

where $\mathbf{v}_{2,1}^\infty$ indicates the background flow from sphere 2 evaluated at the center of sphere 1 (and vice versa). For the externally forced (in-phase) swimmer, the gait is zero $\mathbf{v}_1^S = \mathbf{v}_2^S = \mathbf{0}$. For the anti-phase swimmer, the imposed gait is periodic and given that we are interested in only the mean motion, averaging over a period $\tau = 2\pi/\omega$, for both swimmers, leads to

$$\overline{\mathbf{F}_T} = 6\pi\eta a \left(\alpha \overline{\mathbf{v}_{2,1}^\infty} + \overline{\mathbf{v}_{1,2}^\infty} \right). \quad (8.33)$$

We see clearly, in this far-field result, that the thrust is dictated purely by the *elastic steady streaming flow* generated by each sphere acting on the other.

By solving equations (8.25) to (8.28) asymptotically, one can determine the flow field around an oscillating elastic sphere. This flow field, upon averaging, will give the steady streaming flows $\overline{\mathbf{v}_1^\infty}$ and $\overline{\mathbf{v}_2^\infty}$ (see [153] for technical details). By prescribing an external force of magnitude $F = \delta\omega R_{FU\parallel}$ for the in-phase swimmer, the magnitude of the deformation and thus the magnitude of the steady-streaming flows is equal for both swimmers. We note, in particular, that the elastic steady-streaming flow of each sphere draws fluid inward along the axis of symmetry in much the same way as the viscoelastic steady streaming flow. Here, we find that $\mathbf{v}_{2,1}^\infty \cdot \mathbf{e}_\parallel \propto \delta\omega\epsilon^3/\Delta^2$ and $\mathbf{v}_{1,2}^\infty \cdot \mathbf{e}_\parallel \propto -\delta\omega\epsilon^3/\alpha\Delta^2$. The net thrust is then

$$\overline{\mathbf{F}_T} = \frac{74979}{34048} \pi\eta d_0 \delta\omega\alpha \left(1 - \frac{1}{\alpha^2} \right) \frac{\epsilon^3}{\Delta^3} \mathbf{e}_\parallel. \quad (8.34)$$

8.4. Conclusion

Both oscillating elastic spheres generate steady-streaming flows but the magnitude of each flow is inversely proportional to the radius while the resistance of each sphere is linearly proportional to the radius and so the net thrust force is in the direction of the smaller sphere ($\alpha \geq 1$).

With a hydrodynamic resistance of $R_{FU_{\parallel}} = 6\pi\eta a(1 + \alpha)$, and using the fact that the average external force is zero,

$$\overline{\mathbf{F}_{ext}} = \mathbf{0}, \quad (8.35)$$

(in the case of the anti-phase swimmer the prescribed force itself is zero), we obtain the time-averaged velocity

$$\overline{\mathbf{U}} = \frac{24993}{68096} \delta\omega \left(1 - \frac{1}{\alpha}\right) \frac{\epsilon^3}{\Delta^2} \mathbf{e}_{\parallel}. \quad (8.36)$$

The swimming motion is always in the direction of the smaller sphere, similar to the rigid swimmer in the viscoelastic fluid (the swimmer swims with the smaller sphere as the head). Furthermore, since we solved this problem assuming the spheres are well separated using far-field approximations of the flow, the speed of the swimmer is ultimately independent of whether the spheres oscillate in-phase or anti-phase.

8.4 Conclusion

We studied the effects of elasticity on the motion of two-sphere swimmers where the two spheres oscillate in-line. When the two spheres are rigid and the fluid viscoelastic, we find that the swimmers swim with the smaller-sphere as the head. However, the swimming speed is dependent on the type of swimmer: anti-phase swimmers, in general, swim faster than the in-phase swimmers. We also find that when the spheres themselves are elastic and the fluid Newtonian, the swimmer again moves in the direction of the smaller sphere.

We note that the effects of elasticity on the swimmer are found to be opposite of the effect of inertia described in the theoretical work of Felderhof [74] who showed that the two-sphere swimmer moves with the larger sphere as the head, but we do not observe a reversal of the swimming direction as a function of the Deborah number, analogous to what is observed upon increasing Reynolds number in the numerical work of Dombrowski *et al.* [57].

Chapter 9

Conclusion and outlook

The motivation for the work in this thesis was to understand how some simple motions of particles are affected by the rheological properties of the fluid. We focussed on small particles that can swim, and restricted our attention to two rheological properties, shear-thinning viscosity and viscoelasticity, chosen for their apparent ubiquity in non-Newtonian fluids. We followed a theoretical approach, often drawing from recent experimental and numerical works. In this section, we briefly recapitulate and discuss the findings, the limitations, and the future of this work.

9.1 The findings

We started the thesis by looking at the dynamics of a squirmer in a Newtonian fluid with externally imposed gradients in the fluid viscosity in chapter 3. The work was motivated by the recent study of Liebchen *et al.* [136] explaining the physical mechanism of viscotaxis. We showed that viscosity gradients change the motion of a squirmer drastically in comparison to its motion in a Newtonian fluid of uniform viscosity. Specifically, we find that the squirmers are in general viscophobic, although the details of their dynamics are dependent on whether they swim as pushers, pullers, or neutral swimmers. The differences in these details among the swimmers can be used to sort them based on their swimming style.

Next we discuss the effects of shear-thinning viscosity on the motion of passive particles in Chapter 4. By analysing the motion of a sphere in a background flow field due to an external force, or somewhat equivalently the motion of a rotating and sedimenting sphere (a set-up proposed as a rheometer [82]), we showed how translational and rotational motion can couple even for particle shapes for which no such coupling is present in Newtonian fluids. We also showed that for two equal spheres that sediment along the line joining their centres, while the principle of kinematic reversibility holds and spheres maintain their initial distance of separation, the reduction in their drag is a non-monotonic function of their distance of separation. As for the case of a dilute suspension of rigid spheres in shear-thinning fluids, we found

the corresponding Einstein viscosity, reflecting how the presence of a particle both adds and subtracts from the shear-viscosity; which contribution dominates depends on the applied shear-rate.

The effects of shear-thinning viscosity on the swimming speed of a squirmer were studied in Chapter 5. Prior to our work, there were relatively few studies analysing the motion of swimmers in shear-thinning fluids. We showed that a squirmer can swim both slower and faster in a shear-thinning fluid as compared to a Newtonian fluid for the same swimming stroke. The faster or slower swimming, in general, cannot be explained by a *simple* thrust and drag decomposition of the swimming problem—an approach which previously had been used for developing intuition in shear-thinning fluids. We also showed that squirming modes that do not contribute to swimming in Newtonian fluids can contribute to swimming in shear-thinning fluids, and that, in general, squirming through shear-thinning fluids possesses some rich physics.

While in shear-thinning fluids we showed that higher-order squirming modes, and not just the first mode as in Newtonian fluids, can contribute to swimming, we showed exactly how these modes couple and contribute to the swimming speed in a weakly viscoelastic fluid. In Chapter 6, we give the expression for the swimming speed of a general, n -mode, squirmer in a second-order fluid. As an example of squirmers in which the higher modes are known, we chose diffusiophoretic Janus particles and studied their dynamics both in second-order and shear-thinning fluids. In the particular case of Janus particles, we quantified the error in swimming speeds if one were to use only the first two swimming modes to calculate the effects of the two non-Newtonian properties: viscoelasticity, and shear-thinning viscosity. Whereas in Chapter 6 we studied only the first effects of viscoelasticity through a second-order fluid on the squirmer motion, we considered higher-order effects using two different viscoelastic models—the Giesekus model and a fluid of differential type (grade three)—in Chapter 7. Importantly, we find that the swimming speeds as predicted by the expansion in Deborah number for the two fluid models are qualitatively different. The work raises questions regarding the adequacy of the Deborah number expansion, and the choice of viscoelastic model.

In Chapter 8, we studied an assembly of two spheres connected with a massless, hydrodynamically non-existent, rod for effects of viscoelasticity. We found that on oscillating the two spheres along the rod, the entire assembly moves forward, provided that the two spheres are of unequal sizes. We contrasted this analysis with a similar assembly of two elastic spheres in a Newtonian fluid. We found that in both cases the assembly moves in

the direction of the smaller sphere. Note that, constrained by the scallop theorem, such an assembly of rigid spheres cannot *swim* in a Newtonian fluid; that this simple design *swims* in a viscoelastic fluid is possible only due to the complexity of the fluid.

The topics in this thesis, for most part, concerned the newly emerging field of active matter, which has been attracting researches from the more conventional fields in physics, chemistry and biology. We believe the work in this thesis offers some fundamental contributions to this rapidly growing field, be it in sorting and designing active particles, or more generally through understanding their motions in fluids where they commonly are, or will be, found.

9.2 The limitations

Clearly, many particles are not spherical, and modelling swimmers as squirmers may not be accurate on occasions. Moreover, many non-Newtonian fluids have more complex rheological properties than just shear-thinning viscosity and viscoelasticity. While these points are important, suffice to say we believed disregarding them was essential for any immediate theoretical progress. Hence, we do not delve into these points here.

More importantly, we ask what when no parameter is small in our analysis? As an example, consider the two-sphere swimmer assembly discussed in Chapter 8. Will the direction of the swimmer motion be reversed when the amplitude of oscillations of the spheres is not small? Asymptotic results in this work by themselves cannot answer such questions. Even how small is small enough for the analytical results to hold can be known, generally, only through experiments and numerics.

Further, in the thesis, the quantities of interest were swimming speeds, sedimenting velocities, and drag forces on particles—integral quantities that could be calculated relatively easily using the generalized reciprocal theorem. The shortcut of the reciprocal theorem meant not travelling the more laborious path of calculating the flow field corrections first, and then calculating such quantities as mentioned, but perhaps also a want of a deeper physical intuition developed through analysing flow fields.

In our opinion, we still need more of all—theoretical, numerical, and experimental—research for a complete understanding of the problems we have studied in this work; theoretical work, being more tractable of the three, in part due to its self-declared assumptions, has often struck first in

this battlefield.

9.3 The future

Many microorganisms swim in complex fluids. We know more about microswimmers in Newtonian fluids than in complex fluids. From a problem solving perspective, following Einstein’s suggestion ‘that since the basic equations of physics are nonlinear, all of mathematical physics will have to be done over again’ [183] one may just start solving swimming problems that have been understood in Newtonian fluids in complex (non-linear) fluids. In fact, not a bad advice when comes to understanding nature, owing to the ubiquity of swimming phenomena in biology where many fluids show complex rheological behaviour not restricted to just shear-thinning viscosity and viscoelasticity, but also involving thixotropy and microstructural anisotropy.

Immediate areas to venture into include understanding the interactions between swimmers in complex fluids, for microswimmers, e.g., sperm cells, swim together in large numbers, and understanding how viscoelasticity of the fluid and inertia together affect the motion of a swimmer—microswimmers do accelerate when escaping predators (for effects of inertia alone, see [110, 210] and references therein).

Dynamics of model microswimmers can also be analysed in fluids that are active themselves; such is done in the latest work of Soni *et al.* [186], who answer if an active fluid can do work on a Taylor sheet swimmer, and therefore make it swim faster than in a passive fluid for the same stroke. The same stroke assumption that we have also used in our works, should be relaxed too in order to capture how the strokes themselves are affected by the fluid’s rheological properties. This can be realised by prescribing thrust forces on the swimmers rather than swimming strokes, as Curtis & Gaffney [39] have done for the Najafi-Golestanian three-sphere swimmer in an Oldroyd-B fluid, and thereby showing the qualitative different results achieved through prescribing forces and prescribing kinematics.

One problem, we would like to see addressed in the near future is the stochastic dynamics of active particles in complex fluids. While large macroscopic swimmers can sustain their swimming direction for long times, microswimmers experience orientation decorrelation because of their small sizes [117, 178]. At the size of microswimmers, thermal fluctuations can ‘lead to a Brownian loss of the swimming direction, resulting in a transition from short-time ballistic dynamics to effective long-time diffusion’ [178].

Many bacteria also experience what is called tumbling. In tumbling, ‘a bacterium typically runs in a directed sense for a certain time interval before changing its orientation abruptly, and by a large amount. It then runs in the new direction, possibly correlated to the old one’ [118].

The stochastic dynamics play an important role at the length scale of microswimmers [11, 92]. Even reciprocal swimmers, which on average do not swim, have ‘enhanced diffusivities, possibly by orders of magnitude, above their normal Brownian diffusion’ [123]. As many microswimmers are found in complex fluids, Patteson *et al.* [163] experimentally investigated the run and tumble dynamics of *E. Coli* bacteria in polymeric solutions. The authors found that ‘even small amounts of polymer in solution can drastically change *E. Coli* dynamics: cells tumble less and their velocity increases, leading to an enhancement in cell translational diffusion and a sharp decline in rotational diffusion’ [163]. A theoretical investigation of such phenomena, drawing from and building on recent works on active micro-rheology in non-linear fluids [189, 190], will be interesting.

Bibliography

- [1] ALEXANDER, G. P., POOLEY, C. M. & YEOMANS, J. M. 2009 Hydrodynamics of linked sphere model swimmers. *J. Phys.: Condens. Matt.* **21** (20), 204108.
- [2] ANDERSON, J. L. 1989 Colloid transport by interfacial forces. *Annu. Rev. Fluid Mech.* **21**, 61–99.
- [3] ARDEKANI, A. M. & GORE, E. 2012 Emergence of a limit cycle for swimming microorganisms in a vortical flow of a viscoelastic fluid. *Phys. Rev. E* **85**, 056309.
- [4] ARDEKANI, A. M., RANGEL, R. H. & JOSEPH, D. D. 2008 Two spheres in a free stream of a second-order fluid. *Phys. Fluids* **20** (6), 063101.
- [5] ASTARITA, G. & MARRUCCI, G. 1974 *Principles of non-Newtonian fluid mechanics*. McGraw-Hill Companies.
- [6] AVRON, J. E., KENNETH, O. & OAKNIN, D. H. 2005 Pushmepullyou: an efficient micro-swimmer. *New J. Phys.* **7**, 234.
- [7] BAHAT, A., TUR-KASPA, I., GAKAMSKY, A., GIOJALAS, L. C., BREITBART, H. & EISENBACH, M. 2003 Thermotaxis of mammalian sperm cells: A potential navigation mechanism in the female genital tract. *Nat. Med.* **9** (2), 149–150.
- [8] BARBATI, A. C., DESROCHES, J., ROBISSON, A. & MCKINLEY, G. H. 2016 Complex fluids and hydraulic fracturing. *Annu. Rev. Chem. Biomol. Engng* **7** (1), 415–453.
- [9] BARNES, H. A. 2003 Review of the rheology of filled viscoelastic systems. *Rheology Reviews* p. 49.
- [10] BATCHELOR, G. K. 1970 The stress system in a suspension of force-free particles. *J. Fluid Mech.* **41** (3), 545–570.

Bibliography

- [11] BECHINGER, C., DI LEONARDO, R., LÖWEN, H., REICHHARDT, C., VOLPE, G. & VOLPE, G. 2016 Active particles in complex and crowded environments. *Rev. Mod. Phys.* **88**, 045006.
- [12] BECKER, L. E., KOEHLER, S. A. & STONE, H. A. 2003 On self-propulsion of micro-machines at low Reynolds number: Purcell's three-link swimmer. *J. Fluid Mech.* **490**, 15–35.
- [13] BENDER, C. M. & ORSZAG, S. A. 2013 *Advanced mathematical methods for scientists and engineers I: Asymptotic methods and perturbation theory*. Springer Science & Business Media.
- [14] BENNETT, R. R. & GOLESTANIAN, R. 2015 A steering mechanism for phototaxis in *Chlamydomonas*. *J. R. Soc. Interface* **12** (104), 20141164–20141164.
- [15] BERG, H. C. & BROWN, D. A. 1972 Chemotaxis in *Escherichia coli* analysed by three-dimensional tracking. *Nature* **239** (5374), 500–504.
- [16] BIRD, R. B., ARMSTRONG, R. C. & HASSAGER, O. 1987 *Dynamics of polymeric liquids. Vol. 1: Fluid mechanics*. John Wiley.
- [17] BLAKE, J. R. 1971 A spherical envelope approach to ciliary propulsion. *J. Fluid Mech.* **46**, 199–208.
- [18] BÖHME, G. 1992 On steady streaming in viscoelastic liquids. *J. Non-Newton. Fluid Mech.* **44**, 149 – 170.
- [19] BÖHME, G. & MÜLLER, A. 2015 Propulsion of axisymmetric swimmers in viscoelastic liquids by means of torsional oscillations. *J. Non-Newton. Fluid Mech.* **224**, 1 – 16.
- [20] BRADY, J. F. 2011 Particle motion driven by solute gradients with application to autonomous motion: continuum and colloidal perspectives. *J. Fluid Mech.* **667**, 216–259.
- [21] BRAY, D. 2000 *Cell Movements*. Garland Publishing, New York, NY.
- [22] BRENNEN, C., & WINET, H. 1977 Fluid mechanics of propulsion by cilia and flagella. *Annu. Rev. Fluid Mech.* **9**, 339–398.
- [23] BRENNER, H. 1961 The slow motion of a sphere through a viscous fluid towards a plane surface. *Chem. Engng. Sci.* **16** (3), 242–251.

- [24] BRENNER, H. 1964 The Stokes resistance of an arbitrary particle—IV arbitrary fields of flow. *Chem. Eng. Sci.* **19**, 703–727.
- [25] BRETHERTON, F. P. 1962 The motion of rigid particles in a shear flow at low reynolds number. *J. Fluid Mech.* **14** (2), 284–304.
- [26] BROWN, E. & JAEGER, H. M. 2011 Through thick and thin. *Science* **333**, 1230–1231.
- [27] VAN DEN BRULE, B.H.A.A. & GHEISSARY, G. 1993 Effects of fluid elasticity on the static and dynamic settling of a spherical particle. *J. Non-Newtonian Fluid Mech.* **49** (1), 123–132.
- [28] BRUNN, P. 1977 Interaction of spheres in a viscoelastic fluid. *Rheol. Acta* **16** (5), 461–475.
- [29] BRUNN, P. 1980 The motion of rigid particles in viscoelastic fluids. *J. Non-Newtonian Fluid Mech.* **7**, 271–288.
- [30] BUSH, M.B. & PHAN-THIEN, N. 1984 Drag force on a sphere in creeping motion through a carreau model fluid. *J. Non-Newtonian Fluid Mech.* **16** (3), 303 – 313.
- [31] BUTTINONI, I., VOLPE, G., KÜMMEL, F., VOLPE, G. & BECHINGER, C. 2012 Active Brownian motion tunable by light. *J. Phys. Condens. Matter* **24**, 284129.
- [32] CHHABRA, R. P. 1998 Rising velocity of a swarm of spherical bubbles in power law fluids at high reynolds numbers. *Can. J. Chem. Eng.* **76** (1), 137–140.
- [33] CHHABRA, R. P. 2006 *Bubbles, drops, and particles in non-Newtonian fluids*. CRC press.
- [34] CHHABRA, R. P., TIU, C. & UHLHERR, P. H. T. 1980 *Shear-Thinning Effects in Creeping Flow about a Sphere*, pp. 9–16. Boston, MA: Springer US.
- [35] CHHABRA, R. P. & UHLHERR, P. H. T. 1980 Creeping motion of spheres through shear-thinning elastic fluids described by the Carreau viscosity equation. *Rheol. Acta* **19** (2), 187–195.
- [36] CHISHOLM, N. G., LEGENDRE, D., LAUGA, E. & KHAIR, A. S. 2016 A squirmer across reynolds numbers. *J. Fluid Mech.* **796**, 233–256.

- [37] CHRISTOV, I. C. & JORDAN, P. M. 2016 Comment on “locomotion of a microorganism in weakly viscoelastic liquids”. *Phys. Rev. E* **94**, 057101.
- [38] COOLEY, M. B. A. & O’NEILL, M. E. 1969 On the slow motion of two spheres in contact along their line of centres through a viscous fluid. *Math. Proc. Camb. Philos. Soc.* **66** (2), 407–415.
- [39] CURTIS, M. P. & GAFFNEY, E. A. 2013 Three-sphere swimmer in a nonlinear viscoelastic medium. *Phys. Rev. E* **87**, 043006.
- [40] DABADE, V., MARATH, N. K. & SUBRAMANIAN, G. 2015 Effects of inertia and viscoelasticity on sedimenting anisotropic particles. *J. Fluid Mech.* **778**, 133–188.
- [41] DANIELS, M. J., LONGLAND, J. M. & GILBART, J. 1980 Aspects of motility and chemotaxis in spiroplasmas. *Microbiology* **118** (2), 429–436.
- [42] DASGUPTA, M., LIU, B., FU, H. C., BERHANU, M., BREUER, K. S., POWERS, T. R. & KUDROLLI, A. 2013 Speed of a swimming sheet in Newtonian and viscoelastic fluids. *Phys. Rev. E* **87**, 013015.
- [43] DATT, C. & ELFRING, G. J. 2018 Dynamics and rheology of particles in shear-thinning fluids. *J. Non-Newton. Fluid Mech.* **262**, 107–114.
- [44] DATT, C., NATALE, G., HATZIKIRIAKOS, S. G. & ELFRING, G. J. 2017 An active particle in a complex fluid. *J. Fluid Mech.* **823**, 675–688.
- [45] DATT, C., ZHU, L., ELFRING, G. J. & PAK, O. S. 2015 Squirming through shear-thinning fluids. *J. Fluid Mech.* **784**, R1.
- [46] DAUGAN, S., TALINI, L., HERZHAFT, B. & ALLAIN, C. 2002 Aggregation of particles settling in shear-thinning fluids. *Euro. Phys. J. E* **7** (1), 73–81.
- [47] D’AVINO, G., GRECO, F. & MAFFETTONE, P. L. 2017 Particle migration due to viscoelasticity of the suspending liquid and its relevance in microfluidic devices. *Annu. Rev. Fluid Mech.* **49** (1), 341–360.
- [48] D’AVINO, G., HULSEN, M. A., SNIJKERS, F., VERMANT, J., GRECO, F. & MAFFETTONE, P. L. 2008 Rotation of a sphere in a viscoelastic liquid subjected to shear flow. Part I: Simulation results. *J. Rheol.* **52** (6), 1331–1346.

- [49] D’AVINO, G. & MAFFETTONE, P.L. 2015 Particle dynamics in viscoelastic liquids. *J. Non-Newtonian Fluid Mech.* **215**, 80–104.
- [50] DAVIS, A. M. J., O’NEILL, M. E., DORREPAAL, J. M. & RANGER, K. B. 1976 Separation from the surface of two equal spheres in stokes flow. *J. Fluid Mech.* **77** (4), 625–644.
- [51] DE CORATO, M. & D’AVINO, G. 2017 Dynamics of a microorganism in a sheared viscoelastic liquid. *Soft Matt.* **13**, 196–211.
- [52] DE CORATO, M., GRECO, F. & MAFFETTONE, P. L. 2015 Locomotion of a microorganism in weakly viscoelastic liquids. *Phys. Rev. E* **92**, 053008.
- [53] DE CORATO, M., GRECO, F. & MAFFETTONE, P. L. 2016 Reply to “Comment on ‘Locomotion of a microorganism in weakly viscoelastic liquids’ ”. *Phys. Rev. E* **94**, 057102.
- [54] DELFAU, J.-B., MOLINA, J. & SANO, M. 2016 Collective behavior of strongly confined suspensions of squirmers. *Europhys. Lett.* **114**, 24001.
- [55] DENN, M. M. 1990 Issues in viscoelastic fluid mechanics. *Annu. Rev. Fluid Mech.* **22** (1), 13–32.
- [56] DENN, M. M. & MORRIS, J. F. 2014 Rheology of non-brownian suspensions. *Annu. Rev. Chem. Biomol. Engng.* **5** (1), 203–228.
- [57] DOMBROWSKI, T., JONES, S. K., KATSIKIS, G., BHALLA, A. P. S., GRIFFITH, B. E. & KLOTSKA, D. 2019 Transition in swimming direction in a model self-propelled inertial swimmer. *Phys. Rev. Fluids* **4**, 021101.
- [58] DOMURATH, J., SAPHIANNIKOVA, M., FÉREC, J., AUSIAS, G. & HEINRICH, G. 2015 Stress and strain amplification in a dilute suspension of spherical particles based on a bird-carreau model. *J. Non-Newtonian Fluid Mech.* **221**, 95–102.
- [59] DOWNTON, M. T. & STARK, H. 2009 Simulation of a model microswimmer. *Journal of Physics: Condensed Matter* **21**, 204101.
- [60] DUNKEL, J., HEIDENREICH, S., DRESCHER, K., WENSINK, H. H., BÄR, M. & GOLDSTEIN, R. E. 2013 Fluid dynamics of bacterial turbulence. *Phys. Rev. Lett.* **110**, 228102.

- [61] DUNN, J.E. & RAJAGOPAL, K.R. 1995 Fluids of differential type: Critical review and thermodynamic analysis. *Int. J. Eng. Sci.* **33** (5), 689 – 729.
- [62] DUNN, J. E. & FOSDICK, R. L. 1974 Thermodynamics, stability, and boundedness of fluids of complexity 2 and fluids of second grade. *Arch. Ration. Mech. Anal.* **56** (3), 191–252.
- [63] EARL, D. J., POOLEY, C. M., RYDER, J. F., BREDBERG, I. & YEO-MANS, J. M. 2007 Modeling microscopic swimmers at low Reynolds number. *J. Chem. Phys.* **126** (6), 064703.
- [64] EINARSSON, J. & MEHLIG, B. 2017 Spherical particle sedimenting in weakly viscoelastic shear flow. *Phys. Rev. Fluids* **2**, 063301.
- [65] EINARSSON, J., YANG, M. & SHAQFEH, E. S. G. 2018 Einstein viscosity with fluid elasticity. *Phys. Rev. Fluids* **3**, 013301.
- [66] EINSTEIN, A. 1956 *Investigations on the Theory of the Brownian Movement*. Courier Corporation.
- [67] ELFRING, G. J. 2015 A note on the reciprocal theorem for the swimming of simple bodies. *Phys. Fluids* **27**, 023101.
- [68] ELFRING, G. J. 2017 Force moments of an active particle in a complex fluid. *J. Fluid Mech.* **829**, R3.
- [69] ELFRING, G. J. & GOYAL, G. 2016 The effect of gait on swimming in viscoelastic fluids. *J. Non-Newtonian Fluid Mech.* **234**, 8–14.
- [70] ELFRING, G. J. & LAUGA, E. 2015 *Theory of locomotion through complex fluids*, pp. 283–317. Springer.
- [71] ELGETI, J., WINKLER, R. G. & GOMPPER, G. 2015 Physics of microswimmers—single particle motion and collective behavior: a review. *Rep. Prog. Phys.* **78**, 056601.
- [72] FAUCI, L. J. & DILLON, R. 2006 Biofluidmechanics of reproduction. *Annu. Rev. Fluid Mech.* **38**, 371–394.
- [73] FELDERHOF, B. U. 2006 The swimming of animalcules. *Phys. Fluids* **18** (6), 063101.
- [74] FELDERHOF, B. U. 2016 Effect of fluid inertia on the motion of a collinear swimmer. *Phys. Rev. E* **94**, 063114.

- [75] FOSDICK, R. L., RAJAGOPAL, K. R. & CHADWICK, PETER 1980 Thermodynamics and stability of fluids of third grade. *Proc. R. Soc. Lond. A.* **369** (1738), 351–377.
- [76] FU, H. C., SHENOY, V. B. & POWERS, T. R. 2010 Low-Reynolds-number swimming in gels. *Europhys. Lett.* **91** (2), 24002.
- [77] GAGNON, D. A., KEIM, N. C. & ARRATIA, P. E. 2014 Undulatory swimming in shear-thinning fluids: experiments with *caenorhabditis elegans*. *J. Fluid Mech.* **758**.
- [78] GAO, W. & WANG, J. 2014 The environmental impact of micro/nanomachines: A review. *ACS Nano* **8** (4), 3170–3180.
- [79] GAO, W. & WANG, J. 2014 Synthetic micro/nanomotors in drug delivery. *Nanoscale* **6** (18), 10486–10494.
- [80] GHEISSARY, G. & VAN DEN BRULE, B.H.A.A. 1996 Unexpected phenomena observed in particle settling in non-newtonian media. *J. Non-Newtonian Fluid Mech.* **67**, 1 – 18.
- [81] GILPIN, W., PRAKASH, V. N. & PRAKASH, M. 2016 Vortex arrays and ciliary tangles underlie the feeding-swimming trade-off in starfish larvae. *Nat. Phys.* pp. 1745–2481.
- [82] GODÍNEZ, F. A., DE LA CALLEJA, E., LAUGA, E. & ZENIT, R. 2014 Sedimentation of a rotating sphere in a power-law fluid. *J. Non-Newtonian Fluid Mech.* **213**, 27–30.
- [83] GOLESTANIAN, R. & AJDARI, A. 2008 Analytic results for the three-sphere swimmer at low Reynolds number. *Phys. Rev. E* **77**, 036308.
- [84] GOLESTANIAN, R., LIVERPOOL, T. B. & AJDARI, A. 2005 Propulsion of a molecular machine by asymmetric distribution of reaction products. *Phys. Rev. Lett.* **94**, 220801.
- [85] GOLESTANIAN, R., LIVERPOOL, T. B. & AJDARI, A. 2007 Designing phoretic micro- and nano-swimmers. *New J. Phys.* **9**, 126.
- [86] GOMEZ-SOLANO, J. R., BLOKHUIS, A. & BECHINGER, C. 2016 Dynamics of self-propelled Janus particles in viscoelastic fluids. *Phys. Rev. Lett.* **116**, 138301.

- [87] GRECO, F., D'AVINO, G. & MAFFETTONE, P.L. 2007 Rheology of a dilute suspension of rigid spheres in a second order fluid. *J. Non-Newton. Fluid Mech.* **147** (1), 1–10.
- [88] GUASTO, J. S., RUSCONI, R. & STOCKER, R. 2012 Fluid mechanics of planktonic microorganisms. *Ann. Rev. Fluid Mech.* **44** (1), 373–400.
- [89] GUAZZELLI, E., MORRIS, J. F. & PIC, S. 2009 *A Physical Introduction to Suspension Dynamics*. Cambridge University Press.
- [90] GUMMALAM, S. & CHHABRA, R. P. 1987 Rising velocity of a swarm of spherical bubbles in a power law non-newtonian liquid. *Can. J. Chem. Eng.* **65** (6), 1004–1008.
- [91] GURTIN, M. E., FRIED, E. & LALLIT, A. 2010 *The Mechanics and Thermodynamics of Continua*. Cambridge University Press.
- [92] TEN HAGEN, B., VAN TEEFFELLEN, S. & LÖWEN, H. 2011 Brownian motion of a self-propelled particle. *J Phys.: Condens Matt.* **23** (19), 194119.
- [93] HAPPEL, J. & BRENNER, H. 1983 *Low Reynolds Number Hydrodynamics*. Martinus Nijhoff.
- [94] HEWITT, D. R. & BALMFORTH, N. J. 2017 Taylor's swimming sheet in a yield-stress fluid. *J. Fluid Mech.* **828**, 33–56.
- [95] HOUSIADAS, K. D. & TANNER, R. I. 2009 On the rheology of a dilute suspension of rigid spheres in a weakly viscoelastic matrix fluid. *J. Non-Newtonian Fluid Mech.* **162** (1-3), 88–92.
- [96] HOUSIADAS, K. D. & TANNER, R. I. 2012 The drag of a freely sedimentating sphere in a sheared weakly viscoelastic fluid. *J. Non-Newtonian Fluid Mech.* **183-184**, 52–56.
- [97] HOUSIADAS, K. D. & TANNER, R. I. 2016 A high-order perturbation solution for the steady sedimentation of a sphere in a viscoelastic fluid. *J. Non-Newton. Fluid Mech.* **233**, 166 – 180, papers presented at the Rheology Symposium in honor of Prof. R. I. Tanner on the occasion of his 82nd birthday, in Vathi, Samos, Greece.
- [98] HUANG, Z-H, ABKARIAN, M. & VIALLAT, A. 2011 Sedimentation of vesicles: from pear-like shapes to microtether extrusion. *New J. Phys.* **13**, 035026.

- [99] HWANG, S. H., LITT, M. & FORSMAN, W. C. 1969 Rheological properties of mucus. *Rheol. Acta* **8**, 438–448.
- [100] ISHIKAWA, T., KAJIKI, S., IMAI, Y. & OMORI, T. 2016 Nutrient uptake in a suspension of squirmers. *J. Fluid Mech.* **789**, 481–499.
- [101] ISHIKAWA, T., SIMMONDS, M. P. & PEDLEY, T. J. 2006 Hydrodynamic interaction of two swimming model micro-organisms. *J. Fluid Mech.* **568**, 119–160.
- [102] ISHIMOTO, K. & YAMADA, M. 2012 A coordinate-based proof of the scallop theorem. *SIAM J. Appl. Math.* **72**, 1686–1694.
- [103] JEFFERY, G. B. 1922 The motion of ellipsoidal particles immersed in a viscous fluid. *Proc. Roy. Soc. London A* **102** (715), 161–179.
- [104] JOSEPH, D.D. & FENG, J. 1996 A note on the forces that move particles in a second-order fluid. *J. Non-Newtonian Fluid Mech.* **64** (2), 299–302.
- [105] JOSEPH, D.D., LIU, Y.J., POLETTO, M. & FENG, J. 1994 Aggregation and dispersion of spheres falling in viscoelastic liquids. *J. Non-Newtonian Fluid Mech.* **54**, 45–86.
- [106] JÜLICHER, F. & PROST, J. 2009 Generic theory of colloidal transport. *Eur. Phys. J. E* **29**, 27–36.
- [107] KAPRAL, R. 2013 Perspective: Nanomotors without moving parts that propel themselves in solution. *J. Chem. Phys.* **138**, 020901.
- [108] KARIMI, A., YAZDI, S. & ARDEKANI, A. M. 2013 Hydrodynamic mechanisms of cell and particle trapping in microfluidics. *Biomicrofluidics* **7** (2), 021501.
- [109] KEIM, N. C., GARCIA, M. & ARRATIA, P. E. 2012 Fluid elasticity can enable propulsion at low Reynolds number. *Phys. Fluids* **24**, 081703.
- [110] KHAIR, A. S. & CHISHOLM, N. G. 2014 Expansions at small Reynolds numbers for the locomotion of a spherical squirmer. *Phys. Fluids* **26** (1), 011902.
- [111] KHAIR, A. S., POSLUSZNY, D. E. & WALKER, L. M. 2012 Coupling electrokinetics and rheology: Electrophoresis in non-Newtonian fluids. *Phys. Rev. E* **85**, 016320.

- [112] KHAIR, A. S. & SQUIRES, T. M. 2010 Active microrheology: A proposed technique to measure normal stress coefficients of complex fluids. *Phys. Rev. Lett.* **105**, 156001.
- [113] KIM, S. 1985 A note on Faxén laws for nonspherical particles. *Int. J. Multiph. Flow* **11**, 713–719.
- [114] KISHORE, N., CHHABRA, R.P. & ESWARAN, V. 2008 Drag on ensembles of fluid spheres translating in a power-law liquid at moderate reynolds numbers. *Chem. Eng. J.* **139** (2), 224 – 235.
- [115] KLOTSA, D., BALDWIN, K. A., HILL, R. J. A., BOWLEY, R. M. & SWIFT, M. R. 2015 Propulsion of a two-sphere swimmer. *Phys. Rev. Lett.* **115**, 248102.
- [116] KOCH, D. L. & SUBRAMANIAN, G. 2006 The stress in a dilute suspension of spheres suspended in a second-order fluid subject to a linear velocity field. *J. Non-Newtonian Fluid Mech.* **138** (2), 87–97.
- [117] KOCH, D. L. & SUBRAMANIAN, G. 2011 Collective hydrodynamics of swimming microorganisms: Living fluids. *Annu. Rev. Fluid Mech.* **43**, 637–659.
- [118] KRISHNAMURTHY, D. & SUBRAMANIAN, G. 2015 Collective motion in a suspension of micro-swimmers that run-and-tumble and rotary diffuse. *J. Fluid Mech.* **781**, 422–466.
- [119] LAGNADO, R. R., PHAN-THIEN, N. & LEAL, L. G. 1984 The stability of two-dimensional linear flows. *Phys. Fluids* **27** (5), 1094–1101.
- [120] LAI, S. K., WANG, Y.-Y., WIRTZ, D. & HANES, J. 2009 Micro- and macrorheology of mucus. *Adv. Drug Deliv. Rev.* **61**, 86 – 100.
- [121] LAUGA, E. 2007 Propulsion in a viscoelastic fluid. *Phys. Fluids* **19**, 083104.
- [122] LAUGA, E. 2009 Life at high Deborah number. *Europhys. Lett.* **86**, 64001.
- [123] LAUGA, E. 2011 Enhanced diffusion by reciprocal swimming. *Phys. Rev. Lett.* **106** (17), 178101.
- [124] LAUGA, E. 2011 Life around the scallop theorem. *Soft Matt.* **7**, 3060–3065.

- [125] LAUGA, E. 2014 Locomotion in complex fluids: Integral theorems. *Phys. Fluids* **26**, 081902.
- [126] LAUGA, E. 2015 The bearable gooeyness of swimming. *J. Fluid Mech.* **762**, 1–4.
- [127] LAUGA, E. 2016 Bacterial hydrodynamics. *Annu. Rev. Fluid Mech.* **48**, 105–130.
- [128] LAUGA, E. & MICHELIN, S. 2016 Stresslets induced by active swimmers. *Phys. Rev. Lett.* **117**, 148001.
- [129] LAUGA, E. & POWERS, T. R. 2009 The hydrodynamics of swimming microorganisms. *Rep. Prog. Phys.* **72**, 096601.
- [130] LAVEN, J. & STEIN, H. N. 1991 The einstein coefficient of suspensions in generalized newtonian liquids. *J. Rheol.* **35** (8), 1523–1549.
- [131] LEAL, L. G. 1975 The slow motion of slender rod-like particles in a second-order fluid. *J. Fluid Mech.* **69**, 305–337.
- [132] LEAL, L. G. 1979 The motion of small particles in non-Newtonian fluids. *J. Non-Newtonian Fluid Mech.* **5**, 33–78.
- [133] LEAL, L. G. 1980 Particle motions in a viscous fluid. *Annu. Rev. Fluid Mech.* **12**, 435–476.
- [134] LI, C., QIN, B., GOPINATH, A., ARRATIA, P. E., THOMASES, B. & GUY, R. D. 2017 Flagellar swimming in viscoelastic fluids: role of fluid elastic stress revealed by simulations based on experimental data. *J. R. Soc. Interface* **14** (135), 20170289.
- [135] LI, G. J., KARIMI, A. & ARDEKANI, A. M. 2014 Effect of solid boundaries on swimming dynamics of microorganisms in a viscoelastic fluid. *Rheol. Acta* **53**, 911–926.
- [136] LIEBCHEN, B., MONDERKAMP, P., TEN HAGEN, B. & LÖWEN, H. 2018 Viscotaxis: Microswimmer navigation in viscosity gradients. *Phys. Rev. Lett.* **120**, 208002.
- [137] LIGHTHILL, M. J. 1952 On the squirming motion of nearly spherical deformable bodies through liquids at very small Reynolds numbers. *Commun. Pure Appl. Math.* **5**, 109–118.

- [138] LU, X., LIU, C., HU, G. & XUAN, X. 2017 Particle manipulations in non-Newtonian microfluidics: A review. *J. Colloid Interface Sci.* **500**, 182–201.
- [139] MARCHETTI, M. C., JOANNY, J. F., RAMASWAMY, S., LIVERPOOL, T. B., PROST, J., RAO, M. & SIMHA, R. A. 2013 Hydrodynamics of soft active matter. *Rev. Mod. Phys.* **85**, 1143–1189.
- [140] MATHIJSEN, A. J. T. M., SHENDRUK, T. N., YEOMANS, J. M. & DOOSTMOHAMMADI, A. 2016 Upstream swimming in microbiological flows. *Phys. Rev. Lett.* **116**, 028104.
- [141] MAUDE, A. D. 1961 End effects in a falling-sphere viscometer. *Brit. J. Appl. Phys.* **12** (6), 293.
- [142] MERRILL, E. W. 1969 Rheology of blood. *Physiol. Rev.* **49**, 863–888.
- [143] METZNER, A. B. 1985 Rheology of suspensions in polymeric liquids. *J. Rheol.* **29**, 739–775.
- [144] MICHELIN, S. & LAUGA, E. 2011 Optimal feeding is optimal swimming for all Péclet numbers. *Phys. Fluids* **23**, 101901.
- [145] MICHELIN, S. & LAUGA, E. 2014 Phoretic self-propulsion at finite Péclet numbers. *J. Fluid Mech.* **747**, 572–604.
- [146] MICHELIN, S., LAUGA, E. & BARTOLO, D. 2013 Spontaneous autophoretic motion of isotropic particles. *Phys. Fluids* **25**, 061701.
- [147] MONTENEGRO-JOHNSON, T. D. & LAUGA, E. 2014 Optimal swimming of a sheet. *Phys. Rev. E* **89**, 060701.
- [148] MONTENEGRO-JOHNSON, T. D., SMITH, A. A., SMITH, D. J., LOGHIN, D. & BLAKE, J. R. 2012 Modelling the fluid mechanics of cilia and flagella in reproduction and development. *Eur. Phys. J. E* **35**, 1–17.
- [149] MONTENEGRO-JOHNSON, T. D., SMITH, D. J. & LOGHIN, D. 2013 Physics of rheologically enhanced propulsion: Different strokes in generalized stokes. *Phys. Fluids* **25**, 081903.
- [150] MOROZOV, A. & SPAGNOLIE, S. E. 2015 *Introduction to complex fluids*, pp. 3–52. Springer.

- [151] NAJAFI, A. & GOLESTANIAN, R. 2004 Simple swimmer at low Reynolds number: Three linked spheres. *Phys. Rev. E* **69**, 062901.
- [152] NASOURI, B. & ELFRING, G. J. 2018 Higher-order force moments of active particles. *Phys. Rev. Fluids* **3**, 044101.
- [153] NASOURI, B., KHOT, A. & ELFRING, G. J. 2017 Elastic two-sphere swimmer in Stokes flow. *Phys. Rev. Fluids* **2**, 043101.
- [154] NELSON, BRADLEY J., KALIAKATSOS, I. K. & ABBOTT, JAKE J. 2010 Microrobots for minimally invasive medicine. *Annu. Rev. Biomed. Eng.* **12** (1), 55–85.
- [155] NICODEMO, L., NICOLAIS, L. & LANDEL, R.F. 1974 Shear rate dependent viscosity of suspensions in newtonian and non-newtonian liquids. *Chem. Engng. Sci.* **29** (3), 729–735.
- [156] OGDEN, R. W. 1984 *Non-linear elastic deformations*. Dover.
- [157] OPPENHEIMER, N., NAVARDI, S. & STONE, H. A. 2016 Motion of a hot particle in viscous fluids. *Phys. Rev. Fluids* **1**, 014001.
- [158] OZIN, G. A., MANNERS, I., FOURNIER-BIDOZ, S. & ARSENAULT, A. 2005 Dream nanomachines. *Adv. Mater.* **17**, 3011–3018.
- [159] PAK, O. S. & LAUGA, E. 2014 Generalized squirming motion of a sphere. *J.Engng. Math.* **88**, 1–28.
- [160] PAK, O. S., ZHU, L., BRANDT, L. & LAUGA, E. 2012 Micropropulsion and microrheology in complex fluids via symmetry breaking. *Phys. Fluids* **24**, 103102.
- [161] PAL, R. 2015 Rheology of suspensions of solid particles in power-law fluids. *Can. J. Chem. Eng.* **93** (1), 166–173.
- [162] PALACCI, J., SACANNA, S., STEINBERG, A. P., PINE, D. J. & CHAIKIN, P. M. 2013 Living crystals of light-activated colloidal surfers. *Science* **339**, 936–940.
- [163] PATTESON, A.E., GOPINATH, A., GOULIAN, M. & ARRATIA, P.E. 2015 Running and tumbling with *E. coli* in polymeric solutions. *Scientific reports* **5**.

- [164] PATTESON, A. E., GOPINATH, A. & ARRATIA, P. E. 2016 Active colloids in complex fluids. *Curr. Opin. Colloid Interface Sci.* **21**, 86–96.
- [165] PEDLEY, T. J. 2016 Spherical squirmers: models for swimming microorganisms. *IMA J. Appl. Math.* **81**, 488–521.
- [166] PEDLEY, T. J., BRUMLEY, D. R. & GOLDSTEIN, R. E. 2016 Squirmers with swirl: a model for Volvox swimming. *J. Fluid Mech.* **798**, 165–186.
- [167] PETRINO, M. G. & DOETSCH, R. N. 1978 ‘Viscotaxis’, a new behavioural response of *Leptospira interrogans* (biflexa) strain B16. *Microbiology* **109** (1), 113–117.
- [168] POOLE, R. 2012 The Deborah and Weissenberg numbers. *The British Society of Rheology - Rheology Bulletin* **53**, 32–39.
- [169] POPESCU, M. N., USPAL, W. E. & DIETRICH, S. 2016 Self-diffusiophoresis of chemically active colloids. *Eur. Phys. J. Special Topics* **225**, 2189–2206.
- [170] PURCELL, E. M. 1977 Life at low Reynolds number. *Am. J. Phys.* **45**, 3–11.
- [171] QIN, B., GOPINATH, A., YANG, J., GOLLUB, J. P. & ARRATIA, P. E. 2015 Flagellar kinematics and swimming of algal cells in viscoelastic fluids. *Sci. Rep.* **5**.
- [172] QIU, T., LEE, T. C., MARK, A. G., MOROZOV, K. I., MÜNSTER, R., MIERKA, O., TUREK, S., LESHANSKY, A. M. & FISCHER, P. 2014 Swimming by reciprocal motion at low Reynolds number. *Nat. Commun.* **5**.
- [173] RALLISON, J. M. 2012 The stress in a dilute suspension of liquid spheres in a second-order fluid. *J. Fluid Mech.* **693**, 500–507.
- [174] RIDDLE, M. J., NARVAEZ, C. & BIRD, R. B. 1977 Interactions between two spheres falling along their line of centers in a viscoelastic fluid. *J. Non-Newton. Fluid* **2** (1), 23–35.
- [175] RILEY, N. 1966 On a sphere oscillating in a viscous fluid. *Q. J. Mech. Appl. Math.* **19**, 461–472.

- [176] ROBERTS, A. M. 2010 The mechanics of gravitaxis in Paramecium. *J. Exp. Biol.* **213** (24), 4158–4162.
- [177] ROMANCZUK, P., BÄR, M., EBELING, W., LINDNER, B. & SCHIMANSKY-GEIER, L. 2012 Active Brownian particles. *Eur. Phys. J. Special Topics* **202** (1), 1–162.
- [178] SANDOVAL, M., MARATH, N. K., SUBRAMANIAN, G. & LAUGA, E. 2014 Stochastic dynamics of active swimmers in linear flows. *J. Fluid Mech.* **742**, 50–70.
- [179] SAUZADE, M., ELFRING, G. J. & LAUGA, E. 2011 Taylor’s swimming sheet: Analysis and improvement of the perturbation series. *Phys. D* **240** (20), 1567 – 1573, special Issue: Fluid Dynamics: From Theory to Experiment.
- [180] SCHWEITZER, F. & FARMER, J. D. 2007 *Brownian agents and active particles: Collective dynamics in the natural and social sciences*. Springer.
- [181] SHEN, X. N. & ARRATIA, P. E. 2011 Undulatory swimming in viscoelastic fluids. *Phys. Rev. Lett.* **106**, 208101.
- [182] SHERMAN, M. YU., TIMKINA, E.O. & GLAGOLEV, A.N. 1982 Viscosity taxis in Escherichia coli. *FEMS Microbiol. Lett.* **13** (2), 137–140.
- [183] SIMMONS, GEORGE F 2016 *Differential equations with applications and historical notes*. CRC Press.
- [184] SLEIGH, M. A. 1962 *The Biology of Cilia and Flagella*. Pergamon.
- [185] SOKOLOV, A., APODACA, M. M., GRZYBOWSKI, B. A. & ARANSON, I. S. 2010 Swimming bacteria power microscopic gears. *Proc. Natl. Acad. Sci. U.S.A.* **107** (3), 969–974.
- [186] SONI, H., PELCOVITS, R. A. & POWERS, T. R. 2018 Enhancement of microorganism swimming speed in active matter. *Phys. Rev. Lett.* **121**, 178002.
- [187] SPELMAN, T. A. & LAUGA, E. 2017 Arbitrary axisymmetric steady streaming: flow, force and propulsion. *J. Eng. Math.* **105**, 31–65.
- [188] SPIELMAN, L. A. 1970 Viscous interactions in Brownian coagulation. *J. Colloid Interface Sci.* **33** (4), 562 – 571.

Bibliography

- [189] SQUIRES, T. M. 2008 Nonlinear microrheology: bulk stresses versus direct interactions. *Langmuir* **24** (4), 1147–1159.
- [190] SQUIRES, T. M. & BRADY, J. F. 2005 A simple paradigm for active and nonlinear microrheology. *Phys. Fluids* **17** (7), 073101.
- [191] STICKEL, J. J. & POWELL, R. L. 2005 Fluid mechanics and rheology of dense suspensions. *Annu. Rev. Fluid Mech.* **37** (1), 129–149.
- [192] STIMSON, M. & JEFFERY, G. B. 1926 The motion of two spheres in a viscous fluid. *Proc. Roy. Soc. A* **111** (757), 110–116.
- [193] STONE, H. A. & SAMUEL, A. D. T. 1996 Propulsion of microorganisms by surface distortions. *Phys. Rev. Lett.* **77**, 4102–4104.
- [194] SWIDSINSKI, A., SYDORA, B. C., DOERFFEL, Y., LOENING-BAUCKE, V., VANECHOUTTE, M., LUPICKI, M., SCHOLZE, J., LOCHS, H. & DIELEMAN, L. A. 2007 Viscosity gradient within the mucus layer determines the mucosal barrier function and the spatial organization of the intestinal microbiota. *Inflamm. Bowel Dis.* **13** (8), 963–970.
- [195] SZNITMAN, J. & ARRATIA, P. E. 2015 Locomotion through complex fluids: An experimental view. In *Complex Fluids in Biological Systems* (ed. S. E. Spagnolie), pp. 245–281. Springer New York.
- [196] TAKABE, K., TAHARA, H., ISLAM, M. S., AFFROZE, S., KUDO, S. & NAKAMURA, S. 2017 Viscosity-dependent variations in the cell shape and swimming manner of leptospira. *Microbiology* **163** (2), 153–160.
- [197] TAM, D. & HOSOI, A. E. 2007 Optimal stroke patterns for Purcell’s three-link swimmer. *Phys. Rev. Lett.* **98**, 068105.
- [198] TANNER, R. I. 2000 *Engineering rheology*, , vol. 52. OUP Oxford.
- [199] TANNER, R. I., QI, F. & HOUSIADAS, K. D. 2010 A differential approach to suspensions with power-law matrices. *J. Non-Newtonian Fluid Mech.* **165** (23), 1677 – 1681.
- [200] TAYLOR, G. I. 1951 Analysis of the swimming of microscopic organisms. *Proc. R. Soc. Lond. A* **209**, 447–461.
- [201] THURSTON, G.B. 1972 Viscoelasticity of human blood. *Biophys. J.* **12** (9), 1205 – 1217.

- [202] THUTUPALLI, S., SEEMANN, R. & HERMINGHAUS, S. 2011 Swarming behavior of simple model squirmers. *New J. Phys.* **13**, 073021.
- [203] TRUESDELL, C. 1974 The meaning of viscometry in fluid dynamics. *Annu. Rev. Fluid Mech.* **6** (1), 111–146.
- [204] VASQUEZ, P. A. & FOREST, M. G. 2015 *Complex Fluids and Soft Structures in the Human Body*, pp. 53–110. Springer.
- [205] VÉLEZ-CORDERO, J. R. & LAUGA, E. 2013 Waving transport and propulsion in a generalized Newtonian fluid. *J. Non-Newtonian Fluid Mech.* **199**, 37 – 50.
- [206] WAISBORD, N., LEFÈVRE, C. T., BOCQUET, L., YBERT, C. & COTTIN-BIZONNE, C. 2016 Destabilization of a flow focused suspension of magnetotactic bacteria. *Phys. Rev. Fluids* **1** (5).
- [207] WALTHER, A. & MÜLLER, A. H. E. 2013 Janus particles: Synthesis, self-assembly, physical properties, and applications. *Chem. Rev.* **113**, 5194–5261.
- [208] WANG, J. 2009 Can man-made nanomachines compete with nature biomotors? *ACS Nano* **3**, 4–9.
- [209] WANG, S. & ARDEKANI, A. 2012 Inertial squirmer. *Phys. Fluids* **24** (10), 101902.
- [210] WANG, S. & ARDEKANI, A. M. 2012 Unsteady swimming of small organisms. *J. Fluid Mech.* **702**, 286–297.
- [211] WILKING, J. N., ANGELINI, T. E., SEMINARA, A., BRENNER, M. P. & WEITZ, D. A. 2011 Biofilms as complex fluids. *MRS Bulletin* **36** (5), 385–391.
- [212] YANG, M., KRISHNAN, S. & SHAQFEH, E. S.G. 2016 Numerical simulations of the rheology of suspensions of rigid spheres at low volume fraction in a viscoelastic fluid under shear. *J. Non-Newtonian Fluid Mech.* **234** (Supplement C), 51–68.
- [213] YAZDI, S., ARDEKANI, A.M. & BORHAN, A. 2015 Swimming dynamics near a wall in a weakly elastic fluid. *J. Nonlinear Sci.* **25** (5), 1153–1167.

- [214] YOSHIOKA, H., SATO, Y., YOSHIDA, S., OHTSUBO, S. & OTHERS 2006 Hydrogel for cell separation and method of separating cells. US Patent App. 10/545,935.
- [215] YU, Z., WACHS, A. & PEYSSON, Y. 2006 Numerical simulation of particle sedimentation in shear-thinning fluids with a fictitious domain method. *J. Non-Newton. Fluid* **136**, 126–139.
- [216] ZENIT, R. & FENG, J.J. 2018 Hydrodynamic interactions among bubbles, drops, and particles in non-newtonian liquids. *Annu. Rev. Fluid Mech.* **50** (1), 505–534.
- [217] ZHU, L., LAUGA, E. & BRANDT, L. 2012 Self-propulsion in viscoelastic fluids: Pushers vs. pullers. *Phys. Fluids* **24**, 051902.
- [218] ZÖTTL, A. & STARK, H. 2014 Hydrodynamics determines collective motion and phase behavior of active colloids in quasi-two-dimensional confinement. *Phys. Rev. Lett.* **112**, 118101.

Appendix A

Some expressions for motion of spheres

Here we present some expressions which were used to evaluate the integrals in Chapter 4. Additional details on related expressions for both passive and active particles can be found in the recent work of Nasouri & Elfring [152].

For a single sphere of radius a in a Newtonian fluid with viscosity $\hat{\eta}$

$$\hat{\mathbf{R}}_{FU} = 6\pi\hat{\eta}a\mathbf{I}, \quad (\text{A.1})$$

$$\hat{\mathbf{R}}_{L\Omega} = 8\pi\hat{\eta}a^3\mathbf{I}, \quad (\text{A.2})$$

$$\hat{\mathbf{R}}_{LU} = 0, \quad (\text{A.3})$$

$$\hat{\mathbf{R}}_{F\Omega} = 0. \quad (\text{A.4})$$

Additionally,

$$\mathbf{n} \cdot \hat{\mathbf{T}}_U = -\frac{3\hat{\eta}}{2a} [\mathbf{I} \quad 2\boldsymbol{\Theta}], \quad (\text{A.5})$$

where $\Theta_{ij} = \epsilon_{ijk}x_k$ and \mathbf{n} is the unit normal to the surface.

The entities corresponding to $\hat{\gamma}/2 = \hat{\mathbf{E}}_U \cdot \hat{\mathbf{U}}$

$$[\hat{\mathbf{E}}_U]_{ijk} = \frac{3ax_k}{4r^3} \left(\delta_{ij} - \frac{3x_ix_j}{r^2} \right) + \frac{3a^3}{4r^5} \left[x_k \left(-\delta_{ij} + \frac{5x_ix_j}{r^2} \right) - x_i\delta_{jk} - x_j\delta_{ik} \right] \quad (\text{A.6})$$

$$[\hat{\mathbf{E}}_\Omega]_{ijk} = -\frac{3a^3}{2r^5} (x_ix_l\epsilon_{ljk} + x_jx_l\epsilon_{lik}). \quad (\text{A.7})$$

are detailed in [157]. Relevant to the stresslet calculation, we have

$$\begin{aligned} [\hat{\mathbf{E}}_E]_{klij} &= \frac{\hat{\eta}a^5}{2r^5} (\delta_{ik}\delta_{jl} + \delta_{jk}\delta_{il}) + \frac{5\hat{\eta}a^3}{4r^5} (\delta_{il}x_jx_k + \delta_{ki}x_jx_l + \delta_{jl}x_ix_k + \delta_{kj}x_ix_l) \\ &\quad - \frac{5\hat{\eta}a^5}{2r^7} (\delta_{kl}x_ix_j + \delta_{jl}x_ix_k + \delta_{il}x_jx_k + \delta_{jk}x_ix_l + \delta_{ik}x_jx_l) \\ &\quad + 5\hat{\eta} \left(\frac{7a^5}{2r^9} - \frac{5a^3}{2r^7} \right) x_ix_jx_kx_l + \frac{5\hat{\eta}a^3}{2r^5} \delta_{kl}x_ix_j, \end{aligned} \quad (\text{A.8})$$

$$\begin{aligned}
 [\hat{\mathbf{T}}_E]_{klij} &= \frac{\hat{\eta}a^5}{r^5} (\delta_{ik}\delta_{jl} + \delta_{jk}\delta_{il}) + \frac{5\hat{\eta}a^3}{2r^5} (\delta_{il}x_jx_k + \delta_{ki}x_jx_l + \delta_{jl}x_ix_k + \delta_{kj}x_ix_l) \\
 &\quad - \frac{5\hat{\eta}a^5}{r^7} (\delta_{kl}x_ix_j + \delta_{jl}x_ix_k + \delta_{il}x_jx_k + \delta_{jk}x_ix_l + \delta_{ik}x_jx_l) \\
 &\quad + 5\hat{\eta} \left(\frac{7a^5}{r^9} - \frac{5a^3}{r^7} \right) x_ix_jx_kx_l,
 \end{aligned} \tag{A.9}$$

which can be found in the supplementary information of [128].

For the problem involving two spheres sedimenting along their common axis, the stream functions for the two auxiliary cases in Newtonian fluids, two spheres moving with the same velocity and two spheres approaching each other with equal speed, were reported by Stimson & Jeffery [192] and Brenner [23], respectively. The stream functions are expressed in the form of infinite series solutions. To ensure convergence, we considered around the first 30 to 40 terms of the series. The stream functions are used to calculate the strain-rate tensors corresponding to $\hat{\mathbf{E}}_{\overline{U}}$ (Stimson-Jeffery) and $\hat{\mathbf{E}}_{\Delta U}$ (Brenner, Maude). The stress tensor $\boldsymbol{\tau}_{NN}$ for the case considered in the manuscript is evaluated using strain-rates from the Stimson-Jeffery solution.

For the limiting case of two spheres touching each other and sedimenting, we use the solution of the problem in Newtonian fluids by Cooley & O'Neill [38] to evaluate both $\boldsymbol{\tau}_{NN}$ and $\hat{\mathbf{E}}_U$. The stream function for this case is expressed in form of a definite integral from zero to infinity (equation 3.4 in the reference). A non-infinite value of the upper limit of the integral has to be chosen for evaluation; we find that convergence of the solution is achieved at a value of around 15.

Appendix B

Linear viscoelasticity

Equation (8.7) delineates a relationship between forces and velocities and with (8.18) gives, for each Fourier mode,

$$\frac{\hat{\eta}}{\eta^*(p)} \hat{\mathbf{R}}_{FU} \cdot \mathbf{U}^{(p)} = \mathbf{F}_{ext}^{(p)} + \frac{\eta^*(p)}{\hat{\eta}} \int_{\partial\mathcal{B}} \mathbf{v}^{S(p)} \cdot (\mathbf{n} \cdot \hat{\mathbf{T}}_{\mathbf{U}}) dS - \int_{\mathcal{V}} \mathbf{N}^{(p)} : \hat{\mathbf{E}}_{\mathbf{U}} dV. \quad (\text{B.1})$$

For a rigid-body motion under periodic external forcing, $\mathbf{v}^S = \mathbf{0}$. Assuming that the magnitude of the forcing is small so that nonlinear viscoelastic terms are negligible to leading order, we obtain a (complex) linear viscoelastic relationship between force and velocity for each mode,

$$\mathbf{R}_{FU}^{*(p)} \cdot \mathbf{U}^{(p)} = \mathbf{F}_{ext}^{(p)}, \quad (\text{B.2})$$

where the complex resistance $\mathbf{R}_{FU}^* = \frac{\eta^*}{\hat{\eta}} \hat{\mathbf{R}}_{FU}$.

In our problem, there is only a single force mode $2F^{(1)} = F$ (the other modes are zero, see (8.2)). Setting the magnitude of the velocity to be $|U| = \delta\omega$ then leads to a force with magnitude $F = \delta\omega |\eta^*(1)| \hat{R}_{FU_{\parallel}} / \hat{\eta}$. Using the complex viscosity of Oldroyd-B (see (8.19)) we obtain that taking $F = \delta\omega \eta_0 \frac{1+\beta De^2}{1+De^2} \hat{R}_{FU_{\parallel}} / \hat{\eta}$ leads to a velocity $\mathbf{U} = \delta\omega \cos(\omega t + \phi) \mathbf{e}_{\parallel}$ to leading order.